Analytical and numerical studies of Riemann problems for a multiphase mixture model

Dissertation

zur Erlangung des akademischen Grades

doctor rerum naturalium
(Dr. rer. nat.)

von **M. Sc. Hazem Yaghi**

geb. am 04.04.1984 in Jaramana, Syrian

genehmigt durch die Fakultät für Mathematik
der Otto-von-Guericke-Universität Magdeburg

Gutachter: Prof. Dr. Gerald Warnecke
PD Dr. Maren Hantke

eingereicht am: 21.11.2022

Verteidigung am: 31.01.2023

Ehrenerklärung

Ich versichere hiermit, dass ich die vorliegende Arbeit ohne unzulässige Hilfe Dritter und ohne Benutzung anderer als der angegebenen Hilfsmittel angefertigt habe; verwendete fremde und eigene Quellen sind als solche kenntlich gemacht.

Ich habe insbesondere nicht wissentlich:

- Ergebnisse erfunden oder widersprüchliche Ergebnisse verschwiegen,
- statistische Verfahren absichtlich missbraucht, um Daten in ungerechtfertigter Weise zu interpretieren,
- fremde Ergebnisse oder Veröffentlichungen plagiiert oder verzerrt wiedergegeben.

Mir ist bekannt, dass Verstöße gegen das Urheberrecht Unterlassungs- und Schadenersatzansprüche des Urhebers sowie eine strafrechtliche Ahndung durch die Strafverfolgungsbehörden begründen kann. Die Arbeit wurde bisher weder im Inland noch im Ausland in gleicher oder ähnlicher Form als Dissertation eingereicht und ist als Ganzes auch noch nicht veröffentlicht.

Magdeburg, 21.11.2022

Hazem Yaghi

Abstract

In this thesis, we study submodels of a diffuse interface multiphase mixture model which was proposed by Dreyer, Giesselmann, and Kraus in [24]. This model is a type of phase field model which describe the chemically reacting viscous fluid mixtures consisting of N constituents that may develop a transition between a liquid and a vapor phases.
The submodel has N partial mass balance equations, a balance equation of the momentum, and a transport equation of the phase field variable. The phase variable indicates the present phase. The model is supplied with a complicated equation of state. We will consider one space dimension and assume an isothermal flow. We consider the homogeneous part of this model which is a hyperbolic system of partial differential equations for two phase mixture flow with N components.
The main aim of this work is to study the sub-model analytically and numerically. The analytical study reveals that this model is strictly hyperbolic. We presented the analytical structure and the mathematical properties of the sub-model such as the eigenstructure and the wave types of the solutions. We also obtain the exact solution of Riemann initial value problem for the pure phases flow, i.e. $N = 1$ as well as for the multicomponent flow, i.e. $N > 1$.
Any discretization of the full model in [24] has to contain a correct and stable implementation of the homogeneous part. Therefore, it is justified to deal with the problem of numerics for the submodel separately. This is what we do.
In the numerical study, we first consider a vapor-vapor flow. We solve the model using different Riemann solvers and present the results. We compare the numerical solution with the exact results obtained in the analytical study. Further, we consider vapor-liquid flows. In this case, major difficulties appear such as negative pressures, i.e. unphysical results.
We overcome these difficulties using a tracking the interface approach. But actually, these methods are generally not easy to implement. So we also consider discontinuity capturing methods. For these, we also develop a new strategy to deal with this situation. The new approach is called estimating the pressure approach. We applied the new method to several test cases. This gave an undeniable improvement but still leaves some open problems for future research.
Finally, in this work, we include the source term in the sub-model, and we discuss the ability of this model to deal with chemical reactions.

Zusammenfassung

In dieser Arbeit untersuchen wir Teilmodelle eines diffusen Grenzflächen Mehrphasenmischungsmodells, das von Dreyer, Giesselmann und Kraus in [24] vorgeschlagen wurde. Das Modell in [24] ist eine Art Phasenfeldmodell, das chemisch reagierende Fluidgemische beschreibt, die aus N Bestandteilen bestehen, die einen Übergang zwischen einer flüssigen und einer Dampfphase entwickeln können.
Das Teilmodell hat N partielle Massenbilanzgleichungen, eine Bilanzgleichung des Impulses und eine Transportgleichung der Phasenfeldvariablen. Die Phasenvariable zeigt die gegenwärtige Phase an. Das Modell wird mit einer komplizierten Zustandsgleichung geliefert. Wir betrachten eine Raumdimension und gehen von einer isothermen Strömung aus. Wir betrachten den homogenen Teil dieses Modells, das ein hyperbolisches System partieller Differentialgleichungen für eine Zweiphasen-Gemischströmung mit N Komponenten ist.
Das Hauptziel dieser Arbeit ist es, das Teilmodell analytisch und numerisch zu untersuchen.
Die analytische Studie zeigt, dass dieses Modell streng hyperbolisch ist. Wir stellen die analytische Struktur und die mathematischen Eigenschaften des Teilmodells wie die Eigenstruktur und die Wellentypen der Lösungen vor. Wir erhalten auch die exakte Lösung des Riemann-Anfangswertproblems für die reine Phasenströmung, d.h. $N = 1$, sowie für die Mehrkomponentenströmung, d.h. $N > 1$.
Jede Diskretisierung des vollständigen Modells in [24] muss eine korrekte und stabile Implementierung des homogenen Teils enthalten. Daher ist es gerechtfertigt, das Problem der Numerik für das Teilmodell gesondert zu behandeln. Das ist, was wir machen.
Bei der numerischen Untersuchung betrachten wir zunächst eine Dampf-Dampf-Strömung. Wir lösen das Modell mit verschiedenen Riemann-Lösern und präsentieren die Ergebnisse. Wir vergleichen die numerische Lösung mit den exakten Ergebnissen der analytischen Studie. Weiterhin betrachten wir Dampf-Flüssigkeits-Strömungen. In diesem Fall treten große Schwierigkeiten auf, z.B. negative Drücke, d.h. unphysikalische Ergebnisse.
Wir überwinden diese Schwierigkeiten mit einer Verfolgung der Grenzfläche, d.h. einem Tracking-the-Interface-Ansatz. Aber tatsächlich sind diese Methoden im Allgemeinen nicht einfach zu implementieren. Daher betrachten wir auch Diskontinuitätserfassungsmethoden. Auch für diese entwickeln wir eine neue Strategie, um mit dieser Situation umzugehen. Der neue Ansatz wird Druckschätzungsansatz genannt. Wir wenden diese neue Methode auf mehrere Testfälle an. Dies führt zu einer unbestreitbaren Verbesserung, lässt aber noch einige offene Probleme für zukünftige Forschung.
Schließlich nehmen wir in dieser Arbeit den Quellterm in das Teilmodell auf und diskutieren die Fähigkeit dieses Modells, chemische Reaktionen zu berücksichtigen.

Contents

Chapter 1

Introduction

Consider the classical phases of matter gas, liquid, and solid. Multiphase mixtures occur in nature and modern technology such as e. g. gas bubbles in liquids, solid particles transported by liquid or droplets in a gas.
The flow of the multiphase mixtures is an important phenomenon that plays a major role in many fields of science. One can see it when the liquid pressure drops below the vapor pressure, then the liquid vaporizes and forms a bubble. This is called cavitation, see Bachmann [12]. Further examples, gas and water may coexist in a rock, dust clouds in astrophysics and droplets of liquid move in a gas.
The flow of multiphase mixtures can be combined with a chemical reaction. This depends on the nature of the materials in the mixture.
Our main interest in this work is the flow of two phases. The two-phase flow of gases, liquids and solids can be divided into three categories according to the phase materials: Gas-liquid flows, gas-solid flows, and liquid-solid flows.
In many situations, the components are stationary with respect to one another which means one component does not diffuse into another which leads to the complexity of the theoretical treatment.
In this work, we do not consider the solid phase we consider only fluids that can be made to flow, and the study is turned to be the study of multicomponent fluids.
The presence of multicomponent fluids everywhere in nature demands a deep understanding of their behavior so that many models are considered. Of course, mathematical modeling and numerical computations face huge difficulties. One of the main reasons for such difficulties is the treatment of the interfaces. These are the surfaces and layers that separate the phases. One of the difficulties at the interface is the interaction between the phases which includes the transfer of mass, momentum, and energy across the interface. Also, the discontinuities of the fluid properties at the interface are another reason for the complexity. So that the two-phase flows are characterized by the treatment of the interface. The interface can be considered a free boundary in the flow. In this case, we call it the sharp interface. When we consider a thickness of the interface here we call it a diffuse interface.
Based on the nature of the interface one can distinguish two kinds of models. The first one treats the interface as a sharp interface. Many methods were introduced for the treatment of the sharp interface models. These methods are classified into Lagrangian methods, Eulerian methods, combined Euler-Lagrangian methods, and arbitrary Lagrangian-Eulerian methods. More details can be found in Hu et al. [39], Saurel [63], Scardovelli and Zaleski [66], Tryggvason et al. [77], Saurel and Ab-

grall [64] as well as Saurel and Le Metayer [65].
The second kind of models deals with the interface as a diffuse zone so we call this kind of models a diffuse interface models. These models are based either on the Euler equations or the multiphase flow equations, see discussions in Acar [4], Anderson et al. [6], Alzein [5], Bachmann [12], Abgral [1], Shyue [68], Saurel and Abgral [2], [3] as well as Andrianov et al. [10] [9].
One can see that some models are simple and efficient but have limited applications in physics and require a simple equation of state.
On the other hand, some models have many applications in physics but need a large number of equations to be used.
For instance, models of Baer-Nunziato type [13] require a large number of equations. This increase the numerical cost substantially. Further, these models are usually not in the divergence form. Accordingly, their discretization needs special attention. Moreover, the form of the exchange terms is not known. For more details see Herard [37] and Müller et al. [57].
In 2007 Romenski et al. [61] introduced a similar symmetric hyperbolic and thermodynamically compatible two phase flow model. Although the volume fraction is a variable of the system the model is in divergence form. Therefore the model seems to be very interesting from a mathematical point of view even though a conservation law for relative velocity should be discussed extensively. Recently all characteristic fields of the system and all possible wave phenomena were discussed, see Thein et al. [74], but the full Riemann solution is still not available.
Sharp interface models need only a smaller number of equations. Interesting analytical results are available in Hantke et al. [32]. The Riemann problem for the isothermal Euler equations with phase transitions was completely discussed. Mass transfer was modeled by kinetic relations. To solve such systems numerically, the interface has to be resolved more or less exactly. Accordingly, either a very fine grid resolution is required, or the computations have to be performed on a moving mesh or one has to track the interfaces on an additional mesh. This can become quite complicated in higher space dimensions, see for instance Chalons et al. [17] and [18]. In [17] a conservative finite volume method was developed to approximate weak 1d-solutions of conservation laws with phase boundaries. This method was generalized in [18] for 2d-computations and is able to exactly resolve planar phase interfaces. Further interesting results on this topic can be found in Schleper [67] or Fechter et al. [27].
To overcome the disadvantages of the types of models discussed before, the so called phase field models are considered. This kind of models are based on the phase field variable which is a function of time and space. This parameter takes two distinct values to indicate the local phase. It smoothly changes at the interface which is modeled as small zones of finite width.
Dreyer, Giesselmann, and Kraus in their paper [24] have proposed a diffuse interface model which is such a type of phase field model. This model describes chemical reacting viscous fluids mixtures which consist of N constituents. The mixture may develop a transition between a liquid and a vapor.
To describe the phase transition an artificial phase field indicator has been introduced. This phase field variable, say χ, indicates the present phase by giving the values 1 to the liquid and -1 to the vapor phase. Values in $]-1,1[$ indicate a transition layer. The pressure is a constitutive quantity that is related to the phase

function variable χ and the partial densities of the components by an equation of state. The model is supplied with a multi component equation of state and the challenge comes from its very complicated nature.
The diffuse interface multiphase mixture model derived by Dreyer et al. in [24] is the focus of this work. In particular, the homogeneous part of the model obtained by neglecting source terms and terms with second derivatives in space.
The homogeneous submodel has $N+2$ equations: N partial mass balance equations, an equation of balance for the momentum and a transport equation for the phase field variable χ. This work aims to give a full analysis of the Riemann initial value problem for this hyperbolic system of conservation laws. Also, solving the sub-model numerically is one of the main goals of this thesis.
Presenting the model [24] in detail is essential before we start our study. But due to the wide range of applications and the complicated relations in thermodynamics, we will start this thesis by devoting Chapter 2 to present a summary of the thermodynamics concepts.
In Chapter 3 we present the model in its full version. We discuss all the basic quantities and the constitutive laws in detail. A good knowledge of the hyperbolic sub-part of the full model is required for analytical and numerical computations.
Further, we introduced an equation of state which is necessary in order to close the model. The equation of state has a special form presented in [24]. It is based on the phase variable χ and the equation of state of the pure phases.
Chapter 4 is devoted to studying the model analytically. For this goal, we start this chapter by reminding the reader of the main concepts in the theory of the hyperbolic conservation laws in the scalar case as well as in the systems.
We study the analytical structure and the main mathematical properties of the system considered. Studying the eigenstructure of the submodel helps us to understand the wave patterns of the solution. It reveals that the solution consists of three waves. A contact discontinuity wave in the middle, a shock wave and a rarefaction wave either to the right or to the left. Then we discuss the Riemann invariants which are essential to construct the exact solution. We obtain the exact solution for the case $N = 1$. We could generalize those results to the case $N > 1$.
Many interesting examples are given in this chapter and the results are compared with the results presented in Toro [75] and Hantke et al. [32]. Parts of this chapter will appear as [35].
The main focus of Chapters 5 and 6 is to solve the sub-model numerically. Chapter 5 contains a short survey of numerical methods to solve the conservation laws. We present the Godunov scheme and we give an overview of Riemann solvers such as HLL, HLLC, Roe solver, VFRoe, and Rusanov. For higher order, we discuss the MUSCL method. Then we discuss the discretization of the sub-model. We consider the case of vapor-vapor flow. This case is a good test case in order to test the performance of Riemann solvers and to understand the structure of the solutions.
In Chapter 6 we presented the numerical solution for the more complicated case which is the flow of vapor-liquid. In this case, many unexpected difficulties appear. They are namely the negative pressures, i.e. unphysical results. These difficulties are also relevant for the discretization of the full model since they are due to the nature of the equation of state. It is identical for both models. We develop strategies and methods to overcome these difficulties. In this work, first, we used tracking the interface approach in order to avoid negative pressure. This method is applied

successfully in the work of Thein [73]. But this approach deals with the interface as a sharp interface. So we developed a new approach called "estimating the pressure". This new approach is based on the physical properties of the liquid. We consider a liquid phase as a solid wall because most of the effects appear in the vapor phase. This enables us to solve the Riemann problem on the wall. We do this in two ways. The first one by solving the Riemann problem on the wall numerically using Riemann solvers. The other one, by using the exact solution of the Riemann problem on the wall. This method is applied to many examples and gives good results. Parts of Chapter 6 will appear as [34].
In both Chapters 5 and 6 we give some numerical examples and compare those results with the exact solution obtained in Chapter 4.
Finally, in Chapter 7 for chemical reactions, the sub-model is modified by reaction sources. For their discretization, an ODE-solver has to be coupled to the numerical method. We study this new sub-model and give a numerical solution to it. Numerical examples have been presented.

Chapter 2

Thermodynamics

As we have mentioned in the introduction our aim in this work is to study the homogeneous form of the diffuse interface multiphase mixture model proposed by Dreyer et al. in [24]. This model was suggested for chemically reacting viscous fluid mixtures that may develop a transition between the phases. The model is provided with an equation of state. One can notice that a background in thermodynamics is required so we will start this work by providing the reader with a summary of thermodynamics results and highlighting the basic concepts that we will need in this work.
The main references in this chapter are the book by Atkins [11] and the book by Müller and Müller [56]. For further details we recommend the book by Anderson [7], the paper by Müller and Hantke [33] as well as the PhD thesis by Thein [73]. Additionally we also refer to the work of Menikoff and Plohr [52], Landau and Lifshitz [43], Bothe and Dreyer [15] as well as Flatten [29] .
We will start this chapter with some basic definitions before we introduce the famous laws of thermodynamics. After that we present the thermodynamics potentials in Section 2.3. In Section 2.4 we give an overview of the equation of state with some examples. Maybe the most important section is Section 2.5 where we discuss the thermodynamics of mixtures in order to define the stiffened gas equation of state which will play an important role later on in this study.
Thermodynamics is in general used for providing rules that govern the descriptions of macroscopic systems in terms of their properties and their interactions with other systems.
We divide the universe into two parts, **the system**, which is the part of the world in which we have a special interest and its **surroundings**, which comprise the region outside the system and where we make our measurements. The interface separating the system and its surroundings is called **the system boundary**. And we call the combination of system and surrounding **the universe**.
The characteristics of the system boundaries classify the system into:

- **Open system**: if matter can be transferred through the boundaries between the system and its surrounding.
- **Closed system**: if matter cannot pass through the boundary but other properties may be transferred through it.
- **Isolated system**: a closed system that has neither mechanical nor thermal contact with its surrounding.

We have to mention here that both closed and open systems allow energy to transfer, i.e. can exchange energy with their surrounding.
We distinguish the system, which has constant mass, but possibly variable volume, from the **control volume**. The latter one is a fixed volume where mass can pass in and out through its boundary, which is called **the control surface**.

2.1 Basic definitions

We define

- **Phase:** a quantity of matter that is homogeneous throughout, e.g. liquid, gaseous or solid.
- **Phase boundary:** interface between different phases.
- **State:** condition described by observable macroscopic properties.
- **Property:** quantity that only depends on the state of the system and is independent of the history of the system.

There are two important classes of properties we consider:

- **Extensive property:** a property which is doubled if we double the system, in other words a property that depends on the mass of the system like total volume and total energy.
- **Intensive property:** a property which is independent of the mass of the system like temperature and pressure.

Actually, we define properties for systems which are in **Equilibrium**, which is a state in which no spontaneous changes are observed with respect to time, and we will define three types of equilibrium

- Mechanical equilibrium: is characterized by equal pressure and velocity everywhere in the system.
- Thermal equilibrium: is characterized by equal temperature everywhere.
- Chemical equilibrium: is characterized by equal chemical potentials everywhere.

Often systems undergo a change of state, which means one or more properties of the system have changed, a succession of changes of state is called a process, which is given special names like **isothermal** when it has constant temperature, **isobaric** when constant pressure is assumed, and **isochoric** when we consider constant volume.

2.2 The laws of thermodynamics

2.2.1 First law of thermodynamics

Generally, when a system passes through a process, it exchanges energy with its environment. The total energy of a system is called its **internal energy** E. The difference $\Delta E = E_f - E_i$ is the change in internal energy when the system changes from an initial state i with energy E_i to final state f of internal energy E_f.
The energy change in the system, may result from performing **work** W on the system or letting the system perform work, and from exchanging **heat** Q between the system and the environment. Starting from this point, we can set the first law in thermodynamics:

The change of the internal energy is the sum of the heat supplied to the system and the work done to the system.

To summarize this result we write ΔE the change in internal energy as

$$\Delta E = Q + W$$

which is the mathematical state of the first law.
Now we switch attention to infinitesimal changes of state, e.g. like temperature, and infinitesimal changes in the internal energy dE. Then the work done on a system is dW and the energy supplied to it as heat is dQ, which means

$$dE = dQ + dW.$$

Enthalpy

The **enthalpy** H with the volume V and pressure p is defined as

$$H = E + pV.$$

The enthalpy plays an important role in stationary flows of fluids, ΔH is independent of the path between any pair of initial and final states. The change in enthalpy is equal to the energy supplied as heat at constant pressure

$$dH = dQ, \tag{2.1}$$

and for measurable changes

$$\Delta H = Q.$$

As the internal energy of a substance increases when its temperature T is raised, we define **the heat capacities** C_V and C_p as the amount of heat needed to raise the temperature of the material by one degree. We define the heat capacity at constant volume C_V as

$$C_V = \left(\frac{\partial E}{\partial T}\right)_V.$$

The heat capacity at constant pressure is the slope of the tangent to a plot of enthalpy against T at constant pressure

$$C_p = \left(\frac{\partial H}{\partial T}\right)_p.$$

We define γ the ratio of heat capacities

$$\gamma = \frac{C_p}{C_V}.$$

Remark 1 *So far all quantities were denoted by capital letters. From this point we will consider* ***specific*** *quantities, i.e. per amount of substance or per mass, and we will use the corresponding small letter. We will consider only specific quantities in this work.*

Changes in internal energy

When the specific volume v changes to $v + dv$ at constant temperature, the specific energy $e = e(v, T)$ changes to

$$e' = e + \left(\frac{\partial e}{\partial v}\right)_T dv.$$

If instead, T changes to $T + dT$ at constant volume, then the internal energy changes to

$$e' = e + \left(\frac{\partial e}{\partial T}\right)_v dT.$$

Now suppose that v and T both change infinitesimally, the internal energy differs from e by infinitesimal amount de, therefore the new internal energy is the sum of the changes arising from each increment

$$de = \left(\frac{\partial e}{\partial v}\right)_T dv + \left(\frac{\partial e}{\partial T}\right)_v dT.$$

The coefficient $(\frac{\partial e}{\partial v})_T$ plays a major role in thermodynamics because it measures the variation of the internal energy of a substance as its volume is changed at constant temperature. This coefficient is called the **internal pressure** and denoted by π. We have already $c_v = (\frac{\partial e}{\partial T})_v$, which gives

$$de = \pi dv + c_v dT.$$

Now we want to find out how the internal energy varies with temperature when the pressure of the system is constant. We obtain

$$\left(\frac{\partial e}{\partial T}\right)_p = \pi \left(\frac{\partial v}{\partial T}\right)_p + c_v.$$

The partial derivatives on the right in this expression is the slope of the plot of volume against temperature. This property is called **expansion coefficient** α which is defined as

$$\alpha = \frac{1}{v}\left(\frac{\partial v}{\partial T}\right)_p.$$

Physically it is the fractional change in volume that accompanies a rise in temperature. We define **the isothermal compressibility** κ as

$$\kappa = -\frac{1}{v}\left(\frac{\partial v}{\partial p}\right)_T,$$

which is a measure of the fractional change in volume when the pressure is increased.

2.2.2 The second law of thermodynamics

Some changes can only go in one direction, e.g. in the absence of some extra energy heat can only flow from a hotter medium to a colder medium. Such processes are irreversible. So we think it is useful to start this subsection by defining so-called reversible and irreversible processes:

- Reversible process: A process in which it is possible to return both the system and surroundings to their original states.
- Irreversible process: A process in which it is impossible to return both the system and surroundings to their original states.

The second law of thermodynamic in terms of the state function the specific entropy s says

The entropy of a an isolated system can only increase by internal processes

$$\Delta s_{tot} = s_{tot,f} - s_{tot,i} \geq 0,$$

where f and i are the final and initial state respectively and s_{tot} is the total entropy of the system and its surrounding. We use the index "rev" to indicate reversible processes.
The second law can be summarized by **Clausius inequality** which is given by

$$ds \geq \frac{dq_{rev}}{T}.$$

The equality

$$ds = \frac{dq_{rev}}{T},$$

only holds for reversible processes and may be used to define the entropy for these processes. Further details can be found in Atkins [11], Müller and Müller [56] as well as Thein [73].

2.2.3 The fundamental equation

We have seen that the first law of thermodynamics may be written as

$$de = dq + dw.$$

We may set $dw_{rev} = -pdv$ and $dq_{rev} = Tdv$, where p is the pressure of the system, and T is the temperature. Therefore, for a reversible change in a closed system

$$de = Tds - pdv, \tag{2.2}$$

which combines the first and the second laws of thermodynamics. This relation is called the fundamental equation.
We could regard e as a function of the other variables, such as p and T because they are all interrelated, but the simplicity of the fundamental equation (2.2) suggests

that $e(s, v)$ is the best choice. We can express an infinitesimal change de in terms of changes ds and dv by

$$de = \left(\frac{\partial e}{\partial s}\right)_v ds + \left(\frac{\partial e}{\partial v}\right)_s dv.$$

When this expression is compared to the equation (2.2) we see that,

$$\left(\frac{\partial e}{\partial s}\right)_v = T, \qquad \left(\frac{\partial e}{\partial v}\right)_s = -p.$$

2.3 Thermodynamic potentials

2.3.1 The Helmholtz and Gibbs energies

We can develop the Clausius inequality

$$ds - \frac{dq}{T} \geq 0, \tag{2.3}$$

in two ways according to the conditions of constant volume or constant pressure under which the process occurs. First, we consider at constant volume. Then we can write

$$dq_V = de,$$

which means

$$ds - \frac{de}{T} \geq 0,$$

or

$$Tds \geq de. \tag{2.4}$$

Now, when energy is transferred as heat at constant pressure then by (2.1)

$$dq_p = dh.$$

From (2.3) it follows that

$$Tds \geq dh. \tag{2.5}$$

Because of (2.4) and (2.5) we have the inequalities

$$de - Tds \leq 0 \quad \text{and} \quad dh - Tds \leq 0.$$

These inequalities can be expressed more simply by introducing two more thermodynamics quantities. The first one is **the specific Helmholz energy** ψ which is defined as

$$\psi = e - Ts,$$

and the other is **the specific Gibbs energy** g where

$$g = h - Ts.$$

When the state of the system changes at constant temperature, the two properties change as follows

$$d\psi = de - Tds,$$
$$dg = dh - Tds,$$

and from (2.4) and (2.5) we obtain

$$d\psi_{T,V} \leq 0,$$
$$dg_{T,p} \leq 0.$$

Properties of the Gibbs energy

In order to discuss phase transitions and chemical reactions, we need expressions showing how g varies with the pressure and temperature, and as we have seen before

$$g = h - Ts.$$

This can be written for infinitesimal changes as

$$dg = dh - d(Ts) = dh - Tds - sdT.$$

And because $h = e + pv$, we know that

$$dh = de + d(pv) = de + pdv + vdp,$$

and therefore

$$dg = de + pdv + vdp - Tds - sdT.$$

For a reversible changes of a closed system using (2.2) we obtain

$$dg = vdp - sdT.$$

This gives

$$\left(\frac{\partial g}{\partial T}\right)_p = -s, \qquad \left(\frac{\partial g}{\partial p}\right)_T = v. \tag{2.6}$$

Because the equilibrium composition of a system depends on the Gibbs energy, we need to know how g varies with temperature, and the last relation is a good starting point for this, as we can express it in terms of the enthalpy h by using the definition of g we write

$$s = \frac{h - g}{T},$$

then

$$\left(\frac{\partial g}{\partial T}\right)_p = \frac{g - h}{T},$$

which gives the expression

$$\left(\frac{\partial}{\partial T}\frac{g}{T}\right)_p = \frac{-h}{T^2},$$

which is called **the Gibbs-Helmholtz equation.**

2.3.2 The chemical potential

The chemical potential μ is a measure of the potential that a substance has for undergoing physical or chemical change in a system. For a single component system the molar Gibbs energy g_m and the chemical potential μ are synonyms so $g_m = \mu$. It follows from (2.6) that

$$\left(\frac{\partial \mu}{\partial T}\right)_p = -s, \qquad \left(\frac{\partial \mu}{\partial p}\right)_T = v.$$

2.4 Equation of state

The physical state of a sample of a substance is defined by its physical properties. Two samples of a substance that have the same physical properties are in the same state. The state of a pure gas, for example, is specified by giving its mass density ρ, pressure p, and temperature T.
It has been established experimentally that it is sufficient to specify only two of these variables, then the third variable is determined via an equation of state i.e. an equation that interrelates these three variables.
Equations of state are useful in describing the properties of fluids, mixtures of fluids, solids and even the interior of stars. The general form of an equation of state is

$$p = f(T, \rho).$$

This equation tells us that, if we know the values of T and ρ for a particular substance then the pressure has a determined value. One of the simplest equations of state is the ideal gas law,

$$p = \frac{nRT}{V},$$

where R is a constant and n is the total amount of a substance. This law is roughly accurate for gases at low pressures and moderate temperature. However, this equation becomes inaccurate at higher pressures and lower temperature, and fails to predict condensation from a gas to a liquid. Therefore a number of much more accurate equations of state have been developed for gases and liquids, and next we present some examples:

- The equation suggested by J.D. van der Waals, which is an excellent example of an expression that can be obtained by thinking scientifically about mathematically complicated but physically simple problem. **The van der Waals equation** is

  $$p = \frac{nRT}{V - nb} - a\frac{n}{V}^2,$$

  where a and b are the van der Waals coefficients.

- **Tait's EOS**, which has the form

  $$p = p_{ref} + K_{ref}((\frac{V_{ref}}{V})^{\nu} - 1),$$

  where the subscript ref refers to values at given temperature T_{ref}, and K_{ref} is the modulus of compression. The non-linearity is due to the exponent $\nu \geq 1$ and for linear Tait equation of state $\nu = 1$.

It has to be mentioned, that there is no single equation of state that accurately predicts the properties of all substances under all conditions.

2.5 Thermodynamics of mixtures

A mixture is defined as the result of combining two or more substances like the air can be taken as a mixture of nitrogen and oxygen. We analyze here mixtures

of simple non-reacting chemical substances that form a single phase or multiphase system, such that a chemical reaction does not occur between components of the mixture.
Let us consider a thermodynamic property X as a function of the temperature T, the pressure p and the composition given as the amount of the N components $n_1, n_2, ..., n_N$. This implies that when we keep T and p constants

$$dX = \sum_{i=1}^{N} \left(\frac{\partial X}{\partial n_i} \right)_{T,p} dn_i.$$

The quantity X can be found by integration as

$$X = \sum_{i=1}^{N} \left(\frac{\partial X}{\partial n_i} \right)_{T,p} n_i. \tag{2.7}$$

Here we define **the partial molar quantities** X_i as

$$X_i = \sum_{i=1}^{N} \left(\frac{\partial X}{\partial n_i} \right)_{T,p}.$$

That means the quantity X can be calculated as the sum of the contributions of each component, where the individual contribution is the partial molar quantity multiplied by the amount of the component.
Now we want to apply this to the volume and we define the **partial molar volume** v_i of a component i in a mixture. It is the change in volume per mole of substance i added to a large volume of the mixture and it defined as follows

$$v_i = \left(\frac{\partial v_0}{\partial n_i} \right)_{p,T}.$$

From this relation we can derive that

$$v = \sum_{i=1}^{N} v_i n_i.$$

For a substance in a mixture the chemical potential μ_i is defined as the partial molar Gibbs energy

$$\mu_i = \left(\frac{\partial g}{\partial n_i} \right)_{p,T}.$$

By applying the same argument that led to (2.7) we obtain

$$g = \sum_{i=1}^{N} \mu_i n_i.$$

The equation

$$dg = vdp - sdT,$$

then becomes

$$dg = vdp - sdT + \sum_{i=1}^{N} \mu_i n_i.$$

This expression is called **the fundamental equation of chemical thermodynamics.** It follows that at constant volume and entropy

$$\mu_i = \sum_{i=1}^{N} \left(\frac{\partial e}{\partial n_i} \right)_{s,v},$$

therefore, the chemical potential shows how g and e change when the composition changes. In the same way we can find

$$\mu_i = \sum_{i=1}^{N} \left(\frac{\partial h}{\partial n_i} \right)_{s,p}, \qquad \mu_i = \sum_{i=1}^{N} \left(\frac{\partial \psi}{\partial n_i} \right)_{v,T}. \tag{2.8}$$

2.5.1 Equation of state of the mixture

Let N be the number of the constituents, ρ_i the **partial densities**, then the mixture density ρ is given by

$$\rho = \sum_{i=1}^{N} \rho_i.$$

In order to obtain an equation of state usually it is required to to relate the partial pressure p_i and the thermal energy ρe to the partial densities ρ_i and the mixture temperature T.
As we have seen before the specific Helmholz free energy is given as

$$\psi = e - Ts.$$

It follows that

$$\mu_i = \frac{\partial \rho \psi}{\partial \rho_i} \quad \text{and} \quad e = -T^2 \frac{\partial}{\partial T} \left(\frac{\psi}{T} \right).$$

The representation of the pressure

$$p = -\rho\psi + \sum_{i=1}^{N} \rho_i \mu_i, \tag{2.9}$$

is a consequences of the second law and is called the Gibbs-Duhem equation. For further details concerning these relations see Bothe and Dreyer [15], Hantke and Müller [33] as well as Dreyer et. al. [24].

2.5.2 Simple mixtures

The mixture momentum ρv is given by

$$\rho v = \sum_{i=1}^{N} \rho_i v_i.$$

Now we want to apply the previous results to a simple mixture. By simple mixture we mean a mixture of N components where the **partial pressures** and the **partial specific energies** have the form

$$p_i = p_i(T, \rho_i) \quad \text{and} \quad e_i = e(T, \rho_i).$$

Let $\psi_i = \psi_i(T, \rho_i)$ be the **partial** Helmholz free energy. In this case the further partial quantities are given as

$$e_i = -T^2 \frac{\partial}{\partial T}\left(\frac{\psi_i}{T}\right), \tag{2.10}$$

$$\mu_i = \frac{\partial \rho \psi_i}{\partial \rho_i}, \tag{2.11}$$

$$p_i = -\rho_i \psi_i + \rho_i \mu_i, \tag{2.12}$$

see Hantke and Müller [33].

2.5.3 The stiffened gas equation of state

Due to its simplicity and suitability for fluid mechanical applications, many authors consider the stiffened gas equation of state a useful basis for simulating multicomponent flow problems, especially, when considering water under very high pressures, i.e. typical applications are underwater explosions.
Let ρ_i be the partial densities, the parameters: γ_i, π_i, c_{vi} and q_i be the ratio of the specific heats, the minimal pressure, the specific heat capacity at constant volume and the heat of formation of component i respectively. Let the free energy density ψ_i be defined as

$$\psi_i(\rho, T) = -c_{vi} T \ln \frac{T}{T_{ref}} + q_i(1 - \frac{T}{T_{ref}}) + \frac{\pi_i}{\rho_i} + (\gamma_i - 1) c_{vi} T \ln \frac{\rho_i}{\rho_{i,ref}} + \frac{\pi_i}{\rho_i}\frac{T}{T_{ref}}. \tag{2.13}$$

Here T_{ref} and ρ_{ref} are the reference temperature and reference density respectively. The definition (2.13) was taken from Hantke and Müller [33].
To derive an appropriate internal energy law for e_i, we apply $e_i = -T^2 \frac{\partial}{\partial T}(\frac{\psi_i}{T})$ from (2.10), which gives

$$e_i = c_{vi} T + q_i + \frac{\pi_i}{\rho_i}. \tag{2.14}$$

The chemical potential is determined by applying $\mu_i = \frac{\partial \rho \psi_i}{\partial \rho_i}$ from (2.11), which gives

$$\mu_i = -c_{vi} T \ln \frac{T}{T_{ref}} + q_i(1 - \frac{T}{T_{ref}}) + (\gamma_i - 1) c_{vi} T \ln \frac{\rho_i}{\rho_{i,ref}} + (\gamma_i - 1) c_{vi} T - \pi_i \frac{T}{T_{ref}} . \frac{1}{\rho_{i,ref}}. \tag{2.15}$$

By using (2.12) with the free energy density (2.13) and the chemical potential (2.15) we obtain

$$p_i = -\pi_i + \rho_i(\gamma_i - 1) c_{vi} T; \quad \pi_i \geq 0, \tag{2.16}$$

which is the stiffend gas equation of state in terms of pressure.

Speed of sound

The speed of the sound a_i is defined by the slope of the isentropes in the pressure-density plane as

$$a_i^2 = \left(\frac{\partial p_i}{\partial \rho_i}\right) = (\gamma_i - 1) c_{vi} T. \tag{2.17}$$

Using this equation with (2.16) and $d_i = -\pi_i$ leads to the equation of state

$$p_i = a_i^2 \rho_i + d_i, \tag{2.18}$$

which will play an important role later on in order to supply the model with an equation of state.

Chapter 3

The model

3.1 Introduction

In 2014 Dreyer, Giesselmann and Kraus [24] proposed a new diffuse interface model to describe chemically reacting fluid mixtures consisting of N components where phase transition between a liquid and a vapor may occur. The isothermal evolution was exclusively considered. This model is a type of phase field model. This chapter is devoted to introducing this model in detail.
To describe the phase transition, an artificial phase field indicator was introduced. It indicates the present phase by assigning values to the liquid and the vapor phase. Within the transition layer between the phases the phase field indicator changes smoothly between the two values. In our case the indicator has the value -1 in the vapor phase and the value 1 in the liquid phase. The phase field value between the two phases will be in the interval $]-1,1[$.
As the conservation of mass and momentum play a central role in this model we want to start this chapter by presenting one of the most important properties in nature which are the conservation laws. A general introduction to conservation laws was presented in the book by Evans [26]. Also we refer the reader to the book by Warnecke [81] and by Dafermos [22].
Then we will present a diffuse interface multiphase mixture model in detail and we supply this model with an equation of state before discussing the exact and the numerical solution in the next chapters. Interesting discussions can be found in the work of Blesgen [14], Kotschote [41], Saurel et al. [62] and Feireisl et al. [25].

3.2 Conservation laws

Let u be a quantity of interest such as the density of mass, the temperature of a rod or a concentration in a chemical cell. In physics, we know that properties of an isolated physical system do not change as the system evolves over time which means that these quantities are conserved in certain classes of physical processes. We call this principle a conservation law which is one of the most important results in the history of science. It has many applications in nature and all branches of science.
For the time $t \in [0, t_{max}) \subseteq R_{\geq 0}$ we consider that the quantity $u(t,x)$ defined for all the points x of the domain $\Omega \subset \mathbb{R}^d$ where $d = 1, 2, 3$. The unknown quantity u is called the conservative variable. According to the idea of conservation law the change in the quantity u in time in a fixed volume is equal to the total amount of u

and the flux of u across the boundary of the volume. This means that the change in the quantity u comes only from the information entering or leaving the domain of interest, i.e. the change in u comes only from the fluxes f. The flux represents the amount of u which goes in or comes out of the domain. This observation can be summarized by the following partial differential equation

$$u_t + f(u)_x = 0, \tag{3.1}$$

which is called a conservation law.
An extension of this idea is the consideration of additional source terms s which add or subtract a certain amount of u. In this case there are two factors affecting the change of u the first one is the flux f and the second one is the source s. Then the equation will have the form

$$u_t + f(u)_x = s.$$

This equation is often called the balance law due to the fact that the rate of change in u is balanced by the flux and source.

3.3 The derivation of the conservation laws

The basic idea of the conservation laws says that some features of the matter remain constant in the region of space occupied by the same particles for all time t. This region is called the material volume V. Many features are conservative but in this section we restrict ourselves to the classical quantities which are the mass, the momentum and the energy.
The first conservation law is the conservation of mass which means that the mass of a material volume cannot be changed. In other words no mass is generated or annihilated within V. Suppose that A is the surface of V. This means that no mass flow across the surface A.
Another important conservation law is the conservation of momentum which is based on Newton's second law. This law states that the momentum of a material volume V is equal to the force applied to it.
The last conservation law is the conservation of energy which says that energy can be neither created nor destroyed. This law results from the first law in thermodynamics.
Next in this section we will present only the derivation of the conservation laws of mass and momentum because the conservation law of the energy is not considered in the model in which we are interested.
First we want to remind the reader of the Reynolds transport theorem which states that assume that $\mathbf{v}(x,t)$ is the velocity vector of fluid motion and let V be an arbitrary material volume then

$$\frac{\partial}{\partial t}\int_V \phi(x,t)\ dV = \frac{\partial}{\partial t}\int_{V_0} \phi(x,t)\ dV_0 + \int_A \phi(x,t)\,\mathbf{v}\cdot\mathbf{n}\ dS = 0. \tag{3.2}$$

Here ϕ is the quantity of the fluid motion, V_0 is a fixed control volume of the surface A, $\mathbf{n}$ is the unit outward normal and dV, dV_0 are the volume elements of V and V_0 respectively.

3.3.1 Conservation of mass

As we have seen before the mass of a material is a conserved quantity which means that the mass can not be changed. We assume that ρ is the density of the material in V. This means that the mass can be given as

$$M(t) = \int_V \rho(x,t)\ dV.$$

As we assumed that the mass is conservative this means that the rate of change of the mass is zero

$$\frac{d}{dt}M(t) = \frac{d}{dt}\int_V \rho(x,t)\ dV = 0.$$

Now we apply Reynolds transport theorem (3.2). We obtain

$$\frac{\partial}{\partial t}\int_{V_0} \rho(x,t)\ dV_0 + \int_A \rho(x,t)\,\mathbf{v}\cdot\mathbf{n}\ dS = 0.$$

Applying Gauss's divergence theorem and taking into account that V_0 is independent in time we get

$$\int_{V_0} \frac{\partial \rho}{\partial t} + \operatorname{div}(\rho v)\ dV_0 = 0.$$

Since this holds for any volume V_0, we obtain

$$\frac{\partial \rho}{\partial t} + \operatorname{div}(\rho v) = 0, \tag{3.3}$$

which is the differential form of the mass conservation law.

3.3.2 Conservation of momentum

The conservation law of the momentum results from the direct application of Newton's second law of motion. One has to notice that the total force $F(t)$ consists of two forces the volume force F_V and the surface force F_s which are given by

$$F_V(t) = \int_V \rho f_V\ dV, \qquad F_s(t) = \int_A \mathbf{n}\cdot\sigma\ dA,$$

where f_V is the specific volume force per unit mass and σ is the stress tensor which is given as

$$\sigma = -p\mathrm{I} + \Pi,$$

where p is the pressure of the fluid, I is the unit matrix and Π is the viscous stress tensor see Toro [75]. Now we consider Newton's second law which states that

$$\frac{\partial}{\partial t}\int_V (\rho\mathbf{v})\ dV = F(t)$$

As we have done in the previous subsection we apply again Reynolds transport theorem we get

$$\frac{\partial}{\partial t}\int_{V_0} \rho\mathbf{v}\ dV + \int_A (\rho\mathbf{v}\otimes\mathbf{v} + p\mathrm{I} - \Pi)\cdot\mathbf{n}\ dS = \int_{V_0} \rho f_V\ dV.$$

By applying Gauss's divergence theorem we obtain

$$\int_{V_0} \frac{\partial \rho \mathbf{v}}{\partial t} + \operatorname{div}[\rho \mathbf{v} \otimes \mathbf{v} + p\mathrm{I} - \Pi] \; dV = \int_{V_0} \rho f_V \; dV.$$

As this valid for any arbitrary volume V_0 we obtain

$$\frac{\partial \rho \mathbf{v}}{\partial t} + \operatorname{div}[\rho \mathbf{v} \otimes \mathbf{v} + p\mathrm{I} - \Pi] = \rho f_V,$$

which is the differential form of the momentum equation including a source term due to volume forces. One can neglect the volume forces f_V and set the viscous stresses Π to be zero in order to obtain

$$\frac{\partial \rho \mathbf{v}}{\partial t} + \operatorname{div}[\rho \mathbf{v} \otimes \mathbf{v} + p\mathrm{I}] = 0. \tag{3.4}$$

3.4 A diffuse interface multi-phase mixture model

A diffuse interface multi-phase mixture model, with chemical reactions, was proposed by Dreyer, Giesselmann and Kraus [24] in order to describe the phases in the diffuse interface setting. They proposed a model for chemically reacting viscous fluid mixtures that may develop a transition between a liquid and a vapor where the interface between adjacent liquid and vapor phases is modeled by a thin layer. The thermodynamic quantities change smoothly within the layer in one phase to different values in the other phase. This model belongs to the class of diffuse interface models which solve the partial differential equations in the transition region while the sharp interface models deal with jump conditions across the interface between the phases.
In this study we consider that the mixture consists of N constituents and occupies a region $\Omega \subseteq \mathbb{R}^m$. At any time $t \geq 0$, the phsical state of Ω is described by N partial mass densities ρ_i, the velocity v and the pressure p. These quantities may be functions of time $t \geq 0$ and space $x \in \Omega$.
In this work we exclusively consider isothermal evolutions. This means that the temperature T is fixed to be constant.

3.4.1 The basic quantities

We consider multi-component liquid (L) and/or vapor (V) mixtures of N constituents A_1, A_2, ..., A_N where the constituents A_i for $i = 1, ..., N$ of a fluid mixture allow chemical reactions. This means that we have N_R reactions of the type

$$a_1^j A_1 + a_2^j A_2 + ... + a_N^j A_N \rightleftharpoons b_1^j A_1 + b_2^j A_2 + ... + b_N^j A_N,$$

where the constant stoichiometric coefficients a_i^j and b_i^j are positive integers for $j = 1, ..., N_R$. We define their differences as

$$\nu_i^j = b_i^j - a_i^j.$$

In order to explain the stoichiometric coefficients we present the following example

Example 1 *In this example we consider a mixture of liquid water* $A_1 = (H_2O)_{liquid}$ *and water vapor* $A_2 = (H_2O)_{vapor}$.

$$(H_2O)_{vapor} \rightleftharpoons (H_2O)_{liquid}.$$

In this case we have a mixture that consists of two components $i = 1, 2$. *One can notice that the stoichiometric coefficient sare*

$$a_1 = 0, \quad a_2 = 1, \quad b_1 = 1, \quad b_2 = 0,$$

this means that ν *is*

$$\nu_1 = -1, \quad \nu_2 = 1.$$

The stoichiometric coefficients play an important role in the treatment of two phase flow with chemeical reactions as we shall see in Chapter 7.
Now we consider as basic variables the partial mass densities ρ_i where $i = 1, ..., N$ the number of the constituents N, the partial velocities $\mathbf{v}_i$ and the temperature T. The partial mass densities and the partial velocities are used to define the total mass density ρ and the velocity $\mathbf{v}$ as

$$\rho = \sum_{i=1}^{N} \rho_i, \qquad \mathbf{v} = \frac{1}{\rho} \sum_{i=1}^{N} \rho_i \mathbf{v}_i.$$

To describe phase transitions we introduce a phase field variable χ indicating the present phase at (t, x). We introduce χ to distinguish between the two possible phases. It assumes values in the interval [-1,1] where the values 1 and -1 indicate the liquid and vapor phase respectively and within the transition layer between the phases it changes between -1 and 1.

3.4.2 The constitutive laws

There are further quantities which are given by constitutive equations such as

- The stress σ which models the volume changes, viscosity and capillarity. This is discussed in details in [24]. We will mention it in the model but not use it later.

- Chemical potentials and the pressure which are given by (2.11) and (2.12) as

$$\mu_i = \frac{\partial \rho\psi}{\partial \rho_i}, \qquad p = -\rho\psi + \sum_{i=1}^{N} \mu_i \rho i, \qquad i = 1, ..., N.$$

  Here $\rho\psi$ is the free energy density. The chemical potentials, the pressure and the free energy density were presented in detail in Chapter 2.

- The Reaction rates R_b^j and R_f^j given by

$$R_b^j = R_f^j \exp(\frac{A^j}{kT}), \qquad j = 1, ..., N_R,$$

  where k is Boltzman constant and the chemical affinities A^j defined by

$$A^j = \sum_{i=1}^{N} m_i \nu_i^j \mu_i,$$

  where m_i the atomic mass of constituent i, see Dreyer et al. [24].

- The chemical reaction term which is given as

$$r_i = \sum_{j=1}^{N_R} m_i \nu_i^j (R_f^j - R_b^j).$$

3.4.3 The model

After introducing the main variables we now present the diffused interface model of Dreyer et al. [24] which is given by the system of the partial differential equation

$$\begin{aligned} \tfrac{\partial}{\partial t}\rho + \operatorname{div}(\rho v) &= 0, \\ \tfrac{\partial}{\partial t}\rho_i + \operatorname{div}(\rho_i v) - \operatorname{div}(\textstyle\sum_{\beta=1}^{N-1} M_{i\beta}\nabla(\mu_i - \mu_N)) &= \textstyle\sum_{j=1}^{N_R} \nu_i^j m_i M_r^j (1 - \exp(\frac{A^j}{kT})), \\ \tfrac{\partial}{\partial t}(\rho v) + \operatorname{div}(\rho v \otimes v) + \nabla p + \operatorname{div}(\gamma \nabla\chi \otimes \nabla\chi - \sigma_{NS}) &= 0, \\ \rho \tfrac{\partial}{\partial t}\chi + \rho \mathbf{v} \cdot \nabla\chi &= -M_p(\tfrac{\partial \rho\psi}{\partial \chi} - \gamma\Delta\chi). \end{aligned} \tag{3.5}$$

Here M_r^j and M_p are the mobilities. The reaction mobility have been chosen as constant $M_r^j > 0$.
To solve such systems numerically we use splitting methods. This means that the system is split into two subproblems. The first one is the flow part of the system and the other one is the reacting part by integrating the source term. In this work we will focus on the flow part and we will restrict ourselves to the $1-d$ homogeneous subsystem of first order terms. In the last chapter we will discuss the system with source term.

3.5 The equation of state

The main goal of this section is to present an equation of state in order to close the model (3.5). The pressure p is a constitutive quantity that is related to the phase field variable χ and the partial densities $\rho_i, i = 1, ..., N$ of the components by an equation of state $p = p(\chi, \rho_1, ..., \rho_N)$ which is proposed in [24]. This equation of state has the form

$$p(\chi, \rho_1, ..., \rho_N) = -W(\chi) + h(\chi)p_L(\chi, \rho_1, ..., \rho_N) + (1 - h(\chi))p_V(\chi, \rho_1, ..., \rho_N), \tag{3.6}$$

where

$$p_L = \sum_{i=1}^{N} p_{Li} \qquad \text{and} \qquad p_V = \sum_{i=1}^{N} p_{Vi},$$

are the equation of state in terms of pressure of the liquid and vapor phases respectively. Further the double well potential function $W(\chi) = w_0(\chi - 1)^2(\chi + 1)^2$ is considered and it has its minima in the pure phases and controls the phase transition. The function h is the interpolation function which relates the phases given below.

3.5.1 Relate the phases

In order to relate the phases we consider two phases: a liquid where the phase field variable χ will take the value 1 and vapor where $\chi = -1$. Our aim now is to define a function h which relates the two phases. We consider that this function has the value 1 in the liquid and the value zero in the vapor. In order to relate the two phases considered we will use the function $h : \mathbb{R} \to [0, 1]$ to be the interpolation function satisfying

$$h(\chi) = \begin{cases} 1 & \chi \geq 1 \\ (-\frac{1}{4}\chi + \frac{1}{2})(\chi + 1)^2 & -1 < \chi < 1 \\ 0 & \chi \leq -1. \end{cases}$$

and having the following properties

$$h(1) = 1, \quad h(-1) = 0 \quad \textit{and} \quad h'(1) = h'(-1) = 0.$$

Further the double well function $W(\chi) = w_0(\chi - 1)^2(\chi + 1)^2$ is considered and it has its minima in the pure phases and controls the phase transition.

3.5.2 The equation of state of the mixtures

We consider two phases a Liquid L and a vapor V. Each phase has N constituents. As each phase has to be governed by its own equation of state. We consider now that the equation of state in the pure phases is the stiffened gas equation. This equation of state was discussed in Chapter 2. It is given by (2.18) as

$$p_{ki} = a_{ki}^2 \rho_{ki} + d_{ki}, \qquad i = 1, ..., N, \tag{3.7}$$

where a_k are the isothermal sound speed. The parameters d_L, d_V are given constants which equal to zero for ideal gases. Using (3.6) we obtain

$$p(\chi, \rho_1, ..., \rho_N) = -W(\chi) + \sum_{i=1}^{N} [h(\chi)(a_{Li}^2 \rho + d_{Li}) + (1 - h(\chi))(a_{Vi}^2 \rho + d_{Vi})], \tag{3.8}$$

which is the equation of state of the mixture in terms of the pressure. For more details see Dreyer and Bothe [15] as well as Hantke and Müller [33].

Sound speed of the mixture

The sound speed of the mixture is given as

$$A^2 = (\frac{\partial p(\chi, \rho)}{\partial \rho_i}) = \sum_{i=1}^{N} [h(\chi) a_{Li}^2 + (1 - h(\chi)) a_{Vi}^2].$$

3.6 The homogeneous form

After neglecting the second order diffusion terms and chemical reactions the model consists of N + 2 equations and can be written in the simplified form as following

$$\begin{aligned} \tfrac{\partial}{\partial t}\rho + \tfrac{\partial}{\partial x}(\rho v) &= 0, \\ \tfrac{\partial}{\partial t}\rho_1 + \tfrac{\partial}{\partial x}(\rho_1 v) &= 0, \\ &\vdots \\ \tfrac{\partial}{\partial t}\rho_{N-1} + \tfrac{\partial}{\partial x}\left(\rho_{N-1} v\right) &= 0, \\ \tfrac{\partial}{\partial t}(\rho v) + \tfrac{\partial}{\partial x}(\rho v^2 + p) &= 0, \\ \rho\tfrac{\partial}{\partial t}\chi + \rho v\tfrac{\partial}{\partial x}\chi &= 0, \end{aligned} \tag{3.9}$$

where

- The equation $\rho\frac{\partial}{\partial t}\chi + \rho v\frac{\partial}{\partial x}\chi = 0$ is the transport equation for the phase field variable χ.
- The equations $\frac{\partial}{\partial t}\rho_i + \frac{\partial}{\partial x}(\rho_i v) = 0$, $i = 1, ..., \mathrm{N}-1$ are N-1 continuity equations for the partial mass densities ρ_1, ρ_2,..., ρ_{N-1}.
- The equation $\frac{\partial}{\partial t}\rho + \frac{\partial}{\partial x}(\rho v) = 0$ is the continuity equation for the total mass density $\rho = \sum_{i=1}^{N}\rho_i$. This equation can be replaced by the transport equation for the density of the N^{th} constituent.
- The equation $\frac{\partial}{\partial t}(\rho v) + \frac{\partial}{\partial x}(\rho v^2 + p) = 0$ is the total momentum balance equation involving the total pressure p.

The pressure p is not among the basic variables and it is therefore called a constitutive quantity which is related to the variables χ and ρ by an equation of state $p = p(\chi, \rho)$ which is given in (3.8).
In order to write the system in the conservative form we can replace the transport equation of the phase field variable by the conservative form

$$\frac{\partial}{\partial t}(\rho\chi) + \frac{\partial}{\partial x}(\rho v\chi) = 0.$$

One can clearly see using the continuity equation for total mass density that the both forms are equivalent, i.e. have the same smooth solutions. For discontinues solutions see the discussions in Chapter 4.
One should mention that writing the transport equation of the phase field variable in the conservative form has no physical meaning because physically the phase field variable is not conservative. It can lead to some difficulties but writing the system in the conservative form provides us good way to deal with the model in the context of conservative form. This benefits the methods and solvers considered.

3.7 The case of pure phases N=1

In this section and the rest of our work we will consider two pure phases $N = 1$. In this case the model has the form

$$\begin{aligned} \frac{\partial}{\partial t}\rho + \frac{\partial}{\partial x}(\rho v) &= 0, \\ \frac{\partial}{\partial t}(\rho v) + \frac{\partial}{\partial x}(\rho v^2 + p) &= 0, \\ \rho\frac{\partial}{\partial t}\chi + \rho v\frac{\partial}{\partial x}\chi &= 0, \end{aligned} \tag{3.10}$$

supplied with the equation of state of the form

$$p(\chi, \rho) = -W(\chi) + h(\chi)(a_L^2\rho + d_L) + (1 - h(\chi))(a_V^2\rho + d_V). \tag{3.11}$$

The system can be written in the conservative form

$$\frac{\partial \mathbf{u}}{\partial t} + \frac{\partial}{\partial x}\mathbf{f}(\mathbf{u}) = 0, \tag{3.12}$$

where $\mathbf{u}$ is the vector of the conservative variables and $\mathbf{f}$ is the fluxes vector

$$\mathbf{u} = \begin{pmatrix} \rho \\ \rho v \\ \rho\chi \end{pmatrix}, \qquad \mathbf{f} = \begin{pmatrix} \rho v \\ \rho v^2 + p \\ \rho\chi v \end{pmatrix},$$

Our aim in the following chapters is to find the analytical and numerical solution of this submodel.

Chapter 4

Analytical structure and some exact solutions

4.1 Introduction

In the previous chapter we presented the diffuse interface multiphase mixture model. We have seen that the homogeneous form of this model is a system of conservation laws. One of the main targets of this work is to study this system analytically and obtain the exact solutions for the Riemann initial value problem. Of course we expect some difficulties especially in the discussions of the case $N > 1$ where the mixture consists of N components in each phase. This is actually the exciting part. Due to the main role of the hyperbolic conservation laws we want to start this chapter by giving a brief introduction to the hyperbolic conservation laws. For general background we recommend the books by Toro [75] and LeVeque [47]. Further details can be found in the books of Evans [26], LeFloch [44], Smoller [69], as well as Godlewski and Raviart [31]. Further interesting references in the field of hyperbolic problems Caraso [59], Hoermander [38] as well as Tveito and Winther [78].
In the first part of this chapter we start by reminding the reader of the scalar conservation laws and their properties such as the characteristics, the weak solutions and the Rankine-Hugoniot condition. As an example we consider the advection equation and the Burgers equation.
Presenting some basic concepts on hyperbolic systems of conservation laws is very essential. A summary is given in Section 4.3.
In Section 4.4 we consider the diffuse interface model for the case $N = 1$. We study the analytical structure of the model and we construct the exact solutions to the Riemann problem. The main challenge was to extend this study to the case $N > 1$. One of the main results of this work is to present an analytical study of the case $N > 1$ and obtain the exact solution, see section 4.5.
In Section 4.6 we test the exact solution for the cases $N = 1$ and $N > 1$ into some numerical examples.

4.2 The scalar conservation laws

The partial differential equation

$$\frac{\partial}{\partial t}u(x,t) + \frac{\partial}{\partial x}f(u(x,t)) = 0, \tag{4.1}$$

where $u : \mathbb{R} \to \mathbb{R}$, is said to be a scalar equation. We classify the scalar conservation laws into linear and nonlinear equation. The scalar conservation law is linear if the flux f is a linear function of u. As an example we consider the advection equation. For the nonlinear case we will present the Burgers equation.

4.2.1 The advection equation

The simplest conservation law is the linear advection equation of the form

$$u_t + au_x = 0,$$

where a is constant and represents the wave propagation speed.
The solution of the advection equation is obtained using the method of characteristics. We define the characteristic as the curve $x(t)$ in the $x-t$ plane where the PDE can be reduced to an ODE. Thus we can obtain the unknown function $u(t, x(t))$.
Along the characteristic curves where u is constant we can set

$$\frac{du}{dt} = \frac{\partial u}{\partial t} + \frac{\partial u}{\partial x}\frac{dx}{dt} = 0. \tag{4.2}$$

Comparing the coefficients gives

$$\frac{dx}{dt} = a,$$

which means that the characteristics are straight lines with the characteristic speed a which is the slope of the line in the $x - t$ plane.
Now we supply the advection equation with the initial data $u(x, 0) = u_0(x)$. The corresponding characteristic to the point $x(0) = x_0$ is given as

$$x = x_0 + at.$$

As x_0 represents the values of the x-axis we get a family of characteristics all of them are parallel.
One can observe that the solution of the advection equation means that the profile of the initial data is shifted without any changes with speed a to the right if $a > 0$ or to the left if $a < 0$. The solution is given as

$$u(x, t) = u_0(x - at),$$

for $t > 0$.

4.2.2 Burgers equation

If the flux function f is a nonlinear function then we call the partial differential equation (4.1) nonlinear. The most famous example is Burgers equation where the flux is $f(u) = \frac{1}{2}u^2$. In this case the equation has the form

$$u_t + \left(\frac{1}{2}u^2\right)_x = 0.$$

In the Burgers equation one notices that $a = a(u) = u$. We consider two initial value problems

$$u(x, 0) = \begin{cases} u_- = 3 & if \quad x < 0, \\ u_+ = 1 & if \quad x > 0, \end{cases} \tag{4.3}$$

and

$$u(x,0) = \begin{cases} u_- = 1 & if \quad x < 0, \\ u_+ = 3 & if \quad x > 0, \end{cases} \tag{4.4}$$

where $-$ and $+$ denote the left hand side and the right hand side respectively. The solution as explained before is given as

$$\frac{du}{dt} = u_t + uu_x = 0, \tag{4.5}$$

with

$$\frac{dx}{dt} = u \qquad x(0) = x_0. \tag{4.6}$$

The characteristics in this case are also straight lines but with the slope $1/u_0(x_0)$ in the $x-t$ plane i.e. $u_0(x_0)$ in the $t-x$ plane. The solution is given as

$$u(x.t) = u_0(x_0) = u_0(x - u_0(x_0)t), \tag{4.7}$$

which means that the slope of the characteristic lines depends on the initial data. Figure 4.1 illustrates the initial data and the characteristics for the both examples. Here we discuss two cases

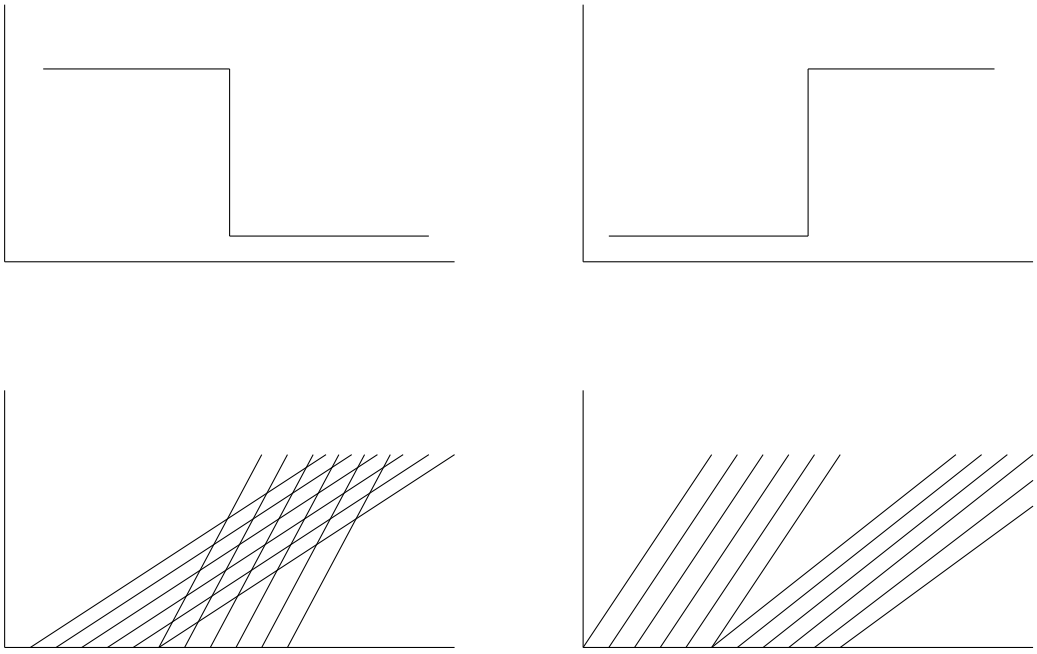

Figure 4.1: Left: The initial data and the characteristics for Example (4.3). Right: The initial data and the characteristics for Example (4.4).

- **Case1**
  In this case the characteristics intersect and a discontinuity arises inevitably. The propagation speed of the discontinuity s fulfills the **jump condition**

$$s = \frac{f_+ - f_-}{u_+ - u_-}, \tag{4.8}$$

which will be disused later in this section. For the Burgers equation we obtain

$$s = \frac{\frac{1}{2}u_+^2 - \frac{1}{2}u_-^2}{u_+ - u_-} = \frac{u_+ + u_-}{2}.$$

The discontinuity is called a **shock** which fulfills the **Lax admissibility condition**

$$u_- > s > u_+.$$

The characteristics go into the shock, see Figure 4.2, and determine its speed by their jump condition (4.8).

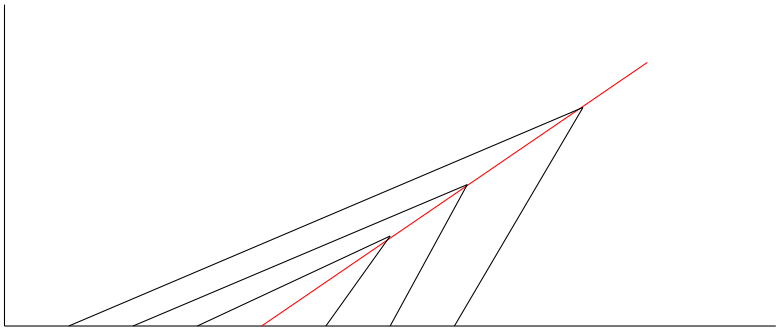

Figure 4.2: The characteristics at the shock.

- **Case2**
  In this case with the initial date $u_- < u_+$ there is a multitude of possible mathematical solutions with admissible and non-admissible discontinuities. But there is one unique continuous solution which is called a **rarefaction**, see Figure 4.3. This solution is unphysical and the characteristics go away from the discontinuity. In this case the entropy condition is not fulfilled.
  The solution for this case can be constructed using intermediate characteristics method. The solution consists of two regions with constant states u_- and u_+. The region between the constant states is the solution which is called the rarefaction wave The solution is given as

$$u(x,t) = \begin{cases} u_- & \frac{x-x_-}{t} \leq u_- \\ \frac{x-x_-}{t} & u_- \leq \frac{x-x_-}{t} \leq u_+ \\ u_+ & \frac{x-x_-}{t} \geq u_+. \end{cases}$$

4.2.3 Characteristics and the weak solution

In this subsection we consider the conservation law

$$u_t + f(u)_x = 0, \tag{4.9}$$

with the initial data

$$u(x,0) = u_0(x).$$

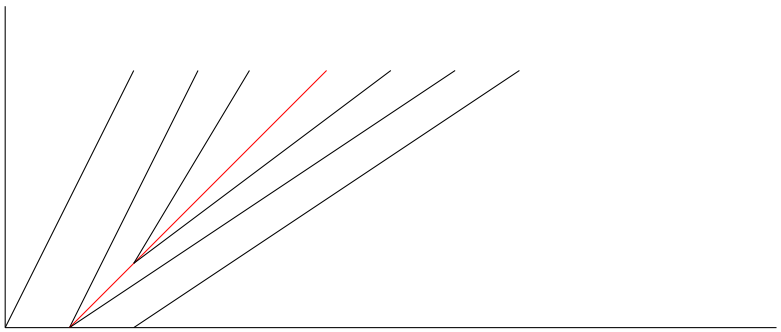

Figure 4.3: The characteristics at the rarefaction, unphysical.

The equation (4.9) can be written in the nonconservative form

$$u_t + a(u)u_x = 0,$$

where

$$a(u) = f'(u).$$

Characteristics or characteristic curves are defined as curves $x = x(t)$ along which the PDE becomes ODE. Let $u = u(x(t), t)$ the solution of the conservation law (4.9). The rate of change of u along $x = x(t)$ is

$$\frac{du}{dt} = \frac{\partial u}{\partial t} + \frac{dx}{dt}\frac{\partial u}{\partial x}.$$

One can notice that if the characteristic curve $x = x(t)$ satisfies

$$\frac{dx}{dt} = a(u),$$

then

$$\frac{du}{dt} = \frac{\partial u}{\partial t} + a(u)\frac{\partial u}{\partial x}.$$

Therefore the rate of changes of u along the characteristic curve $x = x(t)$ is zero which means that the characteristic curves $x = x(t)$ are straight lines along which u is constant.
The speed a is called the characteristic speed. From the initial data one can set that $x(0) = x_0$. The characteristic straight line passing through the point $(x_0, 0)$ is

$$x = x_0 + ta(u_0(x_0)),$$

As the solution remains constant along the characteristics, for the initial data $u(x, 0) = u_0(x)$ then the solution is

$$u(x, t) = u_0(x_0) = u_0(x - at).$$

This solution means that the initial data remains unchanged with the time evolved and it propagates with speed a to the right if $a > 0$ and to the left if $a < 0$.
Now we assume two points x_1 and x_2 and the characteristic curves C_1 and C_2 which are drawn from the points x_1 and x_2 respectively. Let The characteristics C_1 and C_2 have two different slops. In this case the characteristics will intersect at some

point say p.
At this point p the solution should take the same values $u_0(x_1)$ and $u_0(x_2)$ which is impossible. This means that the solution u can not be continuous at the point p.
The solution to this initial value problem may be discontinuous even if $u_0(x)$ is smooth, see Smoller [69] for examples. In this case it will not be possible to determine the differentiation in the conservation law. In order to overcome this situation the idea of a weak solution is considered. The idea of the weak solution is based on multiplying the PDE by a test function say $\phi \in C_0^1(\mathbb{R} \times \mathbb{R})$, where C_0^1 is the space of function that is continuously differentiable with compact support i.e. the test function $\phi(x,t)$ is zero outside of some bounded set. Then integrate one or more times and use the integration of parts to move the derivatives of the function u and onto the smooth test function. This procedure gives an equation with fewer derivatives on u which require less smoothness.
In order to apply this idea to the conservation laws we multiply it by the test function ϕ and integrate. We obtain

$$\int_0^\infty \int_{-\infty}^\infty [\phi u_t + \phi f(u)_x] dx dt = 0.$$

Integrating by parts gives

$$\int_0^\infty \int_{-\infty}^\infty [\phi_t u + \phi_x f(u)] dx dt = -\int_{-\infty}^\infty [\phi(x,0)u(x,0)] dx dt. \tag{4.10}$$

We say that the function $u(x,t)$ is a weak solution of the conservation law if (4.10) holds. For more details about the weak solution see [47].

4.2.4 The Rankine-Hugoniot condition

In this subsection we want to present the Rankine-Hugoniot condition or so called jump condition. This idea is discussed in detail in [47] and [31]. To this end we consider σ to be a surface of discontinuity of u. Let M a point of σ and D a small ball centered at M. We denote by D_+ and D_- the two open components of D on each side of σ. Now we consider ϕ a function in the space of function with compact support. We write

$$0 = \int_D [u \cdot \frac{\partial \phi}{\partial t} + \sum_{i=1}^m f_i(u) \frac{\partial \phi}{\partial x_i}] dx dt = \int_{D_+} + \int_{D_-} .$$

Applying Green's formula in D_+ and D_- and utilizing that u is a solution in D_+ and D_- we obtain

$$\int_{\sigma \cap D} [-n_t(u_+ - u_-) - \sum_{i=1}^m n_{x_i}(f_i(u_+) - f_i(u_-))] \cdot \phi dS = 0,$$

where n is the norm vector to the surface points in the direction of D_+. This means the jump relation along the surface of the discontinuity is

$$(u_+ - u_-)n_t + \sum_{i=1}^m (f_i(u_+) - f_i(u_-))n_{x_i} = 0.$$

We denote by

$$[\![u]\!] = u_+ - u_-,$$

the jump of u across σ and similarly by

$$[\![f_i(u)]\!] = f_i(u_+) - f_i(u_-),$$

the jump of f_i across the discontinuity. Then we can write

$$n_t[\![u]\!] + \sum_{i=1}^{m}[\![f_i(u)]\!] = 0.$$

For the scalar case and smooth σ we can set

$$s[\![u]\!] = [\![f(u)]\!],$$

where s is the speed of propagation of the discontinuity. Discontinuities that satisfy the jump condition are called shocks.

4.3 Notions on hyperbolic systems and conservation laws

Definition 1 ***Conservation laws*** *Let Ω be an open subset of $\mathbb{R}^m$, $\boldsymbol{f}$ be a smooth function from Ω into $\mathbb{R}^m$ and $\boldsymbol{u}$: $\mathbb{R}_{\geq 0} \times \mathbb{R} \to \mathbb{R}^m$ the function of conserved physical states. The general form of systems of conservation laws is*

$$\frac{\partial \boldsymbol{u}}{\partial t} + \frac{\partial \boldsymbol{f}}{\partial x} = 0, \quad x \in \mathbb{R}, \quad t \geq 0, \tag{4.11}$$

where

$$\boldsymbol{u} = \begin{pmatrix} u_1 \\ u_2 \\ \vdots \\ u_m \end{pmatrix}, \quad \boldsymbol{f(u)} = \begin{pmatrix} f_1 \\ f_2 \\ \vdots \\ f_m \end{pmatrix}.$$

Here $\boldsymbol{u}$ is a vector of conserved variables and the function $\boldsymbol{f}$ is a vector of fluxes. One says that the system (4.11) *is written in conservative form.*

The system of one dimensional first order conservation laws (4.11) can be written in the quasilinear form

$$\frac{\partial \mathbf{u}}{\partial t} + \mathbf{A}(\mathbf{u})\frac{\partial \mathbf{u}}{\partial x} = 0 \tag{4.12}$$

where

$$\mathbf{A}(u) = \partial \mathbf{f}/\partial \mathbf{u} = \begin{pmatrix} \partial f_1/\partial u_1 & \dots & \partial f_1/\partial u_m \\ \partial f_2/\partial u_1 & \dots & \partial f_2/\partial u_m \\ \vdots & & \\ \partial f_m/\partial u_1 & \dots & \partial f_m/\partial u_m \end{pmatrix}. \tag{4.13}$$

is the Jacobian matrix of the flux function $\mathbf{f}(\mathbf{u})$. Physically the eigenvalues of the Jacobian matrix represent the speeds of the propagation of information in the solution. We consider that the speed is positive in the direction of positive x and negative

otherwise. We call the eigenvalues $\lambda_i(\mathbf{u})$ for $i = 1, ..., m$ the $i-th$ characteristic speeds which are given by the solution of

$$|\mathbf{A} - \lambda\mathbf{I}| = \mathbf{det}(\mathbf{A} - \lambda\mathbf{I}) = 0.$$

Additionally, we can find a linearly independent right eigenvector $\mathbf{k}_i$ corresponding to an eigenvalue λ_i of the matrix $\mathbf{A}$. The pair $(\lambda_i(\mathbf{u}), \mathbf{k}_i(\mathbf{u}))$ determines the $i-th$ characteristic field of the system (4.11).
The Jacobian matrix and its eigenvalues and eigenvectors play an important role in the study of the analytical structure of the conservation laws as we shall see later on.

Definition 2 ***Hyperbolic systems*** *The system* (4.11) *is called hyperbolic if the Jacobian matrix has m real eigenvalues and m linearly independent corresponding eigenvectors. The system is called strictly hyperbolic if the eigenvalues are distinct, in other words if*

$$\lambda_1 < \lambda_2 < ... < \lambda_m$$

holds.

At time $t = 0$, the system (4.11) with the initial data of the form

$$u(x, 0) = u_0(x), \tag{4.14}$$

is called Cauchy problem or the initial value problem.
One of the difficulties that one may face in the study of the Cauchy problem is that the solution may become discontinuous after some time even if the initial data are smooth. To overcome this situation the weak solution to (4.11) with the initial data (4.14) plays a major role, see the subsection 4.2.3.

Definition 3 ***The Riemann problem*** *The initial value problem* (4.11)-(4.14) *is called Riemann problem if the initial data has the special form*

$$\boldsymbol{u}(x, 0) = \boldsymbol{u}_0(x) = \begin{cases} \boldsymbol{u}_- & if \quad x < 0, \\ \boldsymbol{u}_+ & if \quad x > 0, \end{cases} \tag{4.15}$$

where $\boldsymbol{u}_-$ the left hand side and $\boldsymbol{u}_+$ the right hand side initial date are two constant vectors separated by a discontinuity at x=0. Figure 4.4 illustrates the idea of the Riemann problem.

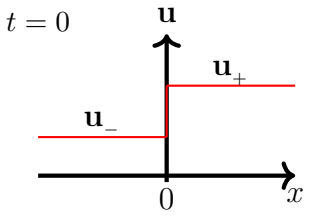

Figure 4.4: The initial data of the Riemann problem.

The Riemann problem plays an important role in the study of hyperbolic conservation laws and it has many applications in science and nature. The solution of the

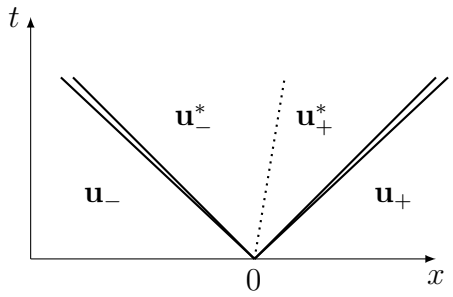

Figure 4.5: The structure of the solution of the Riemann problem.

Riemann problem consists of m waves emanating from the origin. These waves are separated by a discontinuity in the value of the conservative variables $\mathbf{u}$ considered. The solution to the left of the first wave and to the right of the m^{th} wave is given by the initial data $\mathbf{u}_-$ and $\mathbf{u}_+$ respectively. We call the area between the first and the last wave the star region. The main problem is to find the solution in the star region between the first and the last waves. Figure 4.5 illustrate the structure of the solution of the Riemann problem.
In most cases the difference $|\mathbf{u}_- - \mathbf{u}_+|$ plays an essential role in order to find the solution to the Riemann problem, see Andrianov [8]. If the system (4.11) is strictly hyperbolic then the Riemann problem has a solution but only for initial data where the difference $|\mathbf{u}_- - \mathbf{u}_+|$ is small, see Godlewski and Raviart [31]. As an example we consider the flow of two vapors. In this case the difference between the initial data of the conservative variables is small as we shall see in Chapter 5.
For big changes within initial Riemann data, like the flow of vapor and liquid, the corresponding Riemann problem can have no solution, see Keyfitz and Kranzer [40], or at least we can face more difficulties as we shall see in Chapter 6.

Definition 4 ***Linearly degenerate fields*** *A λ_i-characteristic field is said to be linearly degenerate if*

$$\nabla\lambda_i(\boldsymbol{u}) \cdot k_i(\boldsymbol{u}) = 0.$$

Definition 5 ***Genuinely nonlinear fields*** *A λ_i-characteristic field is said to be genuinely nonlinear if*

$$\nabla\lambda_i(\boldsymbol{u}) \cdot k_i(\boldsymbol{u}) \neq 0.$$

Definition 6 ***The generalized Riemann invariants***
Suppose the pair $(\lambda_i(\boldsymbol{u}), k_i(\boldsymbol{u}))$ is the i^{th} characteristic field of the system of hyperbolic conservation laws (4.11)*. Then the i^{th} generalized Riemann invariants are the ordinary differential equation*

$$\frac{du_1}{k_1} = \frac{du_2}{k_2} = ... = \frac{du_m}{k_m},$$

where $\boldsymbol{u} = (u_1, u_2, ..., u_m)^\top$ is the vector of dependent variables which may be conserved or primitive variables and k_i the i^{th}-component of the right eigenvector $k_i(\boldsymbol{u})$ of the i^{th} characteristic field.

The study of the Riemann problem reveals that many kinds of waves occur in the solution. The properties of λ_i-characteristic field provide us with a vision of the nature of the solution. We can distinguish three types of waves that are associated with the genuine nonlinear field and the linearly degenerate field. The waves which are associated to the genuine nonlinear field are the rarefaction waves and the shock waves where the contact discontinuity is the one associated with the linearly degenerated field. One has to mention that the shock and the contact discontinuities satisfy a jump condition. Now we want to present each type of wave and provide the reader a summary of the solution to the Riemann problem. The main references we have used here are the books of Toro [75], Smoller [69] and LeVeque [47] as well as the PhD theses of Matern [51] and Thein [73].

The shock wave

As we have seen previously the characteristics might intersect at some point p. In this case the characteristics form a shock. We understand the shock as a small transition layers of rapid changes in physical quantities such as pressure, density and temperature. The transition layer of a strong shock is very thin so that mathematically this layer can be replaced by discontinuity, for more details see [75].
As we are dealing with the shock as a discontinuity this means that the Rankine-Hugoniot condition

$$[\![\mathbf{f}(\mathbf{u})]\!] = s[\![\mathbf{u}]\!]$$

holds. Here s is the velocity.

The contact discontinuity

The last type of waves is called the contact discontinuity. This type is associated with a linearly degenerated characteristic field. In this case the relation

$$\lambda(\mathbf{u}_-) = \lambda(\mathbf{u}_+) = s,$$

holds. This means that all characteristics are parallel to each other. The Rankine-Hugoniot conditions and the Riemann invariants are fulfilled. The i-th characteristic field speeds are constant across the wave and coincide with the speed of the contact wave.

4.4 The analytical structure and the exact solution of the submodel for the case $N = 1$

In this section we want to study the analytical structure of the diffuse interface multiphase mixture model presented in Chapter 3. We will apply the mathematical tools presented in the previous section and show that the system is a system of hyperbolic conservation laws. We find the eigenvalues and eigenvectors of the Jacobian matrix. Then we analyze the eigenstructure and study the properties of the characteristic fields. We will present the exact solution to the Riemann problem for the case $N = 1$ where we have two pure phases. In this case the homogeneous

form of the diffuse interface model (3.5) is given as

$$\begin{aligned}\chi_t + v\chi_x &= 0,\\ \rho_t + (\rho v)_x &= 0,\\ (\rho v)_t + (\rho v^2 + p)_x &= 0,\end{aligned}$$

with the Riemann initial data

$$(\rho\chi)(x,0) = \begin{cases}(\rho\chi)_- & if \quad x < 0,\\ (\rho\chi)_+ & if \quad x > 0,\end{cases} \quad \rho(x,0) = \begin{cases}\rho_- & if \quad x < 0,\\ \rho_+ & if \quad x > 0,\end{cases} \tag{4.16}$$

$$(\rho v)(x,0) = \begin{cases}(\rho v)_- & if \quad x < 0,\\ (\rho v)_+ & if \quad x > 0.\end{cases}$$

The system is supplied with the equation of state

$$p(\chi,\rho) = -W(\chi) + h(\chi)(a_+^2\rho + d_+) + (1 - h(\chi))(a_-^2\rho + d_-). \tag{4.17}$$

This system also has the conservative form (3.12)

$$\mathbf{u}_t + \mathbf{f}(u)_x = 0,$$

where the conservative variables are $u_1 = \rho\chi$, $u_2 = \rho$, $u_3 = \rho v$.
Now in order to study the eigenstructure of the model we want to compute the Jacobian Matrix $\mathbf{A}(u)$ taking into account that we will need to find p_x. We have $p = p(\chi,\rho)$ which gives

$$\frac{dp}{dx} = \frac{\partial p}{\partial \rho}\frac{\partial \rho}{\partial x} + \frac{\partial p}{\partial \chi}\frac{\partial \chi}{\partial x}.$$

We determine from (4.17)

$$\frac{\partial p}{\partial \rho} = h(\chi)a_+^2 + (1 - h(\chi))a_-^2 = A^2,$$

and

$$\frac{\partial p}{\partial \chi} = -W'(\chi) + p_+h'(\chi) - p_-h'(\chi) = B.$$

This means that

$$\frac{dp}{dx} = A^2\rho_x + B\chi_x,$$

where

$$A^2 = \frac{\partial p}{\partial \rho}, \quad B = \frac{\partial p}{\partial \chi}.$$

In order to find the Jacobian matrix it is easier to write the system in quasi linear form in terms of the primitive variables (χ,ρ,v). The system in quasi linear form is

$$\begin{aligned}\chi_t + v\chi_x &= 0,\\ \rho_t + \rho v_x + v\rho_x &= 0,\\ v_t + vv_x + \frac{A^2}{\rho}\rho_x + \frac{B}{\rho}\chi_x &= 0.\end{aligned}$$

In order to determine the properties of the system, we consider the Jacobian matrix which is

$$\mathbf{A}(u) = \begin{pmatrix} v & 0 & 0 \\ 0 & v & \rho \\ B/\rho & A^2/\rho & v \end{pmatrix}.$$

The eigenvalues of the Jacobian matrix are

$$\lambda_1 = v - A, \quad \lambda_2 = v, \quad \lambda_3 = v + A$$

and the corresponding eigenvectors are

$$\mathbf{k}_1 = \begin{pmatrix} 0 \\ -\rho \\ A \end{pmatrix}, \quad \mathbf{k}_2 = \begin{pmatrix} A^2 \\ -B \\ 0 \end{pmatrix}, \quad \mathbf{k}_3 = \begin{pmatrix} 0 \\ \rho \\ A \end{pmatrix}.$$

One can notice that the eigenvalues are real and satisfy the condition $\lambda_1 < \lambda_2 < \lambda_3$ and we have a set of independent corresponding eigenvectors which means the system is strictly hyperbolic.

4.4.1 Characteristic field of the eigenvalues and Riemann invariants for the case $N = 1$

We classify the eigenvectors $\mathbf{k}_i = (k_{i1}, k_{i2}, k_{i3})$, $i = 1, 2, 3$ to be:

- For $\lambda_1 = v - A$, with the eigenvector

$$\mathbf{k}_1 = \begin{pmatrix} 0 \\ -\rho \\ A \end{pmatrix}.$$

  We find

$$\nabla\lambda_1\mathbf{k}_1 = \frac{\partial\lambda_1}{\partial\chi}k_{11} + \frac{\partial\lambda_1}{\partial\rho}k_{12} + \frac{\partial\lambda_1}{\partial v}k_{13} = 0 + 0 + A \neq 0,$$

  and the first eigenvector is genuinely non-linear. Across the λ_1-wave we have

$$\frac{d\chi}{0} = \frac{d\rho}{-\rho} = \frac{dv}{A},$$

  which gives $\chi =$ constant the first Riemann invariant and we need to solve

$$dv + \frac{A}{\rho}d\rho = 0.$$

  The Riemann invariant is

$$v + A\ln\rho = \text{constant}.$$

- For $\lambda_2 = v$, with the eigenvector is

$$\mathbf{k}_2 = \begin{pmatrix} A^2 \\ -B \\ 0 \end{pmatrix}.$$

We find

$$\nabla\lambda_2\mathbf{k}_2 = \frac{\partial\lambda_2}{\partial\chi}k_{21} + \frac{\partial\lambda_2}{\partial\rho}k_{22} + \frac{\partial\lambda_2}{\partial v}k_{23} = 0\cdot A^2 - 0\cdot B + 0 = 0,$$

and the second eigenvector is linearly degenerate. Across the λ_2-wave we have

$$\frac{d\chi}{A^2} = \frac{d\rho}{-B} = \frac{dv}{0}$$

which gives the first Riemann invariant in this case which is $v =$ constant and

$$\frac{d\chi}{A^2} = \frac{d\rho}{-B} \Leftrightarrow Bd\chi + A^2 d\rho = dp = 0,$$

which gives the second Riemann invariant in this case which is $p =$ constant. Another way to show that $p =$ constant is using the jump condition. The second wave is a contact which means the jump conditions are satisfied. From our system and the jump condition we get $v_l = v_r = s = v$ and from the Rankine-Hungoniot conditions, i.e. $[\![u]\!] = u_l - u_r$, we obtain

$$s = \frac{[\![\rho\chi v]\!]}{[\![\rho\chi]\!]} = \frac{[\![\rho v]\!]}{[\![\rho]\!]} = \frac{[\![\rho v^2 + p]\!]}{[\![\rho v]\!]}.$$

And

$$v = s = \frac{[\![\rho v^2 + p]\!]}{[\![\rho v]\!]} = \frac{[\![\rho v^2]\!]}{[\![\rho v]\!]} + \frac{[\![p]\!]}{[\![\rho v]\!]} = \frac{v^2[\![\rho]\!]}{v[\![\rho]\!]} + \frac{[\![p]\!]}{[\![\rho v]\!]} = v + \frac{[\![p]\!]}{[\![\rho v]\!]}.$$

We find $\frac{[\![p]\!]}{[\![\rho v]\!]} = 0$. Which means $[\![p]\!] = 0$. Then we can find $p_l = p_r$.

- For $\lambda_3 = v + A$, with the eigenvector

$$\mathbf{k}_3 = \begin{pmatrix} 0 \\ \rho \\ A \end{pmatrix},$$

we find

$$\nabla\lambda_3\mathbf{k}_3 = \frac{\partial\lambda_3}{\partial\chi}k_{31} + \frac{\partial\lambda_3}{\partial\rho}k_{32} + \frac{\partial\lambda_3}{\partial v}k_{33} = 0 + 0 + A \neq 0,$$

and the third eigenvector is genuinely non-linear. Across the λ_3-wave we have

$$\frac{d\chi}{0} = \frac{d\rho}{\rho} = \frac{dv}{A}$$

which gives $\chi =$ constant and thus A is a constant. We need to solve

$$dv - \frac{A}{\rho}d\rho = 0.$$

The Riemann invariant is

$$v - A\ln\rho = \text{constant}.$$

4.4.2 The exact solution for the case $N = 1$

In the study of the exact solution of the Riemann problem for the case $N = 1$ we will use the vector $\mathbf{W} = (\rho, v, p)^\top$ of the primitive variables instead of the conservative variables. In this case the initial data in terms of primitive variables consists of the constant data $\mathbf{W}_- = (\rho_-, v_-, p_-)^\top$ to the left and $\mathbf{W}_+ = (\rho_+, v_+, p_+)^\top$ to the right. The initial data are separated by a discontinuity.
As we have seen in the previous section we have three eigenvalues namely

$$\lambda_1 = v - A, \quad \lambda_2 = v, \quad \lambda_3 = v + A,$$

which means that the exact solution of the Riemann problem has three waves. The region between the first and the last wave is called the star region $\mathbf{W}^*$. In this region the data are unknown. We aim to determine the solution in the star region. The wave in the middle divides the star region into two subregions star left $\mathbf{W}^*_- = (\rho^*_-, v^*_-, p^*_-)$ and star right $\mathbf{W}^*_+ = (\rho^*_+, v^*_+, p^*_+)$. This means the waves separate four constant states $\mathbf{W}_-$, $\mathbf{W}^*_-$, $\mathbf{W}^*_+$ and $\mathbf{W}_+$.
The middle wave is a contact discontinuity. Therefore the first and the last waves form four possible wave patterns which are shock-shock, shock-rarefaction, rarefaction-shock, and rarefaction-rarefaction.
The study of the Riemann invariants reveals that

$$p^*_- = p^*_+, \quad \text{and} \quad v^*_- = v^*_+,$$

which means that the pressure and the velocity in the star region are constants. For the sake of the simplicity we use p^* and v^* to denote them. The density has two values in the star region namely ρ^*_- and ρ^*_+. Our goal is now to determine the four unknowns p^*, v^*, ρ^*_- and ρ^*_+.

Solution strategy

The main idea of the solution strategy is based on establishing equations to find the pressure p^* and the velocity v^* in the star region. This benefits the use of the relation between the pressure and the density via the equation of state to find the densities ρ^*_- and ρ^*_+. The main reference is the book by Toro [75] and [49].
For this goal we will define the function f_- below which is a function of the pressure and the data $\mathbf{W}_-$. The function f_- governs the relations across the left wave and connects v^* to the known state $\mathbf{W}_-$.
Similarly, the function f_+ will be a function of the pressure and the data $\mathbf{W}_+$. It relates v^* to the known state $\mathbf{W}_+$. This function governs the relations across the right wave. The solution for the pressure p^* is given by the root of the equation

$$f(p, \mathbf{W}_-, \mathbf{W}_+) = f_-(p, \mathbf{W}_-) + f_+(p, \mathbf{W}_+) + \Delta v = 0, \qquad \Delta v = v_+ - v_-.$$

The solution for the velocity in the star region will be given as

$$v^* = \frac{1}{2}(v_- + v_+) + \frac{1}{2}[f_+(p^*) - f_-(p^*)].$$

Once the pressure p^* is obtained we can find the densities ρ^*_- and ρ^*_+ using the equation of state (4.17).

Shock waves

We start the discussion by considering a shock wave. The shock can move either to the right or to the left. For each of the two cases there are known data and unknown variables which we want to determine. We use the Rankine-Hugoniot condition to derive the relations across the shock waves. First we will assume the case of a shock moving to the left. We will obtain the relation f_- and then we will consider a shock moving to the right and show how we derive a relation of f_+.

Function f_- for a left shock

First we consider a shock moving to the left with speed S_-. We define the relative velocities, see Toro [75] and Hantke et al. [32]

$$\begin{aligned} \hat{v}_- &= v_- - S_-, \\ \hat{v}^* &= v^* - S_-. \end{aligned} \tag{4.18}$$

The calculations at the shocks require the use of the Rankine-Hugoniot conditions which are

$$\rho_-\chi_-\hat{v}_- - \rho_-^*\chi_-^*\hat{v}_-^* = 0, \tag{4.19}$$

$$\rho_-\hat{v}_- - \rho_-^*\hat{v}_-^* = 0, \tag{4.20}$$

$$\rho_-\hat{v}_-^2 + p_- - (\rho_-^*\hat{v}_-^{*2} + p^*) = 0. \tag{4.21}$$

We introduce the mass flux Q_- which from (4.20) can be written as

$$Q_- = \rho_-\hat{v}_- = \rho_-^*\hat{v}_-^*. \tag{4.22}$$

Then from equation (4.21) we have

$$Q_-\hat{v}_- + p_- = Q_-\hat{v}_-^* + p^*.$$

We can get an expression for Q_-, which is given by

$$Q_- = -\frac{p^* - p_-}{\hat{v}_-^* - \hat{v}_-}. \tag{4.23}$$

But from equations (4.18) we can write

$$\hat{v}_-^* - \hat{v}_- = v^* - v_-,$$

which means that we can write the mass flux as

$$Q_- = -\frac{p^* - p_-}{v^* - v_-},$$

and the velocity can be written as

$$v^* = v_- - \frac{p^* - p_-}{Q_-}. \tag{4.24}$$

Our aim now is to relate v^* to p^* and the data $\mathbf{W}_-$ on the left hand side. For this end we need to write Q_- as a function of p^* and the data on the left hand side. So that we use the relations

$$\hat{v}_- = \frac{Q_-}{\rho_-}, \qquad \hat{v}_-^* = \frac{Q_-}{\rho_-^*},$$

which are obtained from (4.22) and substitute into (4.23). This gives that

$$Q_- = -\frac{p^* - p_-}{\frac{Q_-}{\rho_-^*} - \frac{Q_-}{\rho_-}},$$

which implies that

$$Q_-^2 = -\frac{p^* - p_-}{\frac{1}{\rho_-^*} - \frac{1}{\rho_-}}. \tag{4.25}$$

The density is related to the pressure behind the left shock via the stiffened gas equation of state which is presented in detail in Chapter 3, Subsection 3.5.2. In the pure phases the equation of state has the form

$$p = a^2\rho + d,$$

so that

$$Q_-^2 = -\frac{p^* - p_-}{\frac{1}{\frac{p^*-d}{a^2}} - \frac{1}{\frac{p_--d}{a^2}}} = \frac{1}{a^2}(p^* - d)(p_- - d).$$

We substitute into (4.24) and get

$$v^* = v_- - a\frac{p^* - p_-}{\sqrt{(p^* - d)(p_- - d)}}.$$

As the velocity in the star region should satisfy

$$v^* = v_- - f_-(p^*, \mathbf{W}_-),$$

we find that

$$f_-(p^*, \mathbf{W}_-) = a\frac{p^* - p_-}{\sqrt{(p^* - d)(p_- - d)}},$$

which is the expression sought for f_-.

Function f_+ for a right shock

Now we will assume the right wave may be a shock moving with speed S_+. We follow the same approach in the previous discussion taking into account that the information is known to the right in this case. We begin by defining the relative velocities which are given as

$$\begin{aligned} \hat{v}_+ &= v_+ - S_+, \\ \hat{v}^* &= v^* - S_+. \end{aligned} \tag{4.26}$$

Now we apply the Rankine-Hugoniot condition on the system. This gives

$$\rho_+\chi_+\hat{v}_+ - \rho_+^*\chi_+^*\hat{v}_+^* = 0, \tag{4.27}$$

$$\rho_+^*\hat{v}_+^* - \rho_+\hat{v}_+ = 0, \tag{4.28}$$

$$\rho_+^*\hat{v}_+^{*2} + p^* - (\rho_+\hat{v}_+^2 + p_+) = 0. \tag{4.29}$$

We introduce the mass flux

$$Q_+ = -\rho_+\hat{v}_+ = -\rho_+^*\hat{v}_+^*. \tag{4.30}$$

This means that the equation (4.29) can be written as

$$-Q_+\hat{v}_+ + p_+ = -Q_+\hat{v}_+^* + p^*.$$

We can get an expression for Q_+, which is given as

$$Q_+ = \frac{p_+ - p^*}{\hat{v}_+ - \hat{v}_+^*}. \tag{4.31}$$

One can notice that from the definition of the relative velocities we have

$$\hat{v}_+ - \hat{v}_+^* = v_+ - v^*, \tag{4.32}$$

and Q_+ becomes

$$Q_+ = \frac{p_+ - p^*}{v_+ - v^*}. \tag{4.33}$$

This means that the velocity can be written as

$$v^* = v_+ - \frac{p_+ - p^*}{Q_+}. \tag{4.34}$$

Now from (4.30) we get

$$\hat{v}_+ = \frac{-Q_+}{\rho_+}, \qquad \hat{v}_+^* = \frac{-Q_+}{\rho_+^*}.$$

We substitute into (4.31) and get

$$Q_+ = \frac{p_+ - p^*}{\frac{-Q_+}{\rho_+} + \frac{Q_+}{\rho_+^*}}.$$

Then we can write the mass flux in terms of the pressure and the density as

$$Q_+^2 = \frac{p_+ - p^*}{\frac{-1}{\rho_+} + \frac{1}{\rho_+^*}}.$$

Now we use the equation of state $p = a^2\rho + d$ in the pure phases in order to write the mass flux as a function of either the pressure p^* or the density ρ_*. We write the mass flux as a function of the pressure as

$$Q_+^2 = \frac{p_+ - p^*}{\frac{-1}{\frac{p_+ - d}{a^2}} + \frac{1}{\frac{p^* - d}{a^2}}} = \frac{1}{a^2}(p^* - d)(p_+ - d).$$

Next we substitute in (4.34), we get

$$v^* = v_+ - a\frac{p_+ - p^*}{\sqrt{(p^* - d)(p_+ - d)}}.$$

Comparing with the formula of the velocity in the star region satisfying

$$v^* = v_+ + f_+(p^*, \mathbf{W}_+),$$

we find that the function f_+ for the case in which the right wave is shock is

$$f_+ = -a\frac{p_+ - p^*}{\sqrt{(p^* - d)(p_+ - d)}}.$$

Rarefaction waves

Now we want to derive an expression for f_- and f_+ for the case of rarefaction waves. We have two possibilities: the first one when the wave is moving to the left and the second one when the wave is moving to the right. In this case we use the Riemann invariants in order to relate the unknown state $\mathbf{W}_-^*$ with the known data $\mathbf{W}_-$ to the left. Similarly, we relate the unknown $\mathbf{W}_+^*$ with the known date $\mathbf{W}_+$ to the right.

Function f_- for left rarefaction

As we have seen before the Riemann invariant which is associated with the first eigenvalue and the first eigenvector is given as

$$v + A \ln \rho = \text{constant},$$

where A is the speed of sound in the mixture which is already presented previously in this chapter.
As Riemann invariant is constant across the left rarefaction wave and by evaluating the constant on the left data we find

$$v_- + A \ln \rho_- = v^* + A \ln \rho_-^*.$$

This means that v^* is given as

$$v^* = v_- + A \ln \frac{\rho_-}{\rho_-^*}.$$

This leads to

$$f_- = -A \ln \frac{\rho_-}{\rho_-^*}.$$

This equation can be written in terms of p^* as

$$f_- = -A \ln \frac{p_- - d}{p^* - d},$$

which is the required function for the case in which the left wave is a rarefaction wave.

Function f_r for right rarefaction

The Riemann invariant is associated with the third eigenvalue and the corresponding Riemann invariant is given as

$$v - A \ln \rho = \text{constant}.$$

This implies that we can write

$$v_+ - A \ln \rho_+ = v^* - A \ln \rho_+^*,$$

as long as Riemann invariant is constant along the wave to the right. This gives

$$v^* = v_+ + A \ln \frac{\rho_+^*}{\rho_+}.$$

This means that the relation f_+ is given as

$$f_+ = A \ln \frac{\rho_+^*}{\rho_+}.$$

which can be written as

$$f_+ = A \ln \frac{p^* - d}{p_+ - d}.$$

What we have done until now is that we determined the functions f_- and f_+ for the four possible wave patterns. We summarize the expressions f_- and f_+ as follows

$$f_- = \begin{cases} a\frac{p^*-p_-}{\sqrt{(p^*-d)(p_--d)}}, & \text{shock,} \\ -A \ln \frac{p_--d}{p^*-d}, & \text{rarefaction,} \end{cases}$$

and

$$f_+ = \begin{cases} -a\frac{p_+-p^*}{\sqrt{(p^*-d)(p_+-d)}}, & \text{shock,} \\ A \ln \frac{p^*-d}{p_+-d}, & \text{rarefaction.} \end{cases}$$

Now we have a single equation

$$f(p^*, \mathbf{W}_-, \mathbf{W}_+) = f_-(p^*, \mathbf{W}_-) + f_+(p^*, \mathbf{W}_+) + \Delta v = 0, \qquad \Delta v = v_+ - v_-.$$

with one variable p^* which can be determined now by finding the roots of this equation. The velocity v^* can be found by solving

$$v^* = \frac{1}{2}(v_- + v_+) + \frac{1}{2}[f_+(p^*) - f_-(p^*)].$$

We remind the reader that it is an easy task to determine the ρ_-^* and ρ_+^* because the densities are related with the pressure via the equation of state.

4.5 The analytical structure and the exact solution for the case $N > 1$

Our aim in this section is to present a detailed discussion for the analytical structure for the case $N > 1$. We consider a mixture of two phases that consists of N components. In this case the system has the form

$$\begin{aligned} \tfrac{\partial}{\partial t}\rho\chi + \tfrac{\partial}{\partial x}\rho\chi v &= 0, \\ \tfrac{\partial}{\partial t}\rho_i + \tfrac{\partial}{\partial x}(\rho_i v) &= 0 \qquad i = 1, ..., N-1 \\ \tfrac{\partial}{\partial t}\rho + \tfrac{\partial}{\partial x}(\rho v) &= 0 \\ \tfrac{\partial}{\partial t}(\rho v) + \tfrac{\partial}{\partial x}(\rho v^2 + p) &= 0. \end{aligned} \tag{4.35}$$

The transport equation of the total density $\rho = \sum_{i=1}^{N} \rho_i$ can be replaced by the transport equation of the partial density of the $N - th$ component. The system in this case has the form

$$\begin{aligned} \tfrac{\partial}{\partial t}\rho\chi + \tfrac{\partial}{\partial x}\rho\chi v &= 0, \\ \tfrac{\partial}{\partial t}\rho_i + \tfrac{\partial}{\partial x}(\rho_i v) &= 0, \qquad i = 1, ..., N \\ \tfrac{\partial}{\partial t}(\rho v) + \tfrac{\partial}{\partial x}(\rho v^2 + p) &= 0, \end{aligned} \tag{4.36}$$

with the Riemann initial data

$$\chi(x,0)=\begin{cases}\chi_- & \text{if} \quad x<0,\\ \chi_+ & \text{if} \quad x>0,\end{cases} \quad \rho(x,0)=\begin{cases}\rho_{-i} & \text{if} \quad x<0,\\ \rho_{+i} & \text{if} \quad x>0,\end{cases} \qquad i=1,\dots,N$$
$$v(x,0)=\begin{cases}v_- & \text{if} \quad x<0,\\ v_+ & \text{if} \quad x>0.\end{cases} \tag{4.37}$$

Remark 2 *The systems* (4.35) *and* (4.36) *are not only equivalent for the smooth solutions but also for the weak solutions since the jump conditions*

$$s[\![\rho]\!]-[\![\rho v]\!]=0,$$

and

$$s[\![\rho_i]\!]-[\![\rho_i v]\!]=0, \qquad i=1,\dots,N$$

are mutually compatible. Note that this is due to

$$0=\sum_{i=1}^{N}(s[\![\rho_i]\!]-[\![\rho_i v]\!])=s[\![\sum_{i=1}^{N}\rho_i]\!]-[\![\sum_{i=1}^{N}\rho_i v]\!]=s[\![\rho]\!]-[\![\rho v]\!].$$

The pressure p is related to the phase field variable χ and the partial densities ρ_i, $i=1,...,N$ of the components by the equation of state

$$p(\chi,\rho_1,...,\rho_N)=-W(\chi)+\sum_{i=1}^{N}[h(\chi)(a_{+i}^2\rho_i+d_{+i})+(1-h(\chi))(a_{-i}^2\rho_i+d_{-i})], \tag{4.38}$$

where a_{i+} and a_{i-} are the isothermal sound speed of the component i in the liquid and the vapor respectively. We have

$$\frac{dp}{dx}=\frac{\partial p}{\partial \rho_1}\frac{\partial \rho_1}{\partial x}+...+\frac{\partial p}{\partial \rho_N}\frac{\partial \rho_N}{\partial x}+\frac{\partial p}{\partial \chi}\frac{\partial \chi}{\partial x}.$$

From the equation of state (4.38) we introduce the mixture sound speed

$$A_i^2:=\frac{\partial p}{\partial \rho_i}=h(\chi)a_{i+}^2+(1-h(\chi))a_{i+}^2,$$

and the variable

$$B:=\frac{\partial p}{\partial \chi}=-W'(\chi)+h'(\chi)\sum_{i=1}^{N}(a_{i+}^2\rho_i+d_{i+})-h'(\chi)\sum_{i=1}^{N}(a_{i-}^2\rho_i+d_{i-}).$$

One should keep in mind that the abbreviations A_i depend on χ, while B depends on χ and the partial densities ρ_i.
Using the above notations we obtain the quasilinear form of the system (4.36) which has the form

$$\begin{aligned}\tfrac{\partial}{\partial t}\chi+v\tfrac{\partial}{\partial x}\chi &= 0\\ \tfrac{\partial}{\partial t}\rho_i+v\tfrac{\partial}{\partial x}\rho_i+\rho_i\tfrac{\partial}{\partial x}v &= 0 \qquad i=1,...,N\\ \tfrac{\partial}{\partial t}v+\tfrac{B}{\rho}\tfrac{\partial}{\partial x}\chi+\tfrac{1}{\rho}\textstyle\sum_{i=1}^{N}A_i^2\tfrac{\partial}{\partial x}\rho_i+v\tfrac{\partial}{\partial x}v &= 0.\end{aligned} \tag{4.39}$$

The Jacobian matrix in this case is

$$\mathbf{A}(\chi, \rho_1, ..., \rho_N, v) = \begin{pmatrix} v & 0 & 0 & ... & 0 & 0 \\ 0 & v & 0 & ... & 0 & \rho_1 \\ 0 & 0 & v & ... & 0 & \rho_2 \\ \vdots & & & & & \\ 0 & 0 & 0 & ... & v & \rho_N \\ \frac{B}{\rho} & \frac{A_1^2}{\rho} & \frac{A_2^2}{\rho} & ... & \frac{A_N^2}{\rho} & v \end{pmatrix}.$$

The eigenvalues of the Jacobian matrix are

$$\lambda_0 = v - A, \qquad \lambda_1 = \lambda_2 = ... = \lambda_N = v, \qquad \lambda_{N+1} = v + A,$$

where

$$A = \sqrt{\frac{\sum_{i=1}^{N} \rho_i A_i^2}{\rho}}.$$

In case $B \neq 0$ we obtain the full set of linearly independent eigenvectors

$$\mathbf{k}_0 = \begin{pmatrix} 0 \\ -\rho_1 \\ -\rho_2 \\ \vdots \\ -\rho_N \\ A \end{pmatrix}, \quad \mathbf{k}_{N+1} = \begin{pmatrix} 0 \\ \rho_1 \\ \rho_2 \\ \vdots \\ \rho_N \\ A \end{pmatrix},$$

$$\mathbf{k}_1 = \begin{pmatrix} -A_1^2 \\ B \\ 0 \\ \vdots \\ 0 \\ 0 \end{pmatrix}, \quad \mathbf{k}_2 = \begin{pmatrix} -A_2^2 \\ 0 \\ B \\ \vdots \\ 0 \\ 0 \end{pmatrix}, \quad ..., \quad \mathbf{k}_N = \begin{pmatrix} -A_N^2 \\ 0 \\ 0 \\ \vdots \\ B \\ 0 \end{pmatrix}.$$

In the case $B = 0$ we have a full system of linearly independent eigenvectors with

$$\mathbf{k}_1 = \begin{pmatrix} 1 \\ 0 \\ 0 \\ \vdots \\ \vdots \\ 0 \\ 0 \end{pmatrix}, \quad \mathbf{k}_2 = \begin{pmatrix} 0 \\ -A_2^2 \\ A_1^2 \\ 0 \\ \vdots \\ 0 \\ 0 \end{pmatrix}, \quad ..., \quad \mathbf{k}_N = \begin{pmatrix} 0 \\ -A_N^2 \\ 0 \\ \vdots \\ 0 \\ A_1^2 \\ 0 \end{pmatrix},$$

and $\mathbf{k}_0$ and $\mathbf{k}_{N+1}$ as before. The eigensystem in this case looks different because the eigenvectores do not depend smoothly on the entry of the matrix.
This means that in both cases we have a full set of linearly independent eigenvector. This implies that system (4.36) is hyperbolic. For the single component case $N = 1$ it is even strictly hyperbolic.

4.5.1 Characteristic fields

Let $\mathbf{u} = (\chi, \rho_1, \ldots, \rho_N, v)^T$ denote the vector of primitive variables. Across the left wave we have $\lambda_0 = v - A$ with the corresponding eigenvector $\mathbf{k}_0$. We have

$$\begin{aligned}
\nabla_{\mathbf{u}}\lambda_0\mathbf{k}_0 &= \frac{\partial\lambda_0}{\partial\chi}k_{00} + \frac{\partial\lambda_0}{\partial\rho_1}k_{01} + \cdots + \frac{\partial\lambda_0}{\partial\rho_N}k_{0N} + \frac{\partial\lambda_0}{\partial v}k_{0N+1} \\
&= 0 + \frac{\partial\lambda_0}{\partial\rho_1}(-\rho_1) + \cdots + \frac{\partial\lambda_0}{\partial\rho_N}(-\rho_N) + 1\cdot A \\
&= -\frac{A_1^2 - A^2}{2A\rho}(-\rho_1) + \cdots - \frac{A_N^2 - A^2}{2A\rho}(-\rho_N) + A \\
&= \frac{\rho_1 A_1^2 + \cdots + \rho_N A_N^2}{2A\rho} - \frac{\rho_1 A^2 + \cdots + \rho_N A^2}{2A\rho} + A \\
&= \frac{A^2}{2A} - \frac{\rho A^2}{2A\rho} + A \\
&= \frac{A}{2} - \frac{A}{2} + A = A \neq 0.
\end{aligned}$$

The same across the right wave where $\lambda_{N+1} = v + A$ with the corresponding eigenvector $\mathbf{k}_{N+1}$. In this case

$$\begin{aligned}
\nabla_{\mathbf{u}}\lambda_{N+1}\mathbf{k}_{N+1} &= \frac{\partial\lambda_{N+1}}{\partial\chi}k_{N+1,0} + \frac{\partial\lambda_{N+1}}{\partial\rho_1}k_{N+1,1} + \cdots + \frac{\partial\lambda_{N+1}}{\partial\rho_N}k_{N+1,N} + \frac{\partial\lambda_{N+1}}{\partial v}k_{N+1,N+1} \\
&= 0 + \frac{\partial\lambda_{N+1}}{\partial\rho_1}\rho_1 + \cdots + \frac{\partial\lambda_{N+1}}{\partial\rho_N}\rho_N + 1\cdot A \\
&= \frac{A_1^2 - A^2}{2A\rho}(\rho_1) + \cdots + \frac{A_N^2 - A^2}{2A\rho}(\rho_N) + A \\
&= \frac{\rho_1 A_1^2 + \cdots + \rho_N A_N^2}{2A\rho} - \frac{\rho_1 A^2 + \cdots + \rho_N A^2}{2A\rho} + A \\
&= \frac{A^2}{2A} - \frac{\rho A^2}{2A\rho} + A \\
&= \frac{A}{2} - \frac{A}{2} + A = A \neq 0.
\end{aligned}$$

This implies that across the left and the right waves the relations

$$\nabla_{\mathbf{u}}\lambda_0\mathbf{k}_0 \neq 0, \qquad \nabla_{\mathbf{u}}\lambda_{N+1}\mathbf{k}_{N+1} \neq 0,$$

are satisfied. This means that the associated characteristic fields are genuinely nonlinear and the corresponding waves are shocks or rarefactions.
Furthermore for the multiple eigenvalues $\lambda_i = v$ with the corresponding eigenvector $\mathbf{k}_i$ where $i = 1, ..., N$ one can verify that

$$\begin{aligned}
\nabla_{\mathbf{u}}\lambda_i\mathbf{k}_i &= \frac{\partial\lambda_i}{\partial\chi}k_{i0} + \frac{\partial\lambda_i}{\partial\rho_1}k_{i1} + \cdots + \frac{\partial\lambda_i}{\partial\rho_N}k_{iN} + \frac{\partial\lambda_i}{\partial v}k_{iN+1} \\
&= 0\cdot(-A_i^2) + 0\cdot k_{i2} + \cdots + 0\cdot k_{iN} + 1\cdot A = 0,
\end{aligned}$$

which means that the associated characteristic field is linearly degenerate and the corresponding wave is a classical contact.

4.5.2 Riemann invariants for the case $N > 1$

Let λ be an eigenvector of multiplicity m in a system of dimension n. Then there exist $n - m$ Riemann invariants across the wave corresponding to λ.
Here we have $n = N + 2$ accordingly we have $N + 1$ Riemann invariants across the outer waves belonging to λ_0 and λ_{N+1} and we have 2 Riemann invariants across the contact wave in the middle.
To find the Riemann invariants across the field j, for $j = 0, \ldots, N + 1$ one has to solve the system

$$\frac{du_0}{k_{j,0}} = \frac{du_1}{k_{j,1}} = \cdots = \frac{du_{N+1}}{k_{j,N+1}}. \tag{4.40}$$

Case $j = 0$: Then the system of ordinary differential equations to solve becomes

$$\frac{d\chi}{0} = \frac{d\rho_1}{-\rho_1} = \cdots = \frac{d\rho_N}{-\rho_N} = \frac{dv}{A}\,.$$

It is easy to see that the phase field χ is constant across the 0th wave with $\chi \equiv \chi_-$.
For $j = 2, \ldots, N$ we have

$$\frac{d\rho_1}{-\rho_1} = \frac{d\rho_j}{-\rho_j}.$$

This gives for $j = 2, \ldots, N$

$$\ln(\rho_1) - \ln(\rho_j) = \text{const} \qquad \text{resp.} \qquad \rho_j = c_{j-}\rho_1\,.$$

It remains to solve

$$-\frac{A}{\rho_1}d\rho_1 = dv\,.$$

Defining $c_{1-} := 1$ we get

$$dv = -\frac{1}{\rho_1}\sqrt{\frac{\sum_{i=1}^N A_i^2 c_{i-}\rho_1}{\sum_{i=1}^N c_{i-}\rho_1}}d\rho_1 = -\frac{1}{\rho_1}\sqrt{\frac{\sum_{i=1}^N A_i^2 c_{i-}}{\sum_{i=1}^N c_{i-}}}d\rho_1\,.$$

Keeping in mind that the phase field is an invariant we have $A_i = A_i(\chi_-) = \text{const}$ we define $A_{i-} := A_i(\chi_-)$ and we finally obtain

$$v = v_- - \ln(\rho_1)\sqrt{\frac{\sum_{i=1}^N A_{i-}^2 c_{i-}}{\sum_{i=1}^N c_{i-}}} + \ln(\rho_{1-})\sqrt{\frac{\sum_{i=1}^N A_{i-}^2 c_{i-}}{\sum_{i=1}^N c_{i-}}}\,.$$

Case $j = N + 1$: It is quite similar. An analogous calculation with $c_{1+} := 1$ gives the following relations

$$\begin{aligned}
&\chi \equiv \chi_+ \\
&\rho_j = c_{j+}\rho_1 \quad j = 2, \ldots, N \\
&v = v_+ + \ln(\rho_1)\sqrt{\frac{\sum_{i=1}^N A_{i+}^2 c_{i+}}{\sum_{i=1}^N c_{i+}}} - \ln(\rho_{1+})\sqrt{\frac{\sum_{i=1}^N A_{i+}^2 c_{i+}}{\sum_{i=1}^N c_{i+}}} \qquad \text{with } A_{i+} = A_i(\chi_+)\,.
\end{aligned}$$

For the **contact** one can immediately see that the velocity is a Riemann invariant. Nevertheless we fail to determine the second invariant. However, from the single component case with pure phases we know, that also the pressure is a constant across the middle wave. To verify if this is true in general we rewrite the quasilinear system, now using the variables v, p, ρ_i for $i = 1, \ldots, N$.

New choice of variables.

As mentioned before determining Riemann invariants in the middle wave is not an easy task. So that we will rewrite the system (4.36) in terms of the primitive variables ρ_i, $i = 1, \ldots, N$, v and p instead of $\chi, \rho_1, \ldots, \rho_N$ and v.
The equation of state (4.38) has the form $p = p(\rho_1, \rho_2, \ldots, \rho_N, \chi)$. This means that

$$\frac{\partial p}{\partial t} = \sum_{i=1}^{N} A_i^2 \cdot (\rho_i)_t + B\chi_t, \quad \text{and} \quad \frac{\partial p}{\partial x} = \sum_{i=1}^{N} A_i^2 \cdot (\rho_i)_x + B\chi_x,$$

where

$$A_i^2 = \frac{\partial p}{\partial \rho_i} \quad \text{and} \quad B = \frac{\partial p}{\partial \chi}.$$

This implies that

$$\chi_t = \frac{1}{B}(p_t - \sum_{i=1}^{N} A_i^2 (\rho_i)_t) \quad \text{and} \quad \chi_x = \frac{1}{B}(p_x - \sum_{i=1}^{N} A_i^2 (\rho_i)_x).$$

We substitute the last relations into the transport equation of the phase field variable in (4.36) we obtain the smoothly equivalent quasilinear form of the system using the variables v, p, ρ_i for $i = 1, \ldots, N$

$$\partial_t p + v\partial_x p + \sum_{i=1}^{N} A_i^2 \rho_i \partial_x v = 0 \tag{4.41a}$$

$$\partial_t \rho_i + v\partial_x \rho_i + \rho_i \partial_x v = 0 \qquad i = 1, \ldots, N \tag{4.41b}$$

$$\partial_t v + \frac{1}{\rho}\partial_x p + v\partial_x v = 0 \tag{4.41c}$$

with the corresponding Jacobian

$$\begin{pmatrix} v & 0 & \ldots & 0 & \sum_{i=1}^{N} A_i^2 \rho_i \\ 0 & v & \ldots & 0 & \rho_1 \\ \vdots & & \ddots & & \vdots \\ 0 & 0 & \ldots & v & \rho_N \\ \frac{1}{\rho} & 0 & \ldots & 0 & v \end{pmatrix}.$$

The eigenvectors belonging to the multiple eigenvalue $\lambda_1 = \cdots = \lambda_N = v$ are now given by

$$\begin{pmatrix} 0 \\ 1 \\ 0 \\ \vdots \\ 0 \\ 0 \end{pmatrix}, \ldots, \begin{pmatrix} 0 \\ 0 \\ \vdots \\ 0 \\ 1 \\ 0 \end{pmatrix}.$$

Once again we easily can see that the velocity remains constant across the contact wave. In addition we find the pressure to be the further invariant as conjectured above.

4.5.3 The exact solution for the case $N > 1$

In this section we will present the explicit solution of the Riemann problem for the diffuse interface multiphase mixture model (4.36) with the equation of state (4.38). First we summarize the results obtained in the last section as following

- The solution of the Riemann problem consists of four constant states that are separated by three waves. The middle wave is a contact while the outer waves are shocks or rarefactions.
- The phase field χ may change across the contact wave, but stays constant everywhere else. This means that the initial profile of the phase field is shifted with the flow.
- Due to the fact that the solution for the phase field is known, it remains to solve the system consisting of the partial mass balances and the momentum balance. This system is in divergence form. Accordingly the Rankine-Hugeniot jump conditions are satisfied across discontinuities. These are given by

$$\rho_{i+}v_+ - \rho_{i-}v_- = s(\rho_{i+} - \rho_{i-}) \qquad i = 1, \dots, N \tag{4.42}$$

$$\sum_{i=1}^{N}(\rho_{i+}(v_+)^2 - \rho_{i-}(v_-)^2) + (p_+ - p_-) = s\sum_{i=1}^{N}(\rho_{i+}v_+ - \rho_{i-}v_-) \tag{4.43}$$

  where s denotes the propagation speed of the discontinuity and $-$ and $+$ indicate the states to the vapor to the left and the liquid to the right of the discontinuity, resp.
- The velocity and the pressure are Riemann invariants across the contact wave. This allows to follow the strategy described in the book of Toro [75] to construct the Riemann solution.

Rarefactions.

Assume the left wave is a rarefaction. Then from the last section we know that

$$v^* = v_- - \ln(\rho^*_{1-})\sqrt{\frac{\sum_{i=1}^{N} A_{i-}^2 c_{i-}}{\sum_{i=1}^{N} c_{i-}}} + \ln(\rho_{1-})\sqrt{\frac{\sum_{i=1}^{N} A_{i-}^2 c_{i-}}{\sum_{i=1}^{N} c_{i-}}} \tag{4.44}$$

and $\rho^*_{j-} = c_{j-}\rho^*_{1-}$ with $c_{j-} = \frac{\rho_{j-}}{\rho_{1-}}$ and $j = 1, \dots, N$. Using (4.38) we find that

$$\begin{aligned} p^* &= -W(\chi_-) + h(\chi_-)\sum_{i=1}^{N}(a_{i+}^2 c_{j-}\rho^*_{1-} + d_{i+}) + (1 - h(\chi_-))\sum_{i=1}^{N} a_{i-}^2 c_{j-}\rho^*_{1-} \\ &= \mathcal{A}_{0-} + \mathcal{A}_{1-}\rho^*_{1-} \end{aligned}$$

with

$$\mathcal{A}_{0-} = -W(\chi_-) + h(\chi_-)\sum_{i=1}^{N} d_{i+}, \tag{4.45}$$

and

$$\mathcal{A}_{1-} = h(\chi_-)\sum_{i=1}^{N} a_{i+}^2 c_{j-} + (1 - h(\chi_-))\sum_{i=1}^{N} a_{i-}^2 c_{j-}\,.$$

So we can replace ρ^*_{1-} in (4.44) by $\rho^*_{1-} = \frac{p^* - \mathcal{A}_{0-}}{\mathcal{A}_{1-}}$ to give

$$v^* = v_- + \ln\left(\frac{p^* - \mathcal{A}_{0-}}{\mathcal{A}_{1-}}\right)\sqrt{\frac{\sum_{i=1}^N A_{i-}^2 c_{i-}}{\sum_{i=1}^N c_{i-}}} - \ln(\rho_{1-})\sqrt{\frac{\sum_{i=1}^N A_{i-}^2 c_{i-}}{\sum_{i=1}^N c_{i-}}}, \tag{4.46}$$

where

$$A_{i-} = A_i(\chi_-).$$

An analogous calculation for a right rarefaction leads to

$$v^* = v_+ + \ln\left(\frac{p^* - \mathcal{A}_{0+}}{\mathcal{A}_{1+}}\right)\sqrt{\frac{\sum_{i=1}^N A_{i+}^2 c_{i+}}{\sum_{i=1}^N c_{i+}}} - \ln(\rho_{1+})\sqrt{\frac{\sum_{i=1}^N A_{i+}^2 c_{i+}}{\sum_{i=1}^N c_{i+}}}, \tag{4.47}$$

where

$$A_{i+} = A_i(\chi_+).$$

Shocks

Now let us assume that the left wave is a shock propagating with speed S_-. We define the left relative mass fluxes Q_{i-} by rewriting (4.42) as

$$\rho_{\alpha-}(v_- - S_-) = \rho^*_{i-}(v^* - S_-) \quad =: Q_{i-} \qquad i = 1, \ldots, N\,. \tag{4.48}$$

We note that

$$\frac{\rho^*_{i-}}{\rho_{i-}} = \frac{v_- - S_-}{v^* - S_-} \qquad \text{for all } i = 1, \ldots, N. \tag{4.49}$$

Accordingly

$$\rho^*_{i-} = \rho_{i-}\frac{\rho^*_{1-}}{\rho_{1-}} \qquad \text{for all } i = 1, \ldots, N.$$

Using (4.48) this we can rewrite (4.43) as

$$(v_- - v^*)\sum_{i=1}^N Q_{i-} + (p_- - p^*) = 0 \tag{4.50}$$

and we obtain

$$v^* = v_- - \frac{p^* - p_-}{\sum_{i=1}^N Q_{i-}}$$

where we will express $\sum_{i=1}^N Q_{i-}$ in terms of p^*. To do this we rewrite (4.50) as follows

$$\sum_{i=1}^N Q_{i-} = -\frac{p_- - p^*}{v_- - v^*} = -\frac{p_- - p^*}{(v_- - S_-) - (v^* - S_-)} = -\frac{p_- - p^*}{\frac{Q_{j-}}{\rho_{j-}} - \frac{Q_{j-}}{\rho^*_{j-}}}\,. \tag{4.51}$$

Multiplying (4.51) by Q_{j-} and summing up over j we get

$$\sum_{j=1}^N Q_{j-}\sum_{i=1}^N Q_{i-} = -\sum_{j=1}^N \frac{p_- - p^*}{\frac{1}{\rho_{j-}} - \frac{1}{\rho^*_{j-}}}\,.$$

This leads to

$$\sum_{i=1}^{N} Q_{i-} = \sqrt{-\sum_{i=1}^{N} \frac{p_- - p^*}{\frac{1}{\rho_{i-}} - \frac{1}{\rho^*_{i-}}}},$$

and we finally obtain

$$\begin{aligned} v^* = v_- - \frac{\sqrt{p^* - p_-}}{\sqrt{\sum_{i=1}^{N} \frac{\rho_{i-}\rho^*_{i-}}{\rho^*_{i-} - \rho_{i-}}}} &= v_- - \frac{\sqrt{p^* - p_-}}{\sqrt{\frac{\rho^*_{1-}}{\rho^*_{1-} - \rho_{1-}} \sum_{i=1}^{N} \rho_{i-}}} \\ &= v_- - \frac{\sqrt{p^* - p_-}}{\sum_{i=1}^{N} \rho_{i-}} \sqrt{1 - \frac{\mathcal{A}_{1-}\rho_{1-}}{p^* - \mathcal{A}_{0-}}}\,. \end{aligned}$$

Analogously we obtain for a right shock

$$v^* = v_+ + \frac{\sqrt{p^* - p_+}}{\sum_{i=1}^{N} \rho_{i+}} \sqrt{1 - \frac{\mathcal{A}_{1+}\rho_{1+}}{p^* - \mathcal{A}_{0+}}}\,.$$

Existence and uniqueness of the Riemann solution.

We summarize the results of the last subsection in the following

Theorem 1 *Let the function*

$$f(p, \mathbf{W}_-, \mathbf{W}_+) = f_-(p, \mathbf{W}_-) + f_+(p, \mathbf{W}_+) + (v_+ - v_-), \tag{4.52}$$

be given with

$$f_-(p, \mathbf{W}_-) = \begin{cases} \frac{\sqrt{p-p_-}}{\sum_{i=1}^{N} \rho_{i-}} \sqrt{1 - \frac{\mathcal{A}_{1-}\rho_{1-}}{p - \mathcal{A}_{0-}}} & \text{if } p > p_- \text{ (shock)} \\ \ln\left(\frac{p-\mathcal{A}_{0-}}{\mathcal{A}_{1-}}\right) \sqrt{\frac{\sum_{i=1}^{N} A^2_{i-} c_{i-}}{\sum_{i=1}^{N} c_{i-}}} - \ln(\rho_{1-}) \sqrt{\frac{\sum_{i=1}^{N} A^2_{i-} c_{i-}}{\sum_{i=1}^{N} c_{i-}}} & \text{if } p \le p_- \text{ (rarefaction)} \end{cases}$$

$$f_+(p, \mathbf{W}_+) = \begin{cases} \frac{\sqrt{p-p_+}}{\sum_{i=1}^{N} \rho_{i+}} \sqrt{1 - \frac{\mathcal{A}_{1+}\rho_{1+}}{p - \mathcal{A}_{0+}}} & \text{if } p > p_+ \text{ (shock)} \\ \ln\left(\frac{p-\mathcal{A}_{0+}}{\mathcal{A}_{1+}}\right) \sqrt{\frac{\sum_{i=1}^{N} A^2_{i+} c_{i+}}{\sum_{i=1}^{N} c_{i+}}} - \ln(\rho_{1+}) \sqrt{\frac{\sum_{i=1}^{N} A^2_{i+} c_{i+}}{\sum_{i=1}^{N} c_{i+}}} & \text{if } p \le p_+ \text{ (rarefaction)} \end{cases}$$

using

$$\begin{aligned} \mathcal{A}_{0\pm} &= -W(\chi_\pm) + h(\chi_\pm) \sum_{i=1}^{N} d_{i+} \\ \mathcal{A}_{1\pm} &= h(\chi_-) \sum_{i=1}^{N} a^2_{i+} c_{j-} + (1 - h(\chi_-)) \sum_{i=1}^{N} a^2_{i+} c_{j-} \\ c_{i\pm} &= \frac{\rho_{i\pm}}{\rho_{1\pm}} \qquad i = 1, \ldots, N. \end{aligned}$$

Then the function $f(p, \mathbf{W}_-, \mathbf{W}_+)$ has a unique root $p = p^*$ that is the unique solution for the pressure p^* of the Riemann problem (4.36), (4.38), (4.37). *The velocity v^* can be calculated using*

$$v^* = \frac{1}{2}(v_- + v_+) + \frac{1}{2}(f_-(p^*, \mathbf{W}_+) - f_-(p^*, \mathbf{W}_-))\,.$$

Proof
The function f is strictly increasing in p. For $p \to \min\{\mathcal{A}_{0-}, \mathcal{A}_{0+}\}$ the function f tends to $-\infty$. For $p \to +\infty$ we have $f \to +\infty$. Accordingly f has a unique root that by construction is the solution for the pressure p^* of the problem considered. The remaining part of the theorem is obvious.

Remark 3 *To determine the remaining unknown quantities of the solution one has to use the relations above. Here one has to take care for the type of the waves.*

Remark 4 *For the special case $N = 1$, $\chi_- = -1$ and $\chi_+ = 1$ Theorem 1 reduces to Theorem 6.2 (Solution of isothermal two-phase Euler equations without phase transition) in Dreyer et al. [32].*

Remark 5 *The paper [32] mentioned in the previous remark considers the case of single component flow where the phase creation is discussed.*
We can verify that the diffuse interface model with zero order terms is not able to deal with this situation because in the pure phases where $\chi = -1$ or $\chi = 1$ we have $h'(\chi) = 0$. This means that the diffusion term $-M_p(\frac{\partial \rho\psi}{\partial \chi})$ will be zero because

$$\rho\psi = W(\chi) + h(\chi)\rho\psi_L + (1 - h(\chi))\rho\psi_V,$$

which means that

$$\frac{\partial \rho\psi}{\partial \chi} = W'(\chi) + h'(\chi)(\rho\psi_L + \rho\psi_V),$$

which will be zero in the pure phases.

4.6 Numerical results

In this section we find the exact solution for the submodel by applying the results which are obtained before. We discuss the exact solutions for the cases $N = 1$ and $N > 1$ using Theorem 1. We use Newton's method in order to solve the equation (4.52) to determine the value of the pressure p^* in the star region . We selected six problems to illustrate the wave patterns and show the structure of the solution.

The case $N = 1$, Examples 1-4

In this case we will consider two pure phases. First we will discuss the solutions of the case vapor-vapor flow which will appear in the first two examples then we will consider the vapor-liquid case which will be discussed in the Examples 3 and 4. Later we will use those examples as a test cases in order to test various numerical methods.
Each Figure shows the profile of the phase field variable χ, the velocity v, the density ρ and the pressure p. The initial data of the four examples are given in Table 4.1.

Example	χ_-	p_-	v_-	χ_+	p_+	v_+
1	-1	1 Pa	0 m/s	1	0.1 Pa	0 m/s
2	-1	0.4 Pa	-2 m/s	1	0.4Pa	2 m/s
3	-1	2300 Pa	-100 m/s	1	1000 Pa	100 m/s
4	-1	60000 Pa	-200 m/s	1	100000 Pa	-50 m/s

Table 4.1: The initial values for four Riemann problem tests.

The first example is so called Sod test, see Sod [70]. In this example we consider two vapors to the left and to the right. This example is considered a good test case as a beginning. The solution consists of three waves a rarefaction wave moving to the left, a contact in the middle, and a shock moving to the right as we can see in Figure 4.6.
In the second example we consider the 123 problem, see Toro [75]. Figure 4.7 shows the solution which consists of two rarefactions and contact in the middle.
For the vapor-liquid flow we discuss the first two examples in the paper of Hantke et al. [32]. We consider two phases a vapor to the left and a liquid to the right. The solution of the both examples consists of three waves a rarefaction moving to the left, a contact in the middle and a shock moving to the right. Figure 4.8 illustrate the solution for example 3 as well as Figure 4.9 shows the solution of example 4. Table 4.2 shows the values in the star region.

Example	p_*	v_*
1	0.3262076 Pa	1.12022 m/s
2	0.00189 Pa	0 m/s
3	1335.3 Pa	100.0002 m/s
4	43531 Pa	-50.057 m/s

Table 4.2: The initial values for four Riemann problem tests.

The case $N = 2$, Example 5

Now we want to discuss the case of two phases where in each phase we consider $N > 1$ components. First we consider a 2-component example. The initial data of this case is given in Table 4.6

	χ	ρ_1	ρ_2	v
Left	-0.95	2.5	7.5	0
Right	0.5	600	800	0

Table 4.3: The initial values for the case $N = 2$.

The equation of state parameters are given as

	a_1	a_2	d_1	d_2
Vapor	200	300	0	0
Liquid	500	400	$-1.495 \cdot 10^8$	$-6.35 \cdot 10^7$

Table 4.4: The initial values for the case $N = 2$.

The solution consists of 4 constant states separated by a left shock, a contact discontinuity and a right rarefaction, see Figure 4.10. The wave speeds and the states in the star region are summarized in Table 4.5.

S_L	$S_{R,tail}$	$S_{R,head}$	p_*	v_*
-176.3412	289.925	422.207	2716903.0964	-132.2825

Table 4.5: The solution for the case $N = 2$.

The case $N = 3$, Example 6

In this example we consider the 3-component case. The initial data are given as

	χ	ρ_1	ρ_2	ρ_3	v
Left	-0.95	2.5	7.5	1	-50
Right	0.5	300	800	250	20

Table 4.6: The initial values for the case $N = 3$.

The equation of state parameters are

	a_1	a_2	a_3	d_1	d_2	d_3
Vapor	200	300	100	0	0	0
Liquid	250	400	200	$-7.45 \cdot 10^7$	$-6.35 \cdot 10^7$	$-3.15 \cdot 10^7$

Table 4.7: The initial values for the case $N = 3$.

The solution consists of three waves separate 4 states. Figure 4.11 shows two rarefaction waves moving to the left and to the right as well as a contact in the middle. The solution in the star region is

$S_{L,head}$	$S_{R,head}$	$S_{R,tail}$	$S_{R,head}$	p_*	v_*
-317.331	-252.907	343.028	348.604	305261.3806	14.4244

Table 4.8: The solution for the case $N = 3$.

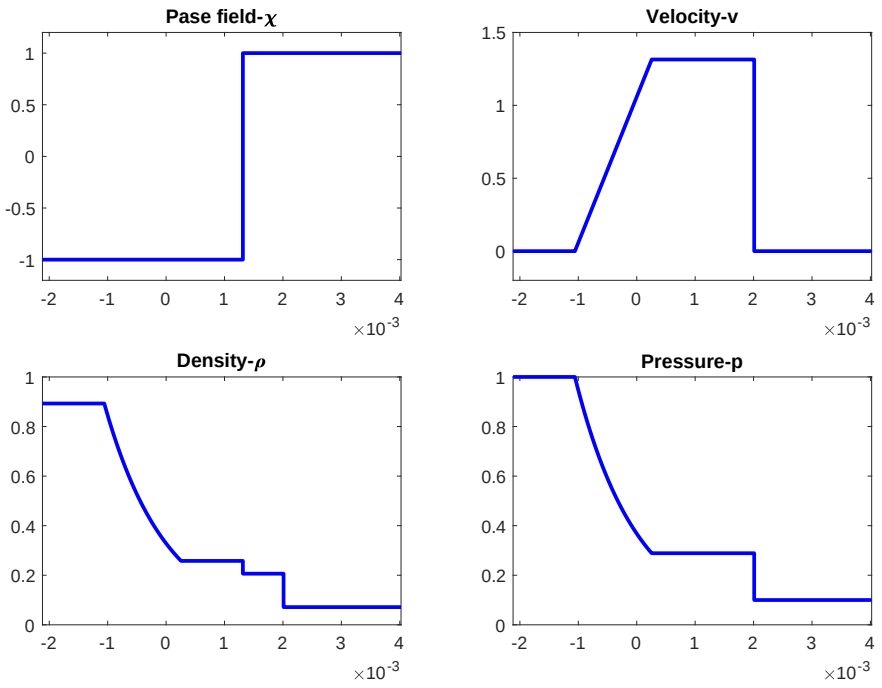

Figure 4.6: The exact solution of Sod test. Example 1.

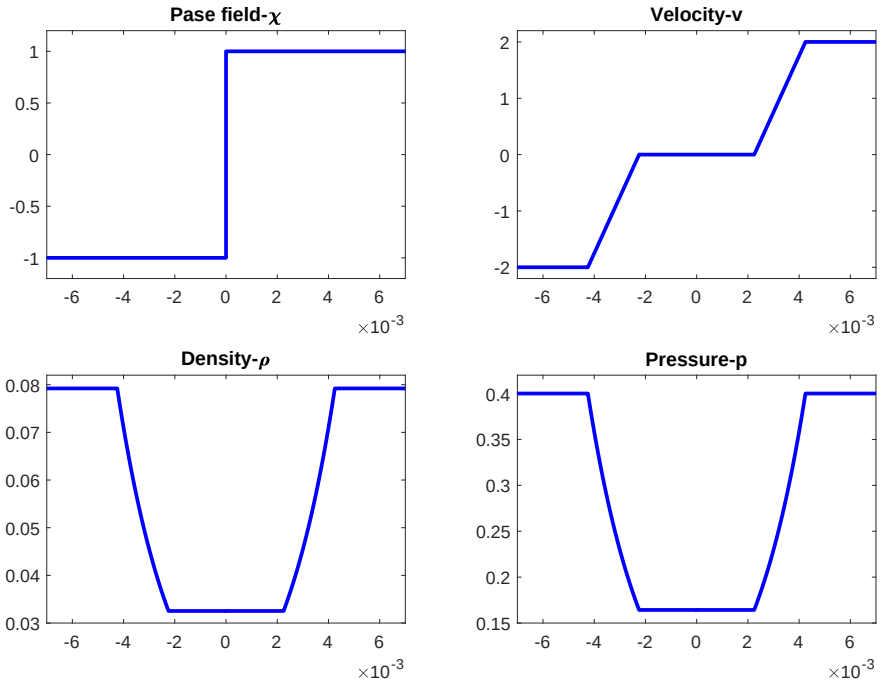

Figure 4.7: The exact solution of 123 problem. Example 2.

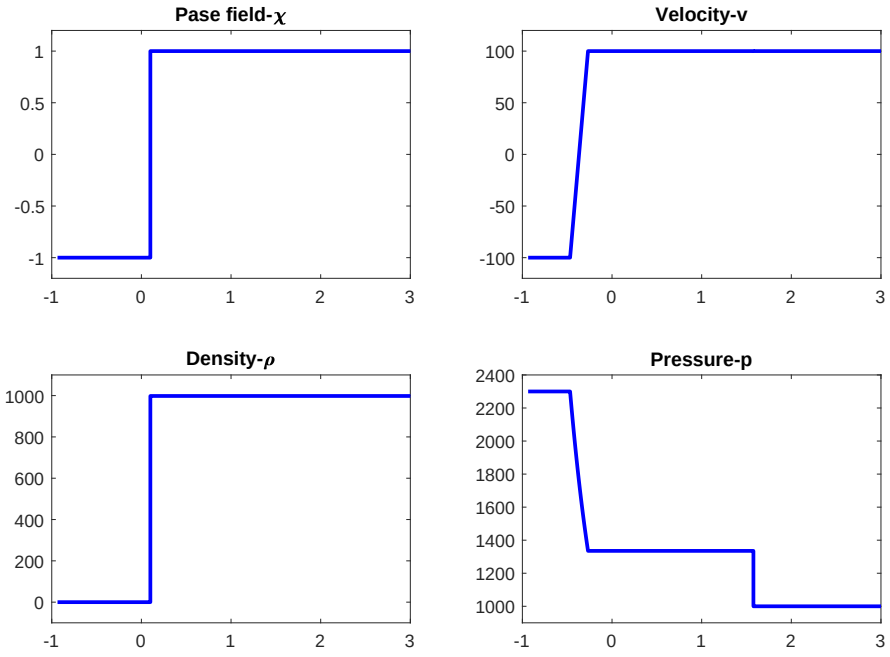

Figure 4.8: The exact solution. Example 3.

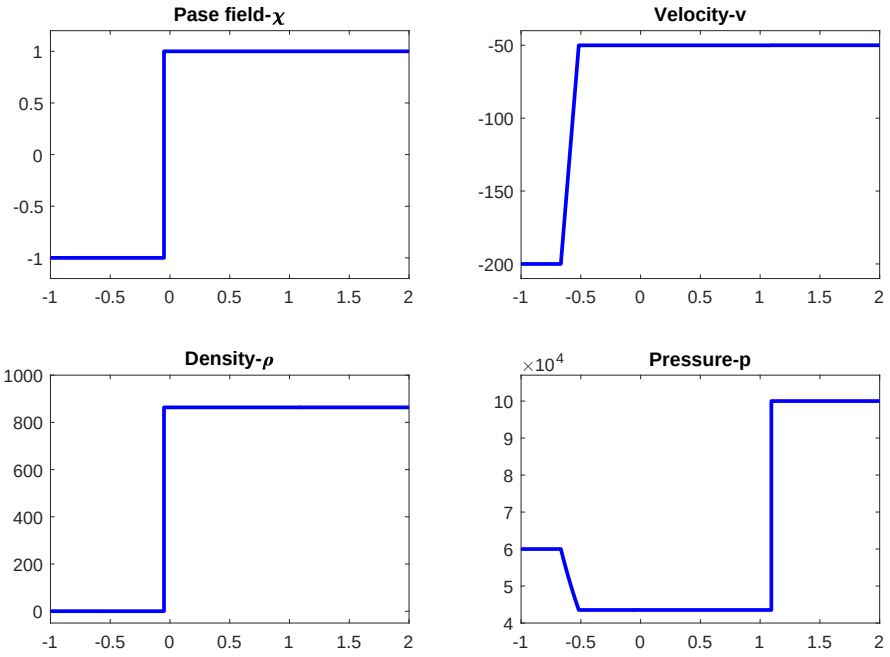

Figure 4.9: The exact solution. Example 4.

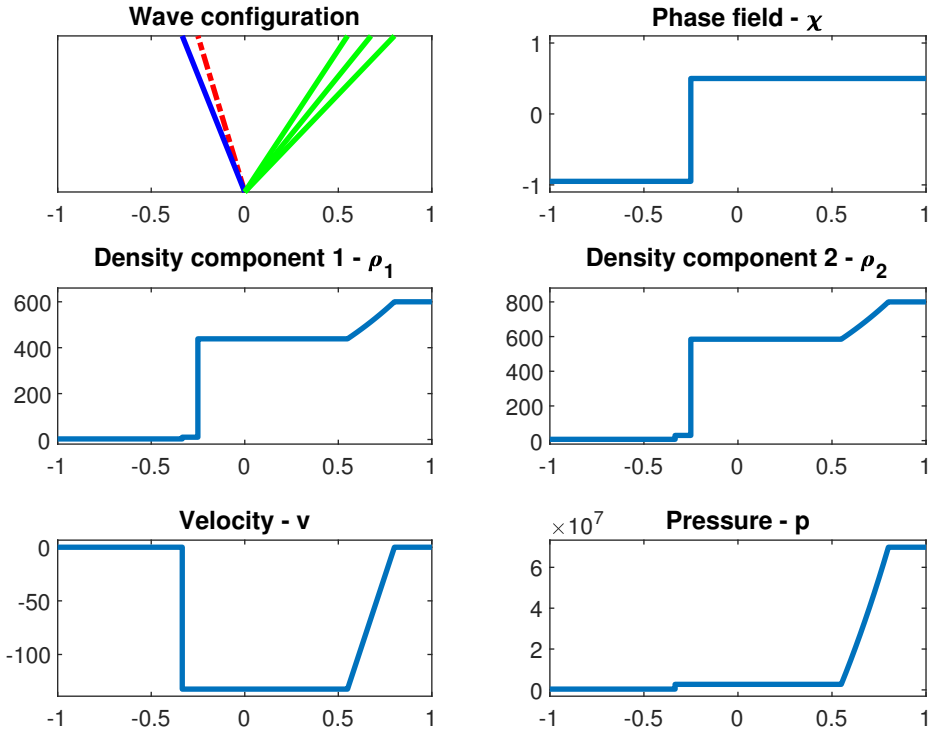

Figure 4.10: The exact solution for the case $N = 2$. Example 5.

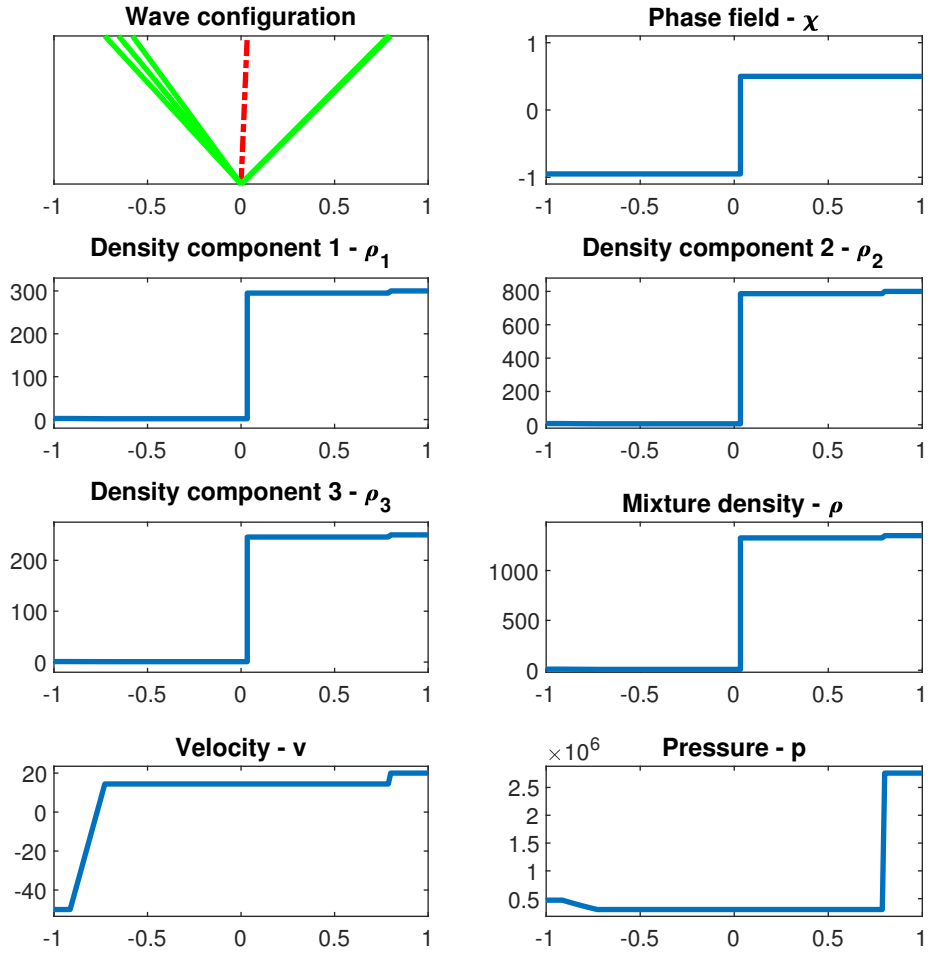

Figure 4.11: The exact solution for the case $N = 3$. Example 6.

Chapter 5

The numerical solution for vapor-vapor flow

5.1 Introduction

One of the main targets of this work is to present a numerical solution for the homogerneous part of a diffuse interface model presented in Chapter 3 and compare the results with the exact solution obtained in Chapter 4. For this goal we will consider two cases. The first one is the vapor-vapor flow which will be discussed in this chapter. Later on in this work we will consider the vapor-liquid flow case.
Actually this chapter is devoted to the vapor-vapor case because we think that this case will be useful in order to test the performance of our solvers and illustrate the structure of the solutions of Riemann problems before we handle the more complicated case which is the vapor-liquid case.
Before we start this study we will remind the reader of some basic concepts of the numerical treatment of hyperbolic conservation laws. Then we will apply those methods to the vapor-vapor case.
Many textbooks can be found in this field. We recommend the textbooks by Toro [75], Kröner [42], LeVeque [47] as well as Godlewski and Raviart [31]. Further details can be found in Murawski et al. [55], Brad er al. [16], Cocchi et al. [21], J. Paulo [23] Chertock et al. [20] and [19], LeVeque [46], Wang et al. [79] and [80], as well as Sohn [71]

5.2 Discretization

In order to utilize numerical methods for solving nonlinear conservation laws, we replace the continuous problem by a finite set of discrete values, which are obtained by discretizing the domain of the PDEs into a finite set of points or volumes via a mesh.
In this work we discretize the upper half plane $\mathbb{R} \times \mathbb{R}_{\geq 0}$ plane by a uniform mesh. The spatial domain $\mathbb{R}$ is discretized into cells with width $h = \Delta x$ and the time interval is discretized with time step $k = \Delta t$. We define the grid points (x_i, t^n) as

$$x_i = (i - \frac{1}{2})h, \quad i \in \mathbb{Z},$$
$$t^n = nk, \quad n \in \mathbb{N}_0.$$

It will be also useful to define the cell boundaries of a cell centered at x_i as

$$x_{i-\frac{1}{2}} = x_i - \frac{h}{2} = (i-1)h,$$
$$x_{i+\frac{1}{2}} = x_i + \frac{h}{2} = ih.$$

The aim of numerical methods is to produce approximations $u_i^n \in \mathbb{R}$ to the solution $u(x_i, t^n)$ applying a finite difference approach and use the point values at the grid points. In developing methods for conservation laws it is often preferable to produce an approximation using the finite volume approach where we use cell averages defined by

$$\bar{u}_i^n = \frac{1}{h}\int_{x_{i-\frac{1}{2}}}^{x_{i+\frac{1}{2}}} u(x, t^n)dx, \tag{5.1}$$

rather than the pointwise value.

5.2.1 Conservative Methods

Consider a scalar conservation law

$$u_t + f(u)_x = 0,$$

where $f = f(u)$ is the flux function. A conservative scheme for the scalar conservation law is a numerical method of the form

$$u_i^{n+1} = u_i^n - \frac{\Delta t}{\Delta x}[\mathrm{F}_{i-\frac{1}{2}} - \mathrm{F}_{i+\frac{1}{2}}],$$

where

$$\mathrm{F}_{i+\frac{1}{2}} = \mathrm{F}_{i+\frac{1}{2}}(u_{i-l_L}^n, ..., u_{i+l_R}^n),$$

with l_L, l_R two non-negative integers, $\mathrm{F}_{i+1/2}$ is called the numerical flux, an approximation to the physical flux $f(u)$. We assume that the flux function satisfies the consistency condition

$$\mathrm{F}_{i+\frac{1}{2}}(u, u, ..., u) = f(u)$$

for any $u \in \mathbb{R}$.

5.2.2 Godunov's method

Our aim is to solve the general initial value problem (IVP)

$$\begin{cases} \mathbf{u}_t + \mathbf{f}(\mathbf{u})_x = 0, \\ \mathbf{u}(x, 0) = \mathbf{u}_0(x), \end{cases} \tag{5.2}$$

for a system of conservation laws numerically. Godunov introduced a conservative extension of the first order upwind scheme to nonlinear system of hyperbolic conservation laws.
In Godunov's method we first define a piecewise constant distribution of the data by defining cell averages

$$\mathbf{u}_i^n = \frac{1}{h}\int_{x_{i-\frac{1}{2}}}^{x_{i+\frac{1}{2}}} \widetilde{\mathbf{u}}(x, t^n)dx, \tag{5.3}$$

where $\widetilde{\mathbf{u}}(x, t^n)$ are the initial data at time $t = t^n$. This produces the piecewise constant distribution $\mathbf{u}(x, t^n) = \mathbf{u}_i^n$, for x in each cell $I_i = [x_{i-\frac{1}{2}}, x_{i+\frac{1}{2}}]$.
A basic assumption of the method is that at a given time level n the data have a piecewise constant distribution of the form (5.3), which at time level n may be seen as a pairs of constant states (u_i^n, u_{i+1}^n) separated by a discontinuity at the intercell boundary $x_{i+1/2}$, which define a local Riemann problem.
The essential ingredient of Godunov's method is the solution of the Riemann problem, which may be the exact solution or some suitable approximation to it. Here we present the scheme in terms of the exact solution.
The Godunov method can be written explicitly in conservative form as

$$\mathbf{u}_i^{n+1} = \mathbf{u}_i^n - \frac{\Delta t}{\Delta x}[\mathbf{F}_{i-\frac{1}{2}} - \mathbf{F}_{i+\frac{1}{2}}], \tag{5.4}$$

where the intercell numerical flux function is

$$\mathbf{F}_{i+\frac{1}{2}} = \mathbf{F}(\mathbf{u}_i^n, \mathbf{u}_{i+1}^n) = \mathbf{f}(\mathbf{u}_{i+\frac{1}{2}}(0)).$$

We assume that the solution of the Riemann problem (5.2) exists. Here for each $i \in \mathbb{Z}$, $\mathbf{u}_{i+\frac{1}{2}}(0)$ is the value of the exact solution $\mathbf{u}_{i+\frac{1}{2}}(x/t)$ of the Riemann problem

$$\mathbf{u}(x, 0) = \begin{cases} \mathbf{u}_L = u_i^n \quad for \quad x < 0, \\ \mathbf{u}_R = u_{i+1}^n \quad for \quad x > 0, \end{cases} \tag{5.5}$$

evaluated at $x/t = 0$.

5.2.3 Approximate Riemann solvers

The method of Godunov requires the solution of Riemann problems which may be exact. This could cause some difficulties due to the complication of the equation of state or by the complexity of the particular system of equations being solved or both. We therefore present extensions of Godunov's scheme that utilize approximate Riemann solvers.
In this work we will present the numerical methods for solving Riemann problems in the one dimensional case. We will use the HLL approach of Harten, Lax, and van Leer, HLLC solver and VFRoe method for deriving an approximate solution to the Riemann problem. We will use the MUSCL method in order to achieve higher order of accuracy, see e.g. Toro [75].

The HLL solver

In this approach an approximation for the intercell numerical flux is obtained directly. It requires estimates for the smallest and the largest signal velocities in the Riemann problem. Assume that the signal speeds S_L and S_R are known. The integral average of the exact solution of the Riemann problem between the slowest and the fastest signals at time T is a known constant given by

$$\mathbf{U}^{hll} = \frac{S_R\mathbf{U}_R - S_L\mathbf{U}_L + \mathbf{F}_L - \mathbf{F}_R}{S_R - S_L}.$$

The approximate solution of the Riemann problem, called the HLL Riemann solver is given by

$$\mathbf{U}(x,t) = \begin{cases} \mathbf{U}_L & if \quad \frac{x}{t} \leq S_L \\ \mathbf{U}^{hll} & if \quad S_L \leq \frac{x}{t} \leq S_R \\ \mathbf{U}_R & if \quad \frac{x}{t} \geq S_R \end{cases}$$

The corresponding intercell flux for the approximate Godunov method is then given by

$$\mathbf{F}^{hll}_{i+1/2} = \begin{cases} \mathbf{F}_L & if \quad 0 \leq S_L \\ \frac{S_R\mathbf{F}_L - S_L\mathbf{F}_R + S_L S_R(\mathbf{U}_R - \mathbf{U}_L)}{S_R - S_L} & if \quad S_L \leq 0 \leq S_R \\ \mathbf{F}_R & if \quad 0 \geq S_R \end{cases}$$

The HLLC solver

As we have seen before, the HLL approximate Riemann solver considers three constant states separated by two waves. This means that the star region consists of a single state which could cause difficulties in some cases where we have a contact wave in the middle. In order to overcome this situation the HLL solver has been modified and applied using 4 constant states separated by 3 waves. This called the HLLC solver.
In this approach the middle wave speed S_* is included corresponding to the eigenvalue λ_2. See Toro [76] as well as Mignone and Bode [53].
The HLLC approximate Riemann solver is given by

$$\mathbf{U}(x,t) = \begin{cases} \mathbf{U}_L & if \quad \frac{x}{t} \leq S_L, \\ \mathbf{U}_{*L} & if \quad S_L \leq \frac{x}{t} \leq S_*, \\ \mathbf{U}_{*R} & if \quad S_* \leq \frac{x}{t} \leq S_R, \\ \mathbf{U}_R & if \quad \frac{x}{t} \geq S_R, \end{cases} \tag{5.6}$$

and the HLLC flux for the approximate Godunov method is given by

$$\mathbf{F}^{hllc}_{i+1/2} = \begin{cases} \mathbf{F}_L & if \quad 0 \leq S_L \\ \mathbf{F}_{*L} = \mathbf{F}_L + S_L(\mathbf{U}_{*L} - \mathbf{U}_L) & if \quad S_L \leq 0 \leq S_* \\ \mathbf{F}_{*R} = \mathbf{F}_R + S_R(\mathbf{U}_{*R} - \mathbf{U}_R) & if \quad S_* \leq 0 \leq S_R \\ \mathbf{F}_R & if \quad 0 \geq S_R \end{cases} \tag{5.7}$$

The Roe solver

We consider the system of the conservation laws of the form

$$\mathbf{U}_t + \mathbf{F}(\mathbf{U})_x = 0, \tag{5.8}$$

with the Riemann initial data

$$\mathbf{U}(x,0) = \mathbf{U}^0(x) = \begin{cases} \mathbf{U}_L & if \quad x < 0, \\ \mathbf{U}_R & if \quad x > 0, \end{cases} \tag{5.9}$$

where $\mathbf{U}$ is the vector of unknown conservative variables and $\mathbf{F}$ is the vector of fluxes.
As we have seen in Chapter 4 the system of conservation laws (5.8) can be written in the form

$$\mathbf{U}_t + \mathbf{A}(\mathbf{U})\mathbf{U}_x = 0, \tag{5.10}$$

where $\mathbf{A}$ is the Jacobian matrix.
Roe's approach based on replacing the Jacobian matrix $\mathbf{A}$ by a constant Jacobian matrix $\tilde{\mathbf{A}}$ which is given as

$$\tilde{\mathbf{A}} = \tilde{\mathbf{A}}(\mathbf{U}_L, \mathbf{U}_R), \tag{5.11}$$

which is a function of the data states $\mathbf{U}_L$ and $\mathbf{U}_R$.
Replacing the constant Jacobian matrix in (5.12) gives a linear system with constant coefficients and the system (5.8) is replaced by an approximate Riemann problem which can be solved exactly.
The Roe Jacobian matrix $\tilde{\mathbf{A}}$ must satisfy the following properties which are given in detail in Toro [75] and Roe [60]:

- The system should be hyperbolic.
- The Roe's matrix $\tilde{\mathbf{A}}$ should be consistent with $\mathbf{A}$.
- Conservative across the discontinuities.

Once we determine the matrix $\tilde{\mathbf{A}}$, its eigenvalues $\tilde{\lambda}$ and its eigenvectors $\tilde{\mathbf{K}}^{(i)}$ we write the data difference as

$$\Delta\mathbf{U} = \mathbf{U}_R - \mathbf{U}_L = \sum_{i=1}^{m} \tilde{\alpha}_i \tilde{\mathbf{K}}^{(i)},$$

from which we can determine the wave strength $\tilde{\alpha}_i = s_{Ri} - s_{Li}$.
The solution is given by

$$\mathbf{U}_{i+\frac{1}{2}} = \mathbf{U}_L + \sum_{\tilde{\lambda}_i \leq 0} \tilde{\alpha}_i \tilde{\mathbf{K}}^{(i)},$$

or

$$\mathbf{U}_{i+\frac{1}{2}} = \mathbf{U}_R - \sum_{\tilde{\lambda}_i \geq 0} \tilde{\alpha}_i \tilde{\mathbf{K}}^{(i)}.$$

The numerical flux is then given as

$$\mathbf{F}_{i+\frac{1}{2}} = \mathbf{F}_L + \sum_{\tilde{\lambda}_i \leq 0} \tilde{\alpha}_i \tilde{\lambda}_i \tilde{\mathbf{K}}^{(i)},$$

or

$$\mathbf{F}_{i+\frac{1}{2}} = \mathbf{F}_R - \sum_{\tilde{\lambda}_i \geq 0} \tilde{\alpha}_i \tilde{\lambda}_i \tilde{\mathbf{K}}^{(i)},$$

We may also write

$$\mathbf{F}_{i+\frac{1}{2}} = \frac{1}{2}(\mathbf{F}_R + \mathbf{F}_L) - \frac{1}{2} \sum_{i=1}^{m} \tilde{\alpha}_i \left|\tilde{\lambda}_i\right| \tilde{\mathbf{K}}^{(i)}.$$

The construction of the Roe matrix $\tilde{\mathbf{A}}$ which satisfies the properties mentioned above is not an easy task. It can be very complicated so that we seek a simpler approach where we can avoid this difficulty. In the next subsection we will introduce the VFRoe method where such difficulty is avoided.

The VFRoe solver

As we have seen before, the Godunov scheme and Roe's method require analytical computations which could be very difficult. In order to overcome such situations, we will present the method introduced by Gallouët and Masella [50], which is called the VFRoe method. This method does not require complicated analytical computations. It is based on the solution of a linearized Riemann problem and the Godunov scheme. In this method we consider the initial value problem (5.2), see [54] We rewrite the system of the conservation laws in terms of primitive variables as

$$\frac{\partial \mathbf{v}}{\partial t} + \mathbf{A}(\mathbf{v})\frac{\partial \mathbf{v}}{\partial x} = 0, \tag{5.12}$$

where $\mathbf{v} = (\rho, v, \chi)^\top$ is the vector of primitive variables and $\mathbf{A}$ is the Jacobian matrix which is given in Chapter 4. In terms of primitive variables we have the initial data of the Riemann problem at each cell boundary $x_{j+\frac{1}{2}}$ of the form

$$\mathbf{v}(x,0) = \begin{cases} \mathbf{v}_j, & x \le x_{j+\frac{1}{2}} \\ \mathbf{v}_{j+1}, & x > x_{j+\frac{1}{2}}. \end{cases} \tag{5.13}$$

Following the approach in [50] the Jacobian matrix $\mathbf{A}(\overline{\mathbf{v}})$ is calculated for the average state

$$\overline{\mathbf{v}} = \frac{\mathbf{v}_j + \mathbf{v}_{j+1}}{2}. \tag{5.14}$$

Hence the intermediate state in the solution of the Riemann problem (5.12), (5.13) is given by

$$\mathbf{v}^*_{j+\frac{1}{2}} = \mathbf{v}_j + \sum_{\lambda_i<0} \alpha_i \mathbf{r}_i, \tag{5.15}$$

where λ_i are the eigenvalues of the Jacobian matrix $\mathbf{A}(\overline{\mathbf{v}}_{j+\frac{1}{2}})$ and $\mathbf{r}_i$ are the corresponding eigenvectors.
Now we recalculate the conservative variables $\mathbf{U}^*_{j+\frac{1}{2}}$ and the Godunove scheme will be

$$\mathbf{u}_j^{n+1} = \mathbf{u}_j^n - \frac{\Delta t}{\Delta x}[\mathbf{f}(\mathbf{u}^*(\mathbf{u}_j^n, \mathbf{u}_{j+1}^n)) - \mathbf{f}(\mathbf{u}^*(\mathbf{u}_{j-1}^n, \mathbf{u}_j^n))]$$

$$\mathbf{u}^* = \mathbf{u}_L + \sum_{\lambda_i<0} \alpha_i \mathbf{r}_i.$$

MUSCL method

In this approach we replace locally the averages values $\mathbf{U}_i^n$ by piecewise linear function $\mathbf{U}_i(x)$ which is given as

$$\mathbf{U}_i(x) = \mathbf{U}_i^n + \frac{(x - x_i)}{\Delta x}\Delta_i, \quad x \in [x_{i-\frac{1}{2}}, x_{i+\frac{1}{2}}],$$

where Δ_i is a chosen slope of $\mathbf{U}_i$ in cell I_i with so called boundary extrapolated values which are the values of $\mathbf{U}_i(x)$ at the extreme points. They are given by

$$\mathbf{U}_i^L = \mathbf{U}_i(0) = \mathbf{U}_i^n - \frac{1}{2}\Delta_i, \quad \mathbf{U}_i^R = \mathbf{U}_i(\Delta x) = \mathbf{U}_i^n - \frac{1}{2}\Delta_i,$$

and evaluated by a time $\frac{1}{2}\Delta t$ according to

$$\begin{cases} \overline{\mathbf{U}}_i^L = \mathbf{U}_i^L + \frac{1}{2}\frac{\Delta t}{\Delta x}[\mathbf{F}(\mathbf{U}_i^L) - \mathbf{F}(\mathbf{U}_i^R)], \\ \overline{\mathbf{U}}_i^R = \mathbf{U}_i^R + \frac{1}{2}\frac{\Delta t}{\Delta x}[\mathbf{F}(\mathbf{U}_i^L) - \mathbf{F}(\mathbf{U}_i^R)]. \end{cases}$$

As a consequence of having modified the data, at each interface $x_{i+\frac{1}{2}}$ one now may consider the so called generalized Riemann problem. We seek now the solution of the generalized Riemann problem after the extrapolated values $\mathbf{U}_i^R$ and $\mathbf{U}_{i+1}^L$ are evolved to $\overline{\mathbf{U}}_i^R$ and $\overline{\mathbf{U}}_{i+1}^L$.
The intercell numerical flux $\mathbf{F}_{i+\frac{1}{2}}$ is then obtained from

$$\mathbf{F}_{i+\frac{1}{2}} = \mathbf{f}(\mathbf{u}_{i+\frac{1}{2}}(0)),$$

where $\mathbf{u}_{i+\frac{1}{2}}(0)$ is the exact similarity solution $\mathbf{u}_{i+\frac{1}{2}}(x/t)$ of the Riemann problem evaluated at $x/t = 0$.

5.3 Numerical methods for the submodel

In this section we consider the homogeneous part of the diffuse interface multiphase mixture model without chemical reactions. We consider first the case $N = 1$ which means we are dealing with two phases in each phase we have only one vapor. The model (3.5) in this case is

$$\begin{aligned} (\rho)_t + (\rho v)_x &= 0, \\ (\rho v)_t + (\rho v^2 + p)_x &= 0, \\ \rho\chi_t + \rho v\chi_x &= 0. \end{aligned}$$

As we consider two pure vapor phases, the mixture equation of state (3.8) is given as

$$p(\rho, \chi) = -W(\chi) + h(\chi)a_{V_1}^2\rho + (1 - h(\chi)a_{V_2}^2\rho. \tag{5.16}$$

Here the constants a_{V_1} and a_{V_2} are the speed of sound in the first vapor and the second vapor respectively. The constants d_{V_1} and d_{V_2} have the value zero in vapors. The Riemann initial data are given by

$$\mathbf{U}(x, 0) = \mathbf{U}^0(x) = \begin{cases} \mathbf{U}_L & if \quad x < 0, \\ \mathbf{U}_R & if \quad x > 0, \end{cases} \tag{5.17}$$

where $\mathbf{U} = (\rho, \rho v, \rho\chi)^\top$ is the vector of the conservative variables.
In order to asses the performance of this model we will not restrict our attention to the isothermal equation of state (5.16) previously considered. We will also consider the isentropic equation of state given by

$$p(\rho) = C\rho^\gamma,$$

where γ is the ratio of specific heat capacities and C is a constant evaluated by taking

$$C = \frac{p}{\rho^\gamma}, \tag{5.18}$$

from a reference state. We will discuss the difference between this equation of state and the isothermal equation of state and compare both results with the exact solution of the system which was obtained in Chapter 4 and the exact solution of the Euler system presented in Toro [75]. We will also see the behavior of the energy e and the temperature T which are given as

$$e = \frac{p}{(\gamma - 1)\rho},$$

and

$$T = \frac{p}{(\gamma - 1)c_v\rho}.$$

The local speed of sound will be obtained by

$$a^2 = \frac{\partial p}{\partial \rho} = C\gamma\rho^{\gamma-1},$$

which is again a function of ρ. The mixture speed of sound needed later is given as

$$A(\chi, \rho) = h(\chi)a_{V_1}^2 + (1 - h(\chi))a_{V_2}^2. \tag{5.19}$$

The mixture equation of state will be in this case

$$p(\rho) = -W(\chi) + h(\chi)C_{V_1}\rho^{\gamma} + (1 - h(\chi))C_{V_2}\rho^{\gamma}. \tag{5.20}$$

Our aim is to solve this system numerically and to show for various examples how the solutions to Riemann problems are influenced by the model used. The three models are the Euler and the diffuse interface equations with the isothermal equation of state (5.16) as well as these equations with the isentropic equation of state (5.21). For this purpose we will use the HLL, HLLC, VFRoe solver in order to find the first order solution. We will also use the MUSCL method to achieve second order.

5.4 Numerical results

In this section we present the numerical results for solving Riemann problems of the diffuse interface model on test cases and illustrate the performance of Riemann solvers considering different phases.
In all chosen tests the data consist of two constant states $\mathbf{W}_l = (\rho_l, v_l, p_l)$ and $\mathbf{W}_r = (\rho_r, v_r, p_r)$ separated by a discontinuity. The variable χ has the value -1 to indicate the phase to the left, and the value 1 to indicate the phase to the right. The spatial domain is the interval $[0, 1]$ which is discretized with $N = 500$ computing cells and the results are given after 250 time steps. All figures show the profiles of the conservative variables which are the density ρ, the momentum ρv and $\rho\chi$, also the constitutive variable, the pressure p, the velocity v and the phase indicator χ.
In the first example we consider the so called Sod test see Sod [70] and in the second one we consider the 123 problem see Toro [75] and Marie et al. [50]. In both tests we consider two vapors, V_1 to the left and V_2 to the right. They are governed by the isothermal equation of state

$$p(\rho) = -W(\chi) + h(\chi)(a_{V_1}^2\rho + d_{V_1}) + (1 - h(\chi))(a_{V_2}^2\rho + d_{V_2}),$$

where a_{V_1} and a_{V_2} are the speed of sound in the first vapor and the second vapor respectively. The parameters mentioned are given in Table 5.2 for the first test and in Table 5.5 for the second test.
In Examples 3 and 4 we consider again the Sod test and the 123 problem but we will use the isentropic equation of state

$$p(\rho) = -W(\chi) + h(\chi)(C_{V_1}\rho^\gamma + d_{V_1}) + (1 - h(\chi))(C_{V_2}\rho^\gamma + d_{V_2}), \tag{5.21}$$

where C is the constant obtained from (5.18). The constants d_{V_1} and d_{V_2} have the value zero in the both cases.

Example 1

First we consider the initial data of the Sod test which are given in Table 5.1. The equation of state parameters are given in Table 5.2 and the Courant number

Initial Data	p_{V_1}	v_{V_1}	ρ_{V_1}	p_{V_2}	v_{V_2}	ρ_{V_2}
Sod test	1.0	0	1.0	0.1	0	0.125

Table 5.1: The initial data for the case vapor-vapor/Sod test, see [70]

coefficient is $C_{cfl} = 0.9$.

Parameters	a_{V_1}	d_{V_1}	a_{V_2}	d_{V_2}
Sod test	1.0	0	0.894427	0

Table 5.2: The parameters for the case vapor-vapor/Sod test

Figures 5.1, 5.2, and 5.3 show the numerical results using the HLL, HLLC and

VFRoe solvers for the Sod test. Figure 5.4 shows the results using the MUSCL method.
The solution of the Sod test consists of a shock that moves to the right, a right going contact in the middle and a rarefaction wave traveling to the left. It has to be mentioned that the contact is not an Euler equation contact but the phase change contact since the energy equation in the Euler system is replaced by the equation for phase field.
Table 5.3 shows the values of the intermediate state in the star region using the solvers mentioned and the exact solution in the star region which is obtained in Chapter 4. One can notice, as expected, that the MUSCL and the exact results are nearly identical. The VFRoe solver presents better results than the HLL and HLLC solvers. While we can notice that the HLLC solver exhibits a better convergence to the exact solution than the HLL solver.

Results	$p^*_{V_1}$	$v^*_{V_1}$	$p^*_{V_2}$	$v^*_{V_2}$
HLL	0.3260862	1.1193367	0.3260865	1.1193293
HLLC	0.3260637	1.1194257	0.3260629	1.11942169
VFRoe	0.3260877	1.1193559	0.3260857	1.1193557
MUSCL	0.3262192	1.12016	0.326228	1.12013
Exact	0.3262076	1.12022	0.3262076	1.12022

Table 5.3: The results: The values in the star region using HLL, HLLC, VFRoe solvers and MUSCL method

Example 2

In the second example we will consider the 123 problem, see Toro [75]. We present the initial data in Table 5.4 where the proper equation of state parameters are given in Table 5.5. In all solvers the Courant number has the value $C_{cfl} = 0.9$ except for the VFRoe solver. We use $C_{cfl} = 0.6$ for it and one can notice that in this particular case the VFRoe scheme no longer provides a convergent solution since it blows up when we exceed this value of the CFL condition. The solution consists of two rarefaction waves where the vapor is pulled to the left and to the right. Due to the symmetrical initial conditions the contact is a ghost wave, see Galloët [30]. Figures 5.5, 5.6 and 5.7 show the first order solution profiles using the HLL, HLLC and VFRoe solvers respectively. Figure 5.8 gives the results using the MUSCL method for the second order as above are given in Table 5.6. As expected the second order methods converges faster to the exact solution. One can notice that the HLL solver is more diffuse than the HLLC solver and VFRoe but it gives good result.

Initial Data	p_{V_1}	v_{V_1}	ρ_{V_1}	p_{V_2}	v_{V_2}	ρ_{V_2}
123 problem	0.4	-2.0	1.0	0.4	2.0	1.0

Table 5.4: The initial data for the case vapor-vapor/123 problem, see [75]

The test	a_{V_1}	d_{V_1}	a_{V_2}	d_{V_2}
123 problem	0.632456	0	0.632456	0

Table 5.5: The parameters for the case vapor-vapor/123 problem

Results	$p^*_{V_1}$	$v^*_{V_1}$	$p^*_{V_2}$	$v^*_{V_2}$
HLL	0.001520186	0.046388889	0.001520681	0.045961276
HLLC	0.001520017	0.04650278	0.001520739	0.0459819
MUSCL	0.001658343	0.01232602	0.001667608	0.00878486
Exact	0.00189	0	0.00189	0

Table 5.6: The results: The values in the star region using HLL, HLLC, VFRoe solvers and MUSCL method

Example 3

In this example we will consider again the Sod test and from the initial data we will find the constant C.
Figure 5.9 presents the solution using the isentropic equation of state (5.21). The solution is monotone as in the Euler system. We have seen that this is not the case using the isothermal equation of state. The solution consists of three waves a rarefaction to the left, contact in the middle moving to the right and shock moving to the right. Comparing the results with the solution using the EOS (5.16) we see a difference in the wave structure where the solution is not monotone and comparing both results with the exact solution of Euler system in Toro [75] we find the similarity between the exact solution and the numerical solution using the isentropic EOS (5.21) where some differences appear when we use the isothermal EOS.
Figure 5.10 shows the structure of the sound speed a, the temperature T as well as the energy e which as expected have the same structure because the all quantities are proportional.

Example 4

In this example we will consider the 123 problem using the isentropic EOS. Figure 5.11 shows the solution. We notice that we have here the same structure comparing with the results using the isothermal equation of state (5.16) in Example 2 because we don't have a shock here.
The behavior of the sound speed a, the temperature T as well as the energy e is presented in Figure 5.12.

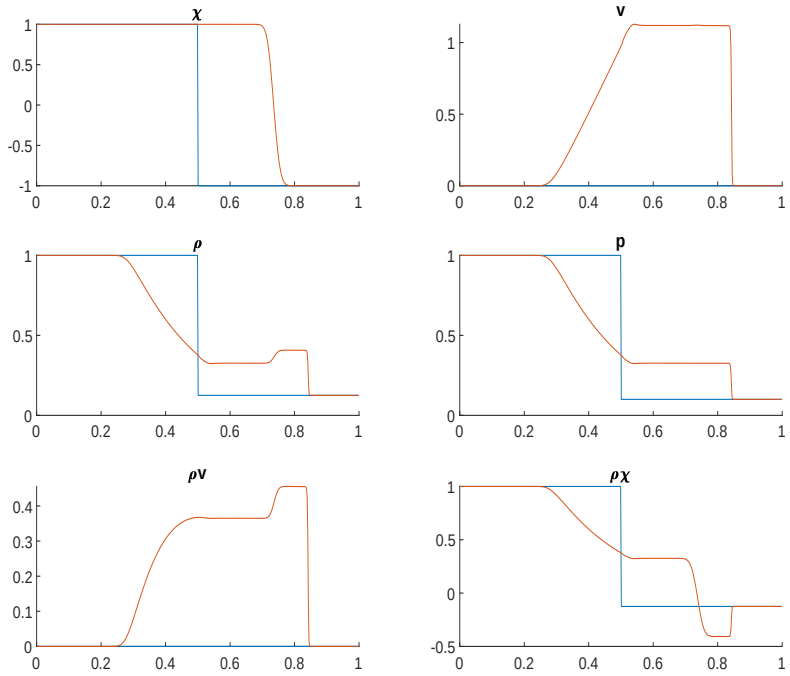

Figure 5.1: The solution: Sod test using the HLL solver, blue: the initial data, red: the numerical solution.

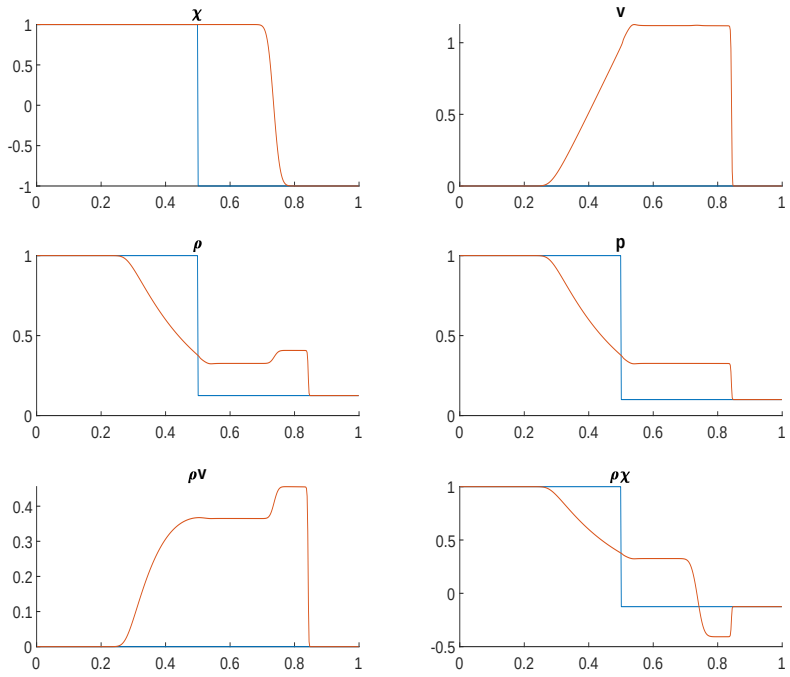

Figure 5.2: The solution: Sod test using the HLLC solver, blue: the initial data, red: the numerical solution.

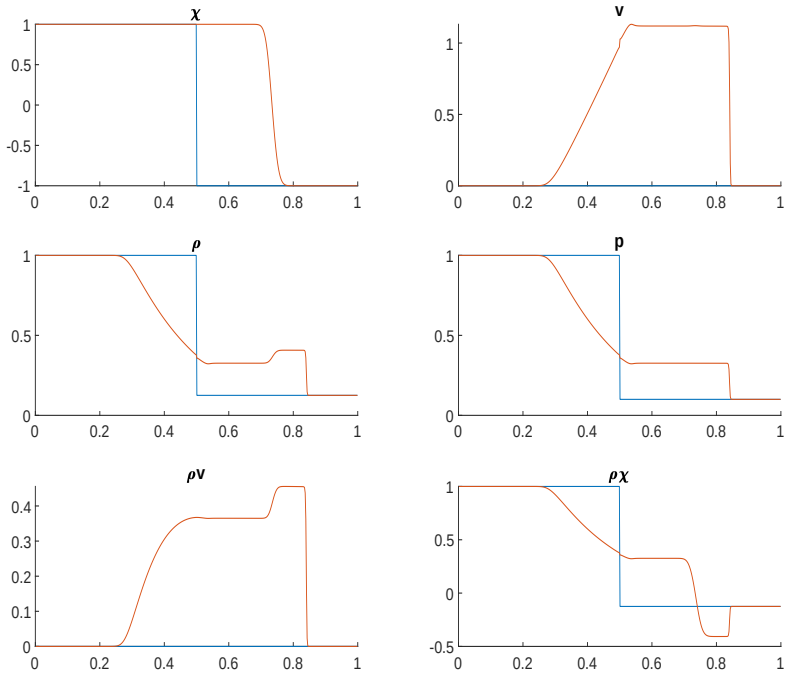

Figure 5.3: The solution: Sod test using the VFRoe solver, blue: the initial data, red: the numerical solution.

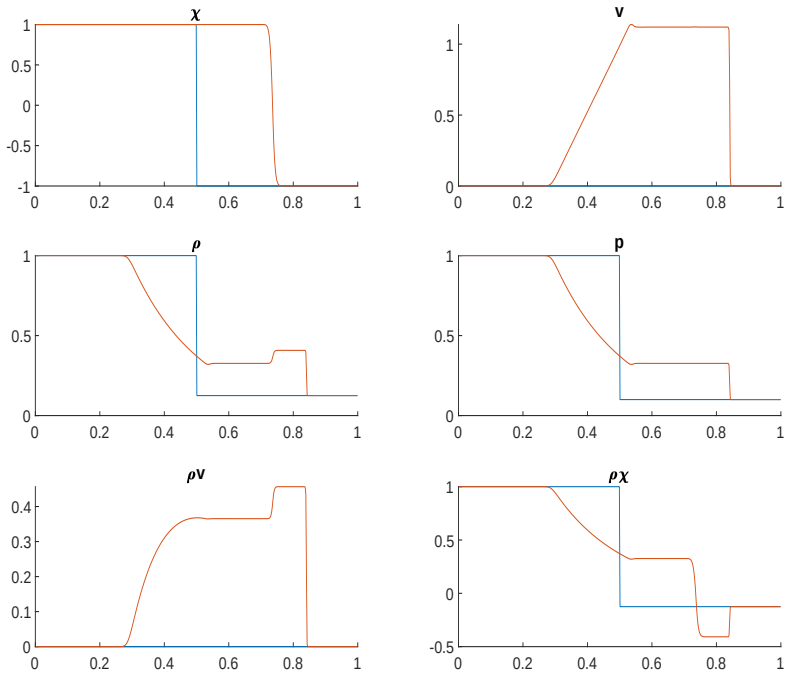

Figure 5.4: The solution: Sod test using the MUSCL method, blue: the initial data, red: the numerical solution.

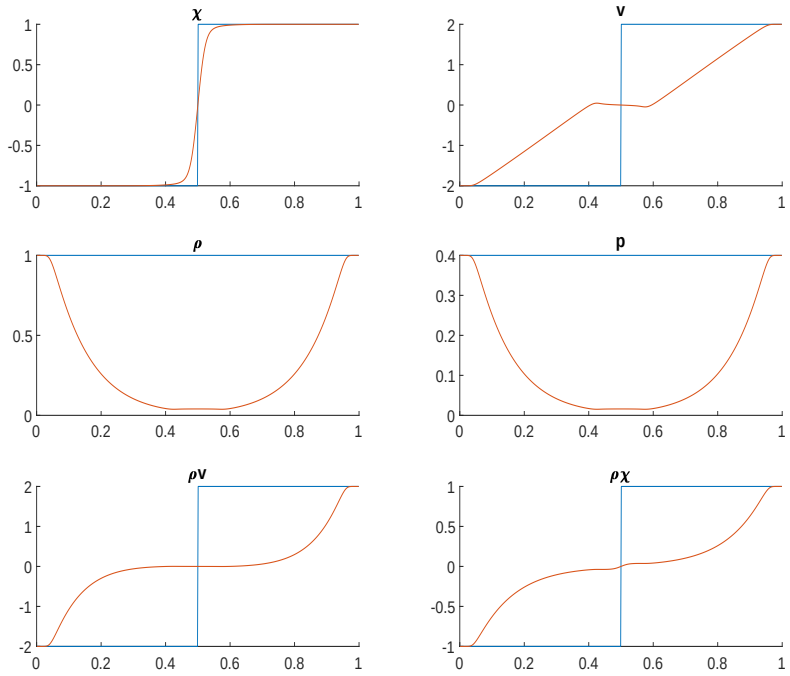

Figure 5.5: The solution: 123 problem using the HLL solver, blue: the initial data, red: the numerical solution.

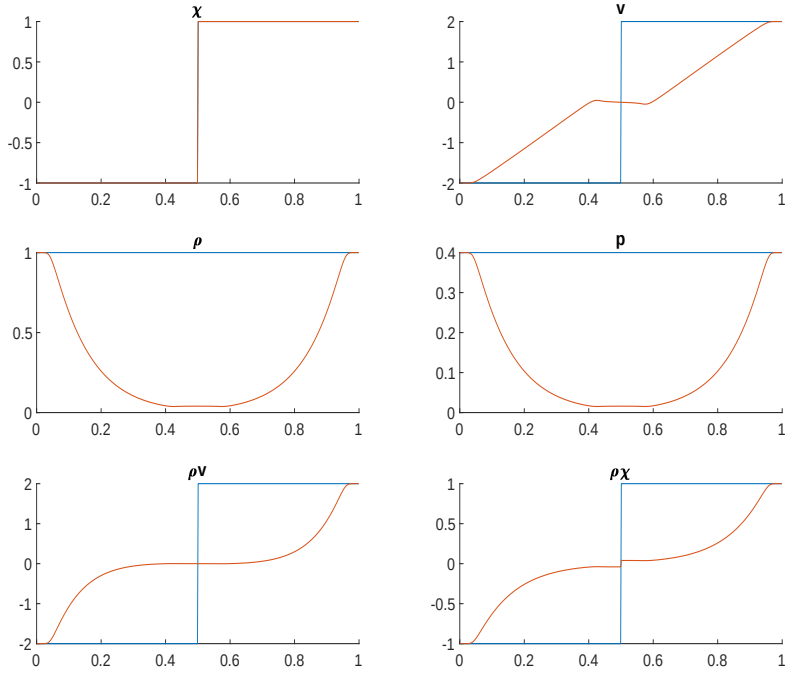

Figure 5.6: The solution: 123 problem using the HLLC solver, blue: the initial data, red: the numerical solution.

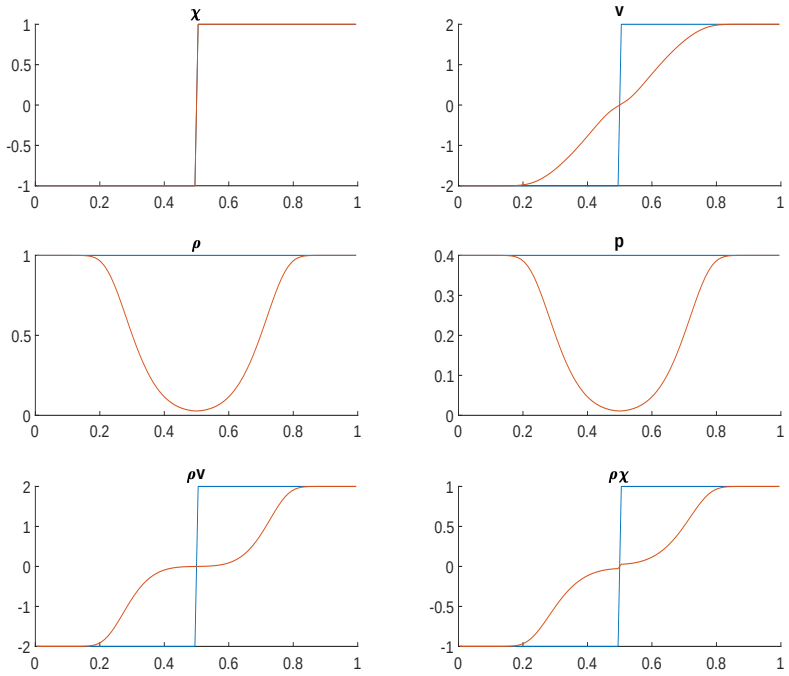

Figure 5.7: The solution: 123 problem using the VFRoe solver, blue: the initial data, red: the numerical solution.

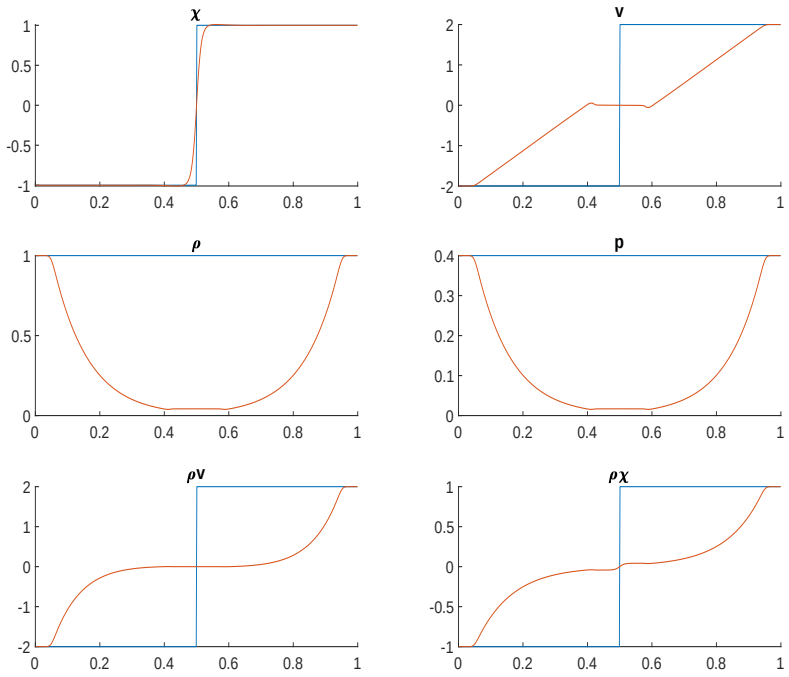

Figure 5.8: The solution: 123 problem using the MUSCL method, blue: the initial data, red: the numerical solution.

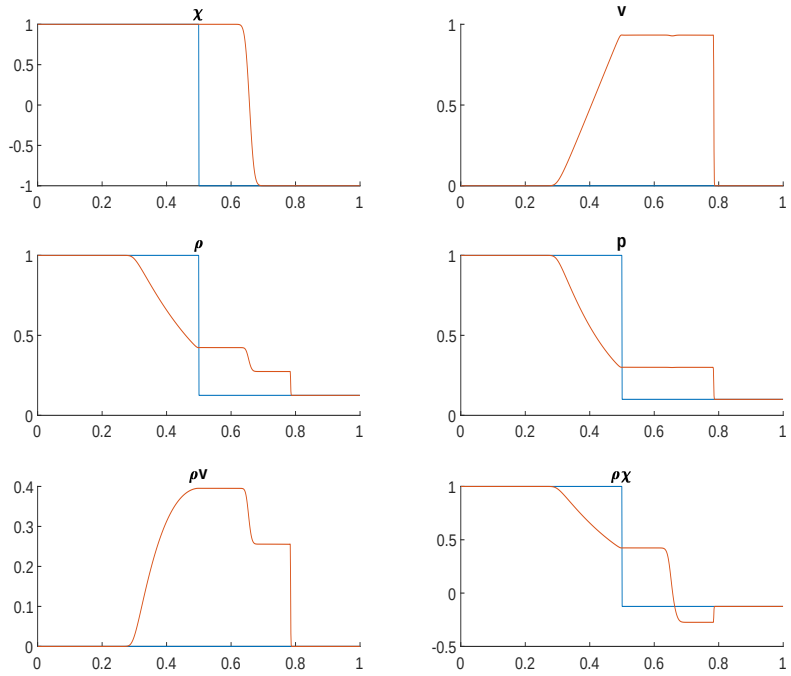

Figure 5.9: The solution: Sod test using the HLL solver with isontropic EOS, blue: the initial data, red: the numerical solution.

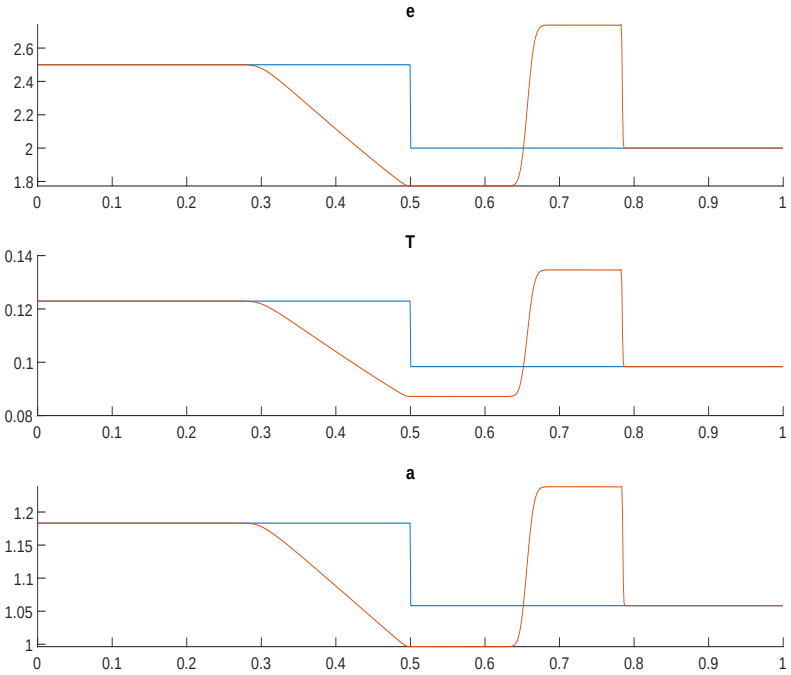

Figure 5.10: The structure of the sound speed a, the temperature T and the energy e for Sod test, blue: the initial data, red: the numerical solution.

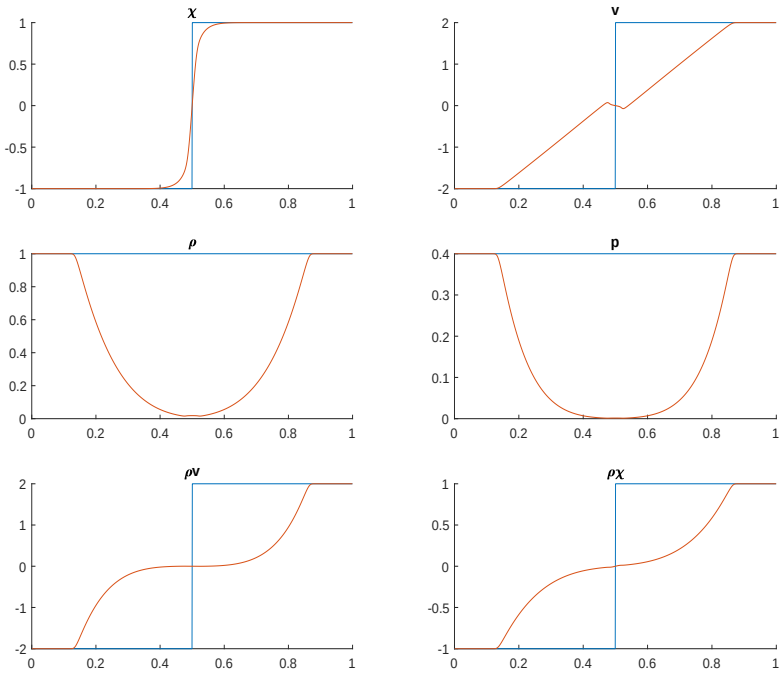

Figure 5.11: The solution: 123 problem using the HLL solver with isontropic EOS, blue: the initial data, red: the numerical solution.

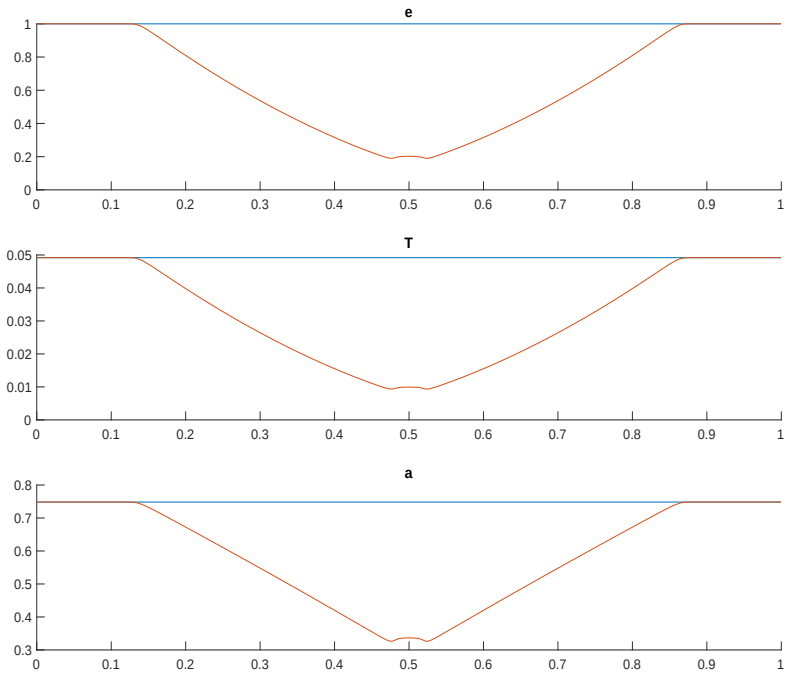

Figure 5.12: The structure of the sound speed a, the temperature T and the energy e for 123 problem, blue: the initial data, red: the numerical solution.

Chapter 6

The numerical solution for vapor-liquid flow

6.1 Vapor-liquid

In Chapter 5 we presented some numerical methods in order to solve the homogeneous part of the diffuse interface multiphase mixture model proposed in [24]. In order to test the performance of the model considered and the numerical methods presented in the previous chapter we assumed a mixture of two phases where in each phase we have vapors only.
Up to this point we could obtain good results and ensured that the numerical methods considered in Chapter 5 were able to solve that model in different examples. But the diversity of materials existing in nature implies that we need to consider more complicated cases such as vapor-liquid flows.
This chapter is devoted to the study of two phase flow without chemical reactions. In each phase we have either liquid or vapor. This case must be treated with some care due to the difficulties which appear.
In all of this chapter our principal goal is to solve Riemann problems for the homogeneous part of a diffuse interface model numerically and figure out which difficulties will occur when we consider the case of vapor-liquid. Furthermore we want to give strategies in order to overcome such difficulties.
First we consider two pure phases liquid (L) and vapor (V). In each phase we have only one constituent. The phase variable χ will indicate the present phase as $\chi = -1$ in a vapor phase. We will consider it on the left hand side. We take $\chi = 1$ for a liquid phase and will consider it on the right hand side. The interpolation function h in this case will have the values 1 in the liquid and 0 in the vapor. The phases will be separated by a diffuse interface and χ in this case will take values in $]-1, 1[$. The mixture is described using the model

$$\begin{aligned} \partial_t \rho + \partial_x(\rho v) &= 0, \\ \partial_t(\rho v) + \partial_x(\rho v^2 + p) &= 0, \\ \partial_t(\rho \chi) + \partial_x(\rho v \chi) &= 0, \end{aligned}$$

with the Riemann initial data

$$\mathbf{U}(x,0) = \mathbf{U}^0(x) = \begin{cases} \mathbf{U}_L & if \quad x < 0, \\ \mathbf{U}_R & if \quad x \geq 0. \end{cases} \tag{6.1}$$

The pressure p is given via the equation of state as a function of χ and ρ. As we have two pure phases the equation of state in this case will have the form

$$p(\rho) = -W(\chi) + h(\chi)(a_L^2\rho + d_L) + (1 - h(\chi))(a_V^2\rho + d_V), \tag{6.2}$$

where a_L and a_V are the sound speed in the liquid and vapor respectively and d_L and d_V are constants.
For the purpose of solving Riemann problems for the system of PDEs numerically, we will use the HLL solver presented in Chapter 5. The HLL solver seems to be an appropriate choice for the conserved quantities of the system, namely ρ and ρv.
In this work we use the computational domain $[0, 1] \times [0, T]$. The spatial domain $[0, 1]$ is discretized into uniform cells with width Δx. The time step Δt is determined via the CFL condition where we use the CFL number $C_{CFL} = 0.9$.
As an example we consider the initial data in Table 6.1 corresponding to Example 1 in [32],

Primitive variables	χ_L	p_L	v_L	χ_V	p_V	v_V
Initial data	1	2300 Pa	-100 m/s	-1	1000 Pa	100 m/s

Table 6.1: The initial data for the case vapor-liquid

with the equation of state parameters which are given in Table 6.2

Parameters	a_L	d_L	a_V	d_V
	1478.4 m/s	$-2.1817 \cdot 10^9$	367.8 m/s	0

Table 6.2: The equation of state parameters. Example 1

Based on the results obtained in [32] and in Chapter 4 the expectations are that we will get three waves, a shock wave moving to the left, contact wave in the middle, and a rarefaction moving to the right.
Starting some simulation for a liquid and a vapor phase with significant differences in the phase densities the computations immediately breaks down.
At first glance this seems to be surprising because the phase field models are developed to deal with phase mixtures. In particular, due to the design of the equation of state one may expect that mixture cells can be handled. Figure 6.1 shows the strange behavior of the solution and one can observe that the results obtained are unphysical.
We illustrate this situation in Figure 6.2 for pure water at room temperature. Here the pressure is presented as a function of the density ρ and the phase field χ.
The states on the left boundary correspond to pure vapor whereas the states on the right boundary indicate pure liquid water. One can see that for most states (χ, ρ) in the phase plane the pressure is negative. This means that these states are not meaningful.
Solving a Riemann problem for initially pure phases means that states on the left boundary are connected to the right boundary. In the exact Riemann solution, see Chapter 4, the intermediate state lies in the reasonable part of the mixture region in between. Our aim now is to preserve this property and explain why we get such results and how we can overcome this situation.

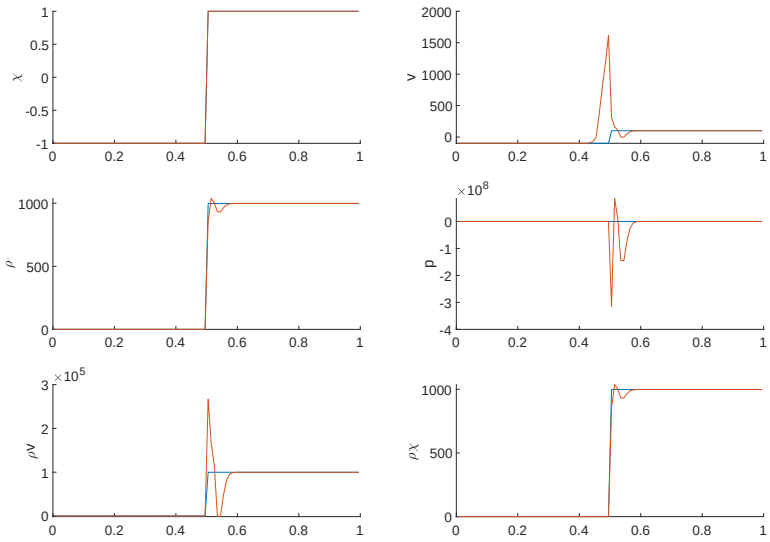

Figure 6.1: The solution: vapor-liquid case using the HLL solver, blue: the initial data, red: the numerical solution.

6.2 Numerical difficulties

The results obtained imply that we have a problem in our solver. It is due to the numerical dissipation in conjunction with the equation of state. In order to understand these results it is useful to solve the system for only one time step. Figure 6.3 shows the results after one time step. We can notice that we give correct values for χ and ρ. But we get a negative pressure. This means that the problem results from the interplay between the solver taking intermediate values at the phase interface leading to unphysical values in the equation of state (6.2). Figure 6.4 shows the area where we get the unphysical results in the ρ-p plane. In this area, once we consider a value of ρ we may get a negative pressure. This is the case in the above computation where usually the phase interface moves and does not coincide with any cell boundary after a certain time and all quantities will smear out during the calculations.

To understand the situation from a numerical point of view, we remind the reader that usually we are dealing with a grid using the cell size Δx. Our aim is to calculate the averages in each cell in order to apply the finite volume approach. We now consider that at time level t^n the phase boundary lies on a cell boundary. The question now is where will it lie after the time step Δt? If we are lucky the phase boundary after Δt will lie on a cell boundary again. But what will happen if the phase boundary lies inside a cell?.

As we do not consider phase transition the phase boundary moves with the velocity $v \neq 0$ during the time Δt. This means the phase boundary will travel the distance $v\Delta t$. Which means that the phase boundary will lie inside a cell, see Figure 6.5. In other words we will have a cell with two different phases and the averaging can lead to unphysical states.

In this chapter we examine two different procedures to overcome the unphysical

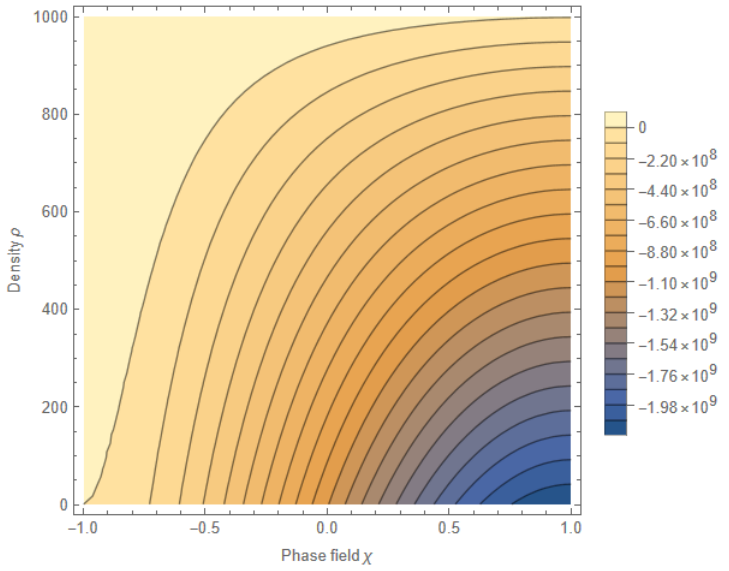

Figure 6.2: Pressure p depending on phase field χ and density ρ.

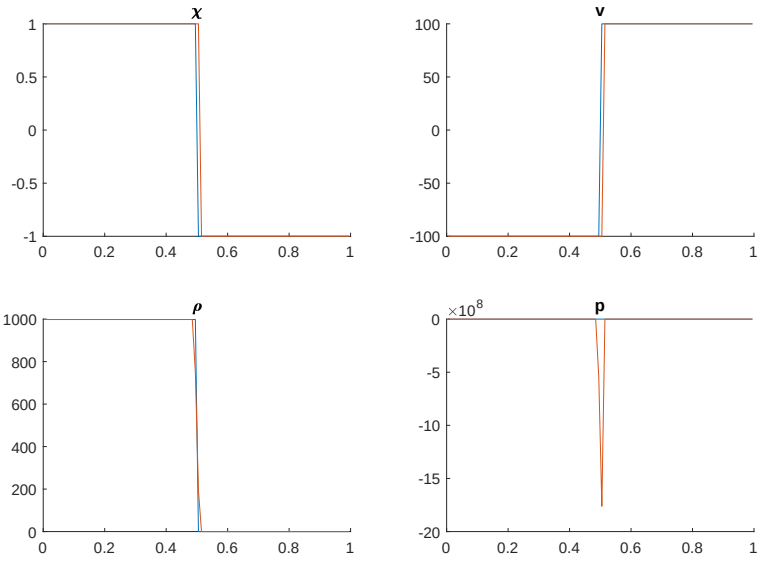

Figure 6.3: The solution after one time step. Blue: the initial data. Red: the numerical solution

results. The two strategies that we are going to use are:

- Tracking the interface.
- Estimating and fixing the pressure.

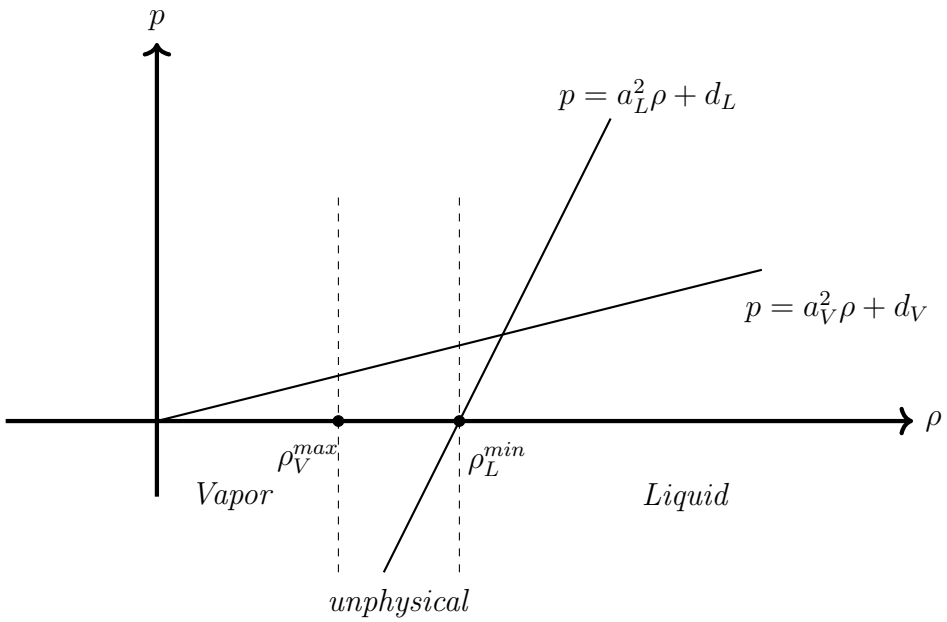

Figure 6.4: The equation of state in the vapor in liquid phases.

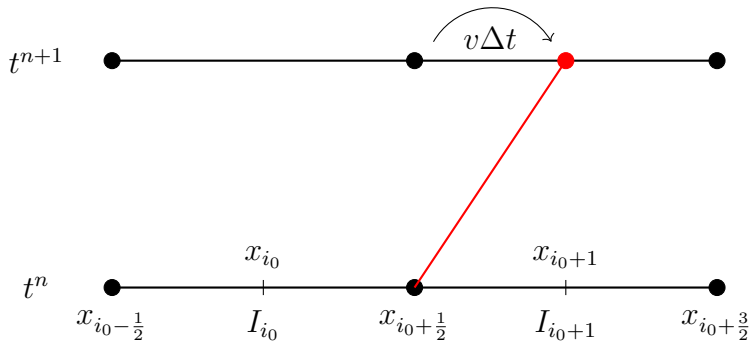

Figure 6.5: the mixture cell.

6.3 Tracking the interface

The main idea of this approach is to check the grid in each time step in order to test if the phase boundary lies on the cell boundary or not. This approach was successfully applied in the thesis of Thein [73] in order to solve the isothermal Euler equations numerically. If the phase boundary lies again on the cell boundary then we can go to the next time step, if not, we will align the grid to the phase boundary. This implies that we have

$$\begin{aligned} &\text{either} \quad \chi = -1 \quad \Rightarrow \quad h(\chi) = 0, \qquad \text{for a vapor phase,} \\ &\text{or} \qquad \chi = 1 \quad \Rightarrow \quad h(\chi) = 1. \qquad \text{for a liquid phase.} \end{aligned}$$

The equation of state (EoS) in this case will be

$$p(\rho) = -W(\chi) + \underbrace{h(\chi)(a_L^2\rho + d_L)}_{=0 \text{ in vapor}} + \overbrace{(1 - h(\chi))(a_V^2\rho + d_V)}^{=0 \text{ in liquid}}. \tag{6.3}$$

Aligning the grid will change the size of the cells and we have to deal with different cell sizes.
Suppose the phase boundary lies on the boundary $x_{i_0+1/2}$ of the cell I_{i_0} at the time step t^n. This means that at the time step $t^{n+1} = t^n + \Delta t$ the phase boundary will move the distance $v\Delta t$. The new cell boundary according to the new location of the phase boundary will be then $x_{i_0+1/2} = x_{i_0+1/2} + w\Delta t$, see Figure 6.6.

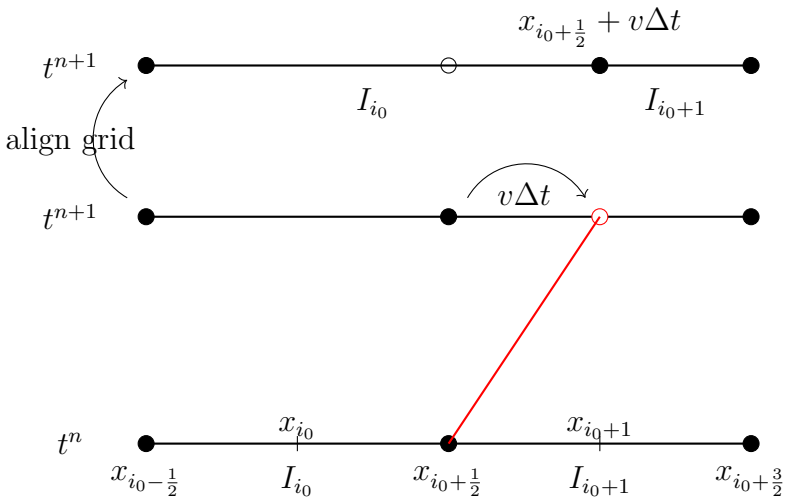

Figure 6.6: after changing the grid.

The new cell size is $\Delta x_{av} + w\Delta t$ could be too large or too small, where $\Delta x_{av} = (b-a)/N$. With a too small cell we get a severe time step restriction to maintain stability via the CFL condition. Too large cells give loss of accuracy. We choose therefore two parameters $0 < \epsilon_1 < 1 < \epsilon_2$. We will determine two cases:

- If a cell satisfies $\Delta x_i < \epsilon_1 \Delta x_{av}$ the cell is too small. We merge it with the neighboring one.
- If a cell satisfies $\Delta x_i > \epsilon_2 \Delta x_{av}$ the cell is too large. We split it into two cells.

Thereby, we get a modified grid where the phase boundary will always lie on a cell boundary. We do the same for the next time level.
The Godunov conservative form in this case reads

$$\mathbf{U}_i^{n+1} = \frac{\Delta x_i^n}{\Delta x_i^{n+1}} \mathbf{U}_i^n - \frac{\Delta t}{\Delta x_i^{n+1}} [\mathbf{F}_{i+\frac{1}{2}} - \mathbf{F}_{i-\frac{1}{2}}],$$

where Δx_i^n and Δx_i^{n+1} are the cell sizes at the time step t^n and t^{n+1}.
In order to calculate and update the time step we start with the initial time step which is obtained by using

$$S_{max}^0 = \max\{|v-a|, |v+a|\} \quad \text{and} \quad \Delta t = C_{CFL} \frac{\Delta x_0}{S_{max}^0}.$$

We recalculate the time step using

$$\Delta x_{min} = \min_{i=1,\dots,N} \{\Delta x_i | \Delta x_i \geq \epsilon_2 \Delta x_{av}\},$$
$$S_{max}^n = \max |S|,$$

as

$$\Delta t = C_{CFL}\frac{\Delta x_{min}}{S^n_{max}}.$$

The solution at the interface

Now we want to present the solution at the phase boundary. As we discuss the case without phase transition and according the results in Chapter 4 we found that $[\![p]\!] = 0$ and $[\![v]\!] = 0$, and using the wave speed estimates for the HLLC solver, see Chapter 5, we get

$$\begin{aligned} S_L &= u_L + a_L, \\ S_V &= u_V - a_V, \\ w &= \frac{p_L - p_V + \rho_V u_V(S_V - u_V) - \rho_L u_L(S_L - u_L)}{\rho_V(S_V - u_V) - \rho_L(S_L - u_L)}, \\ \rho^*_L &= \rho_L \frac{S_L - u_L}{S_V - w}. \end{aligned}$$

Here S_V and S_L denote the velocities of the classical waves. The density is calculated according to the HLLC solver as presented in Chapter 5. The pressure p^* will be calculated using the equation of state.

6.3.1 Numerical results

In this section we will test tracking the interface approch presented in previous section on many examples. We will compare the results with the exact solution obtained before as well as with the exact solution in Toro [75].

Example 1

We consider again Example 1 with the initial data as given in Table 6.3. This Example corresponds to Example 1 in [32] and in Chapter 4 where the exact solution is presented. We will solve the system (6.1) supplied with the equation of state (6.2) using tracking the interface based on the HLL solver.

primitive variables	p_L	v_L	p_V	v_V
Initial Data	2300 Pa	-100 m/s	1000 Pa	100 m/s

Table 6.3: The initial data for the case vapor-liquid

Figure 6.7 shows the solution which consists of two waves, a shock moving to the right and a rarefaction moving to the left.
In Table 6.4 we can see the numerical results after applying the approach discussed before with a different number of cells and the values in the star region.

Example 2

The initial data of this Example are given in Table 6.5 and correspond to Example

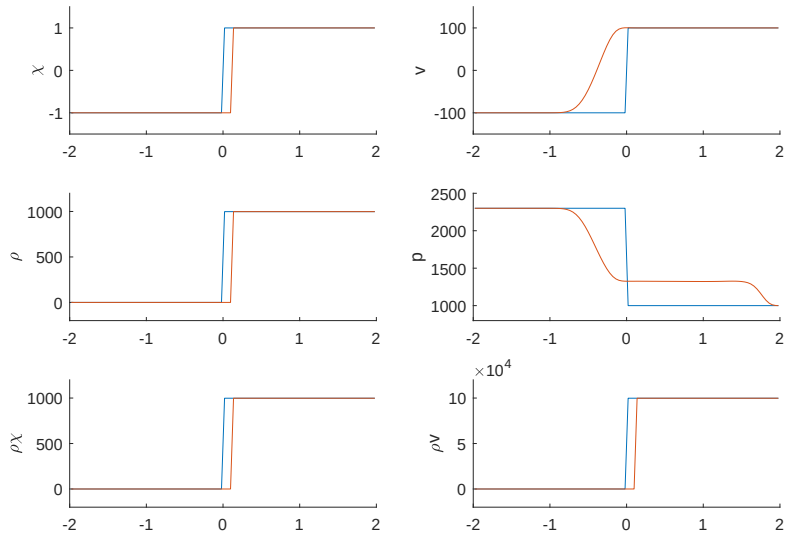

Figure 6.7: The solution of Example 1: vapor-liquid case using the HLL solver, blue: the initial data, red: the numerical solution.

Cells	p_L	v_L	p_V	v_V
100	1329.2 Pa	100.45071 m/s	1328.9 Pa	100.38174 m/s
800	1333.0 Pa	100.1242 m/s	1333.0 Pa	100.1193 m/s
1500	1333.8 Pa	100.0784 m/s	1333.8 Pa	100.0767 m/s
4000	1334.7 Pa	100.0363 m/s	1334.7 Pa	100.0360 m/s
Exact solution	1335.3 Pa	100.0002 m/s	1335.3 Pa	100.0002 m/s

Table 6.4: The values in the star region on different grids

2 in Hantke et al. [32] where the exact solution is presented as well as in Thein [73] where one can see the numerical solution.

primitive variables	p_L	v_L	p_V	v_V
Initial Data	60000 Pa	-200 m/s	100000 Pa	-50 m/s

Table 6.5: The initial data for the case vapor-liquid

Figure 6.8 illustrates the numerical results and shows the wave structure. The solution consists in this case of two rarefaction waves moving to the left and to the right.
The values in the star region are given in Table 6.6 using different number of cells and for comparison we provide the values of the exact solution given in [32].

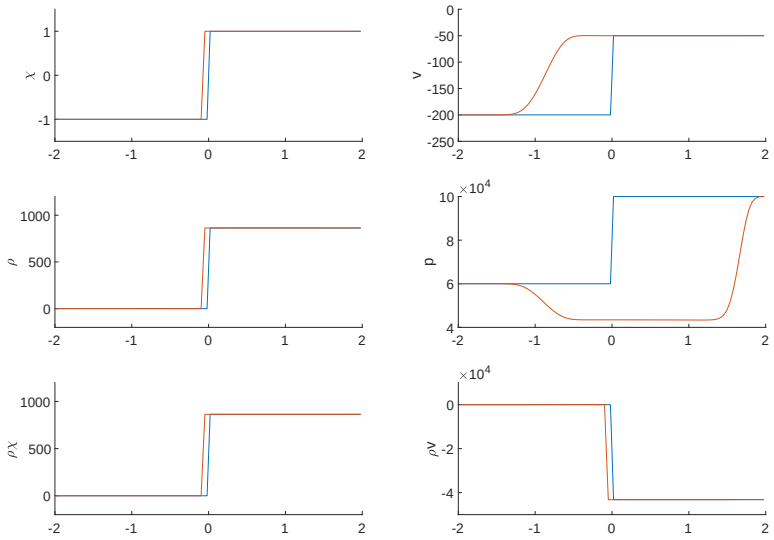

Figure 6.8: The solution of Example 2: vapor-liquid case using the HLL solver, blue: the initial data, red: the numerical solution.

Cells	p_L	v_L	p_V	v_V
100	43451 Pa	-50.057246 m/s	43450 Pa	-50.057247 m/s
800	43511.2 Pa	-50.05718612 m/s	43511.1 Pa	-50.05718617 m/s
1500	43518.65 Pa	-50.05717861 m/s	43518.62	-50.05717865 m/s
4000	43525.407 Pa	-50.057171781 m/s	43525.406 Pa	-50.057171783 m/s
Exact solution	43531 Pa	-50.057 m/s	43531 Pa	-50.057 m/s

Table 6.6: The results after checking the grid

6.4 Estimating the mixture pressure

In the previous section we solved the system (6.1) supplied with the equation of state (6.2) numerically using a tracking of the interface approach. This approach provided us with a numerical solution of the system considered and enabled us to avoid the unphysical results. But one can notice that splitting the mixture cell into two cells means that the phase variables χ will have only two values, either -1 in the vapor phase or 1 in the liquid phase. This means that the equation of state in the vapor phase will be

$$p(\rho) = (a_V^2 \rho + d_V), \tag{6.4}$$

because by definition $h(\chi) = 0$. In the liquid phase $h(\chi) = 1$ which implies that the equation of state will be

$$p(\rho) = (a_L^2 \rho + d_L). \tag{6.5}$$

The phase variable χ will never have a value in]-1,1[. This procedure will prevent us from dealing with the interface as a diffuse interface. However the interface will be treated as a sharp interface which is not our aim. On other words, tracking the

interface approach did not deal with the complete equation of state. Instead of that, only with parts of it.
As we are interested in the complete equation of state our intent is to find another strategy to avoid the unphysical results.
The major focus of this section is to find an approach which maintains the structure of the equation of state (6.2). In order to do that we will introduce an "estimating the pressure approach". In the following sections we will start by explaining the idea of estimating a value of the pressure then use this value to solve the model considered.

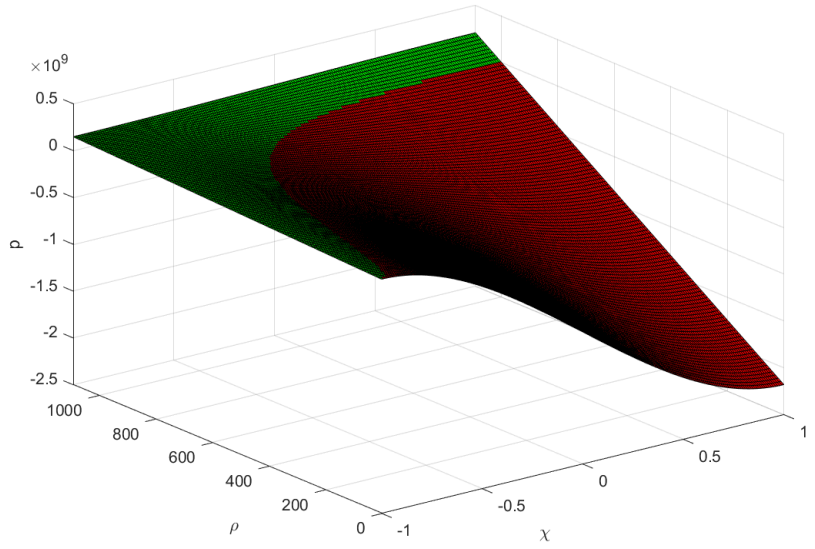

Figure 6.9: The pressure function, green: the positive, red: the negative.

The main idea

Usually, in order to calculate the pressure at the time level n via the equation of state we start with the values of χ^n and ρ^n using the Riemann solvers, in this case the HLL solver. In order to find the pressure p^{n+1} at the time level $n+1$ we find first χ^{n+1} and ρ^{n+1}. Again using the equation of state we evaluate p which in mixture cells most probably gives a negative value due to the nature of the equation of state considered. Figures 6.9 and 6.2 show the graph of the pressure function in the variables χ and ρ. One can see that the negative area is very big especially near the liquid phase. This means it would be useful to find the pressure without using the equation of state in the mixture cells to avoid unphysical values in the liquid phase and for mixtures where $\chi \in]-1, 1[$.
The question now is whether we can find a value for the pressure by estimating a positive value of p^{n+1} directly from p^n without using χ^{n+1} and ρ^{n+1} in the equation of state.
The conserved quantity ρ can be evaluated using Riemann solvers, i.e. in our case the HLL solver.

It remains to find the phase variable χ. This variable is an artificial quantity indicates that the phases present and has no additional meaning. This quantity is not conserved. Discretizing the transport equation of the variable χ will lead sometimes to some difficulties. To avoid such difficulties we use the equation of state to find the third variable χ^{n+1}. We substitute the variables p^{n+1} and ρ^{n+1} in the equation of state.
We summarized this approach as following:

- We estimate a value of the pressure p.
- We find the density ρ using the Riemann solver.
- We find the phase variable χ by substituting p and ρ into the equation of state and then solving it numerically for χ.

Figure 6.10 illustrate the path of the new approach.

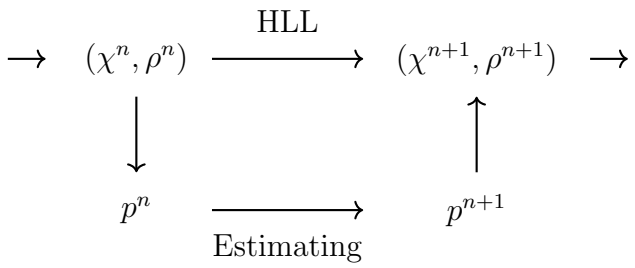

Figure 6.10: The path of the new approach.

It has to mention that this approach is done only local for mixture cells. The question now is how to estimate a value of the pressure without considering χ and ρ?

6.4.1 A piston problem

According to the physical properties of the liquid and the vapor, we observe when we compress or decompress a gas or a liquid that most of the changes occur in the gas phase. This means that most of the effects will appear in the vapor. To illustrate this idea we notice in Figure 6.11 that a small difference in the pressure causes a big difference in the density of the gas phase whereas a big change in the pressure in the liquid phase could be barely noticed and causes a very small change in the density. This is the almost incompressibility of the liquid. The useful interpretation of this comes from the fact that the speed of sound in the liquid phase is much larger than that in the gas phase.
As long as we can consider that there are no effects in the liquid phase, we will treat the liquid phase as an incompressible liquid. In order to make this idea work in practice it is useful to consider the liquid phase as a wall. When this is the case, our main task now is to solve a problem on the boundary of a wall.
To make this idea precise, we consider a Riemann problem with vapor phase to the left and a wall to the right. This is a type of piston problem. We consider again Example 1 where the initial data are given in Table 6.7. This example is illustrated

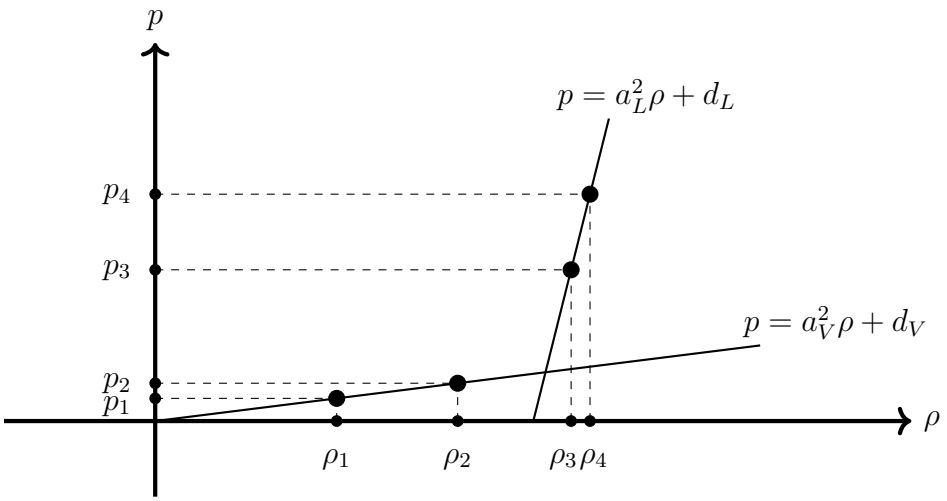

Figure 6.11: The equation of state in the vapor and liquid.

Primitive variables	p_L	v_L	p_V	v_V
Initial data	2300 Pa	-100 m/s	1000 Pa	100 m/s

Table 6.7: The initial data for the case vapor-liquid

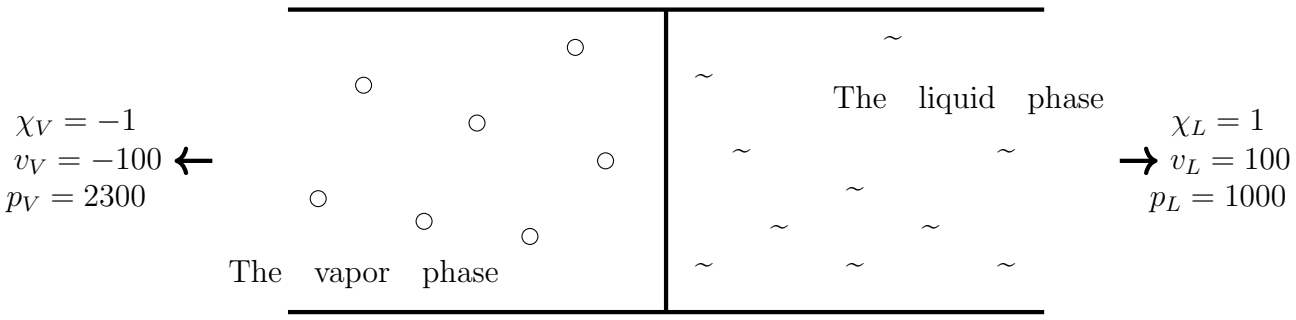

Figure 6.12: The vapor-liquid phases.

in Figure 6.12.
We want to employ the piston problem in the process of solving this example. Note that the velocity difference between the phases is 200 m/s. We use Galilean invariance to assume that the liquid is a solid wall at rest while the vapor moves at -200 m/s. Figure 6.13 illustrates the idea. We will use this problem to obtain an estimated value of the pressure for mixture cells in two ways

- Solving Riemann problem on the wall numerically.
- Finding the exact solution on the wall.

6.4.2 Estimating the pressure numerically

In this subsection we want to discuss the use of the above piston problem for the solution at the phase boundary. This discussion will be based on the idea of esti-

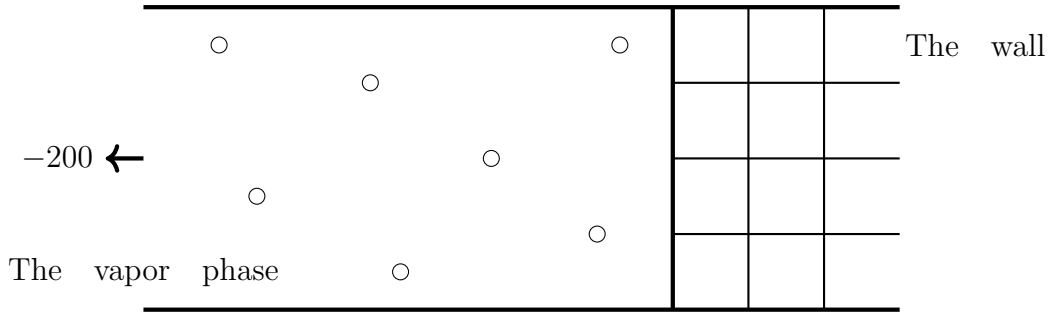

Figure 6.13: the wall.

mating the pressure suggested in the previous section.
We consider first the whole domain as a vapor. We discretize the domain into N cells, where N is an even number. As we have seen in the previous section the liquid phase will be treated as an incompressible liquid which means that we will consider the liquid phase like a solid stationary wall. In order to perform an update on cell $I_{N/2}$, i.e last cell of the vapor phase we need to find the intercell fluxes between this cell and its neighbors. We have no problems with the intercell flux between the cells $I_{N/2-1}$ and $I_{N/2}$. In order to define the second intercell flux we need to add a so called ghost cell $I_{N/2+1}$, see Figure 6.14.
Now we assume that the cell $I_{N/2+1}$ behaves like a wall. The most important feature of the wall is that its velocity is zero. The interface in this case will lie on the cell boundary at $x_{N/2+\frac{1}{2}}$.

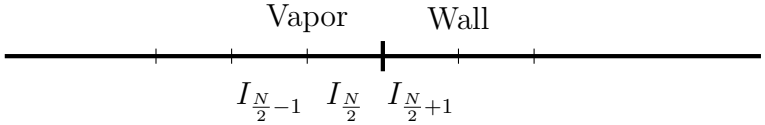

Figure 6.14: Discretization of the domain for determination of $F_{\frac{N}{2}+\frac{1}{2}}$.

The fluxes of a cell I_i where $i = 1, ..., N$ are given as

$$\mathbf{F}_{i\pm\frac{1}{2}} = \begin{pmatrix} \rho_{i\pm\frac{1}{2}} v_{i\pm\frac{1}{2}} \\ \rho_{i\pm\frac{1}{2}} v^2_{i\pm\frac{1}{2}} + p_{i\pm\frac{1}{2}} \\ \rho_{i\pm\frac{1}{2}} \chi_{i\pm\frac{1}{2}} v_{i\pm\frac{1}{2}} \end{pmatrix}.$$

As the speed of the wall is zero the flux $\frac{N}{2} + \frac{1}{2}$ will be

$$\mathbf{F}_{\frac{N}{2}+\frac{1}{2}} = \begin{pmatrix} 0 \\ p_{\frac{N}{2}+\frac{1}{2}} \\ 0 \end{pmatrix}.$$

But as we have seen in Chapter 4 according to the Riemann invariants in (4.4.1) the pressure is constant across this contact discontinuity. Therefore, we set

$$p_{\frac{N}{2}+\frac{1}{2}} = p_{N/2}.$$

It has to mention that we use this only locally at the phase boundary.
What we have now is an estimating value of the pressure at the phase boundary between the two phases based on the physical properties of the vapor and the liquid. Table 6.8 shows the values of the pressure on the phase boundary applied to Examples 1 and 2. Figures 6.15 and 6.16 present the estimating behavior of the pressure for one time step at $x = 1 = x_{\frac{N}{2}+\frac{1}{2}}$.

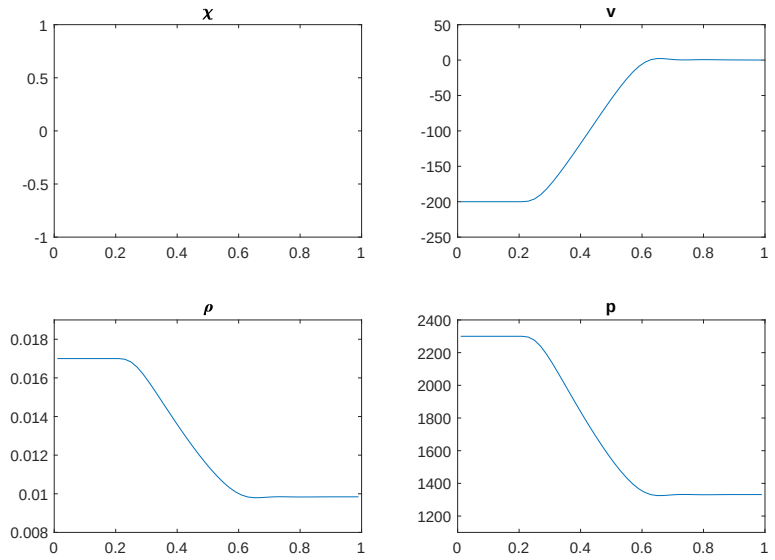

Figure 6.15: Estimating the pressure for the first example at $x = 1 = x_{\frac{N}{2}+\frac{1}{2}}$.

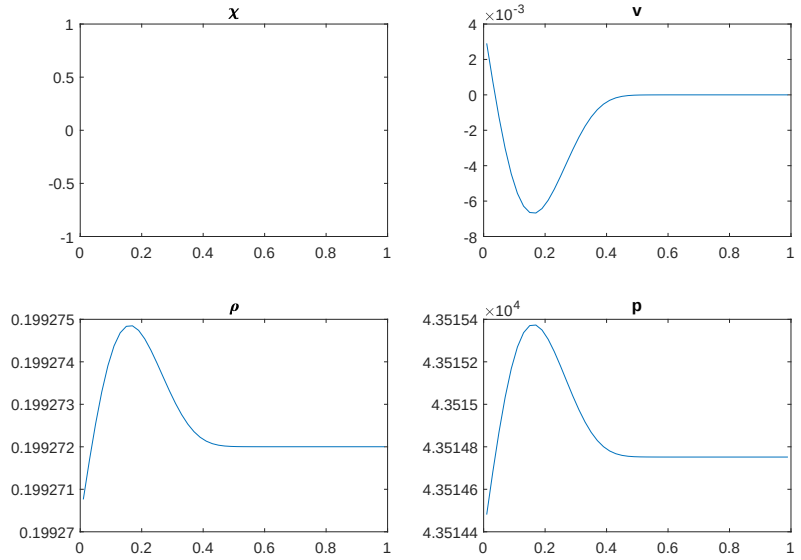

Figure 6.16: Estimating the pressure for the second example at $x = 1 = x_{\frac{N}{2}+\frac{1}{2}}$.

Table 6.8 shows the results obtained using the tracking the interface and estimating the pressure approaches and compares both results with the exact solution in Chapter 4. One can notice that the results are close enough for practical purposes to the exact solution.

Approach	Example 1	Example 2
Trackimg the interface	1334.7 Pa	43525.407 Pa
Estimating the pressure	1334.6 Pa	43514.8 Pa
Exact solution	1335.3 Pa	43531 Pa

Table 6.8: The values of the pressure in the star region using the tracking the interface approach and by estimating the mixture pressure.

6.4.3 The pressure fix

In this subsection we want to use the idea of estimating the pressure presented above in order to find the numerical solution of the model considered, supplied with the equation of state (6.2), for many time steps. For this purpose we calculate the pressure in the pure phases where $\chi = 1$ or $\chi = -1$ using the equation of state (6.2). In order to find the pressure in the mixture cells where $\chi \in]-1, 1[$ we consider that the pressure in this case is the estimated value of the pressure. For more time steps we utilize the property of uniform pressure at the phase boundary. This gives

$$p^{n+1} = p^n, \tag{6.6}$$

where n is the time step. We assume that the value of the pressure in a mixture cell in each time step is the value of the estimated pressure from the first time step. This approach is summarized in the following algorithm:

if $\chi = 1$ *or* $\chi = -1$ **then**
| $p = p(\chi, \rho)$
else
| $p =$ the estimated value of the pressure
end

Algorithm 1: pressure fix algorithm.

In order to test the performance of this approach we test this idea on Example 1 using the data in Table 6.1. We will use the HLL solver in order to find the numerical solution. We consider 50 cells and 5 time steps. The CFL number is fixed at 0.9.
Figure 6.17 shows the solution after 5 time steps. One can notice that the solution consists of three waves, a rarefaction wave, a contact in the middle and a shock wave. The solution has the same structure as the results obtained using the tracking the interface approach, see Section 6.3, as well as with the exact solution obtained in Chapter 4.
One can see that the pressure fix approach treats the difficulties discussed in Section 6.2.
So far this approach provides us a numerical solution for the model considered but

only for a few time steps. Our aim now is to find the numerical solution at any time T. Increasing the number of the time steps will reveal further difficulties.
Unfortunately this approach is not able to solve the problem for many time steps. Figure 6.18 illustrates the solution of the same example considered, but after 20 steps.
Actually this approach is not proper for each example we want to consider. Figure 6.19 shows the solution of Example 2, see Section 6.5, after 5 time steps. One can see the negative pressure problem appears again despite of using a small number of time steps. This confronts us with new questions. Why do we get these results? And how can we overcome this situation? This will be discussed in the next subsection.

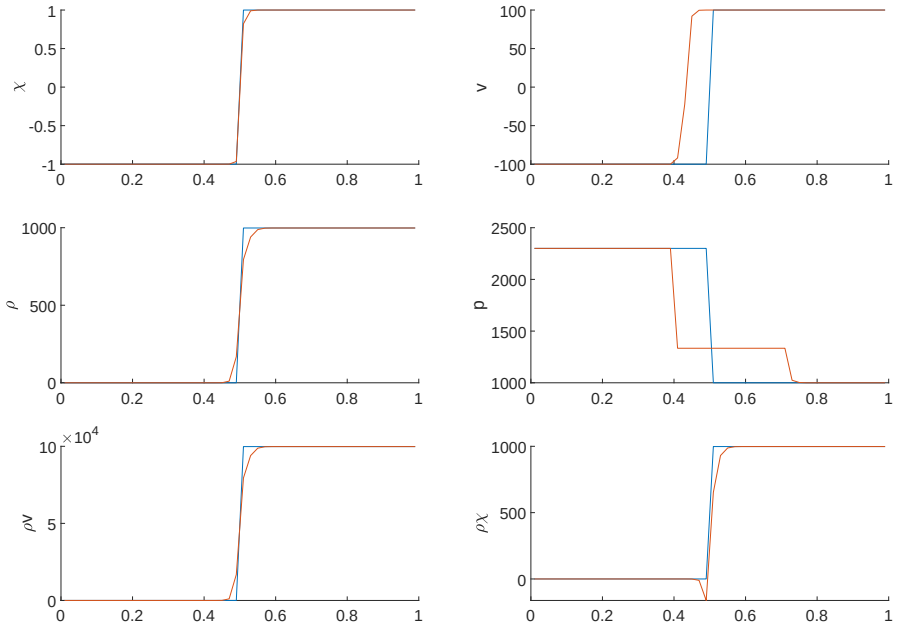

Figure 6.17: Estimating the pressure for the first example after 5 time steps. Blue: the initial data, Red: the numerical solution.

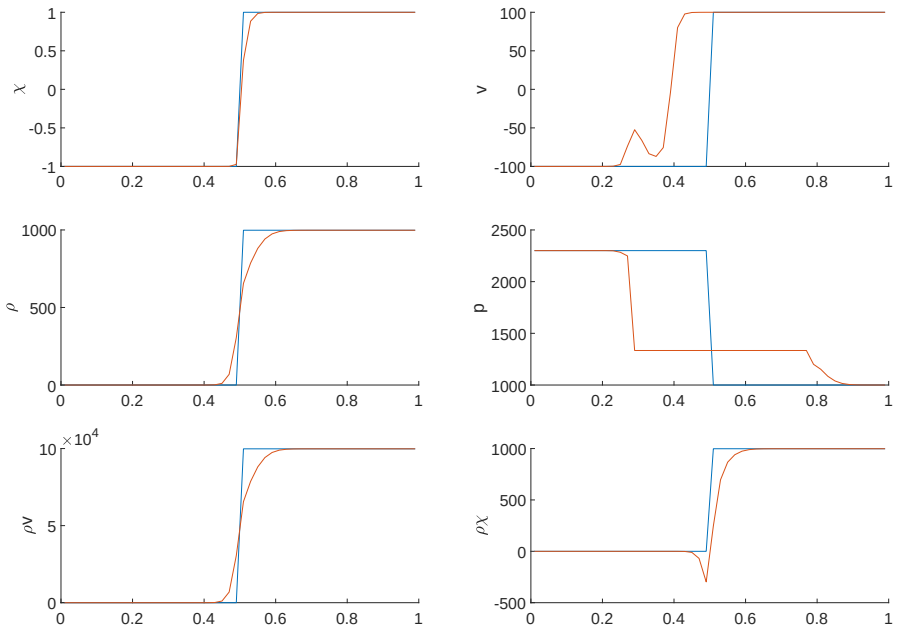

Figure 6.18: Estimating the pressure for the first example after 20 time steps. Blue: the initial data, Red: the numerical solution.

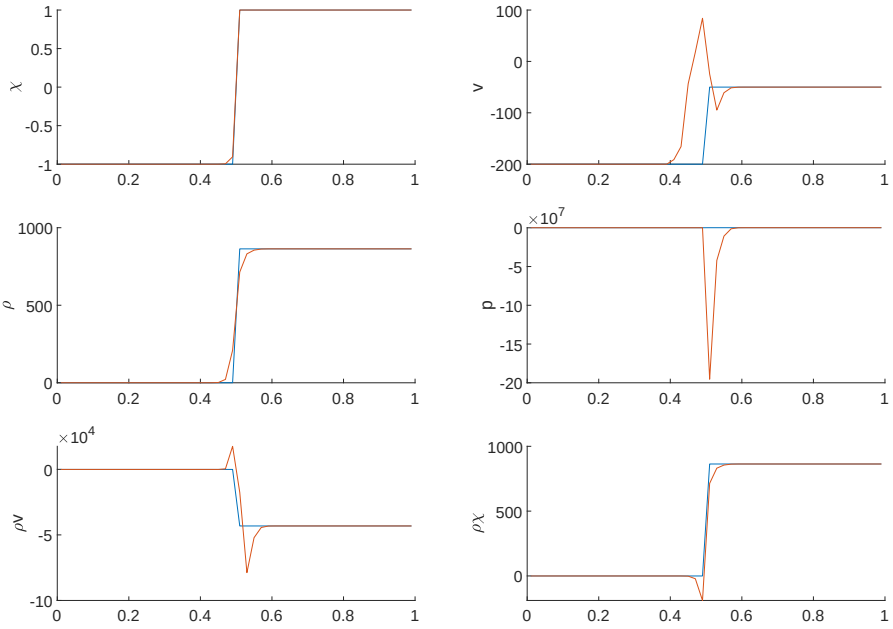

Figure 6.19: Estimating the pressure for the second example after 5 time steps. Blue: the initial data, Red: the numerical solution.

6.4.4 Pressure bounds

As we have seen before, the pressure fix approach provides us a good method in order to find the pressure in a mixture cell and utilize the estimated value of the pressure in order to evaluate the solution in each time step. This idea is applied by calculating the pressure using the equation of state (6.2) as long as we want to find the pressure in the pure vapor phase or in the pure liquid phase. If $-1 < \chi < 1$ indicates a mixture cell then the pressure in this case will have the estimated value of the pressure. We do not use the equation of state (6.2) in order to find the pressure in the mixture cell to avoid negative values. This approach is successfully solving problems as in Example 1.
But as we have seen in the previous section, until now this approach was not able to deal with all situations as in Example 2 where we still get a negative pressure. The negative value of the pressure does not imply the complete failure of the previous approach. But now the nagative value occure in a liquid cell and not in mixture cell. After testing the value of the pressure in the whole mixture cells one can notice that the value of the pressure there is equal to the value of the estimated value of the pressure.
The question now is why we get a negative pressure in a liquid cell?
To overcome this situation we checked the value of the density. One notices that the negative pressure appears in the first cell next to the mixture cells. When we test the value of χ in this cell we get the value 1, i.e. $\chi = 1$ indicates the liquid phase. This means that the negative pressure appears in the first liquid cell next to the mixture cells.
The reason behind this is a small difference in the value of the density of the liquid

in this cell due to the smearing out of the density.
As we have seen in Figure 6.11 a small change in the density of the liquid causes a big change in the pressure. This is the case here.
In order to avoid this situation we define a minimum value of the density in the liquid phase and find the pressure using the equation of state only when the density is bigger than this value. Otherwise we extend the estimated value of the pressure to the cells where the density does not exceed the expected value of the density. In this way we guarantee avoiding the consequences of the smearing out of the density. Figure 6.4 illustrates the idea of the minimal density $\rho_{L_{min}}$ in the liquid phase.
We modify the algorithm of the pressure fix by including the pressure bound to be

if $(\chi = 1 \text{ and } \rho > \rho_{L_{min}})$ *or* $(\chi = -1)$ **then**
| $p = p(\chi, \rho)$
else
| p= the estimated value of the pressure,
end

Algorithm 2: pressure fix with pressure bound algorithm.

Applying this approach gives us better results. As we can see in Example 1 we can find the solution for further time steps. In Example 2 we can see that the negative pressure is avoided now. In both cases we get good results comparing with the exact solution. But in general, this method is not able to solve the problem for arbitrary large time.

6.5 Numerical results

In this section we want to reconsider the two examples discussed before and present the solution using different solvers. We obtain the results using the idea of fixing the pressure and solve the following examples using the Lax-Friedrich, HLL and Rusanov solvers. In both examples we consider 50 cells with 10 time steps. The CFL condition is 0.9.

Example 1
We consider the initial date as in Table 6.9.

primitive variables	p_V	v_V	χ_V	p_L	v_L	χ_L
Initial Data	2300 Pa	-100 m/s	-1	1000 Pa	100 m/s	1

Table 6.9: The initial data for the case vapor-liquid - Example 1.

Figures 6.20, 6.21 and 6.22 illustrate the solution of Example 1 using the Lax-Friedrich, HLL and Rusanov solvers respectively. The solution consists of three waves. A rarefaction wave moving to the left, a shock wave moving to the right and a ghost contact in the middle.
The values in the star region are given in Table 6.10.

	p_L^*	v_L^*	p_R^*	v_R^*
The solution	1335 Pa	99.996 m/s	1335 Pa	99.998 m/s

Table 6.10: The values in the star region - Example 1.

Example 2

In this example we consider the data as in Table 6.11 The solution of Example 2

primitive variables	p_L	v_L	p_V	v_V
Initial Data	60000 Pa	-200 m/s	100000 Pa	-50 m/s

Table 6.11: The initial data for the case vapor-liquid - Example 2

after fixing the pressure is presented in Figures 6.23 and 6.24 using the HLL and Rusanov. The solution in this case consists of two rarefaction waves moving to the left and right and a contact wave in the middle.
Table 6.12 shows the solution of this example in the star region.

	p_V^*	v_v^*	p_L^*	v_L^*
The solution	43514.75 Pa	-50.074 m/s	43514.75 Pa	-50.065 m/s

Table 6.12: The values in the star region - Example 2

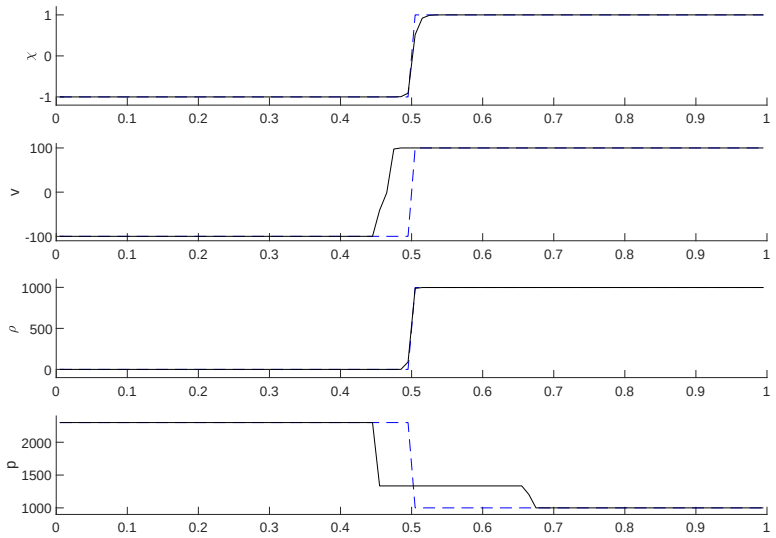

Figure 6.20: Lax-Friedrich. Example 1. Blue: the initial data, Black: the numerical solution.

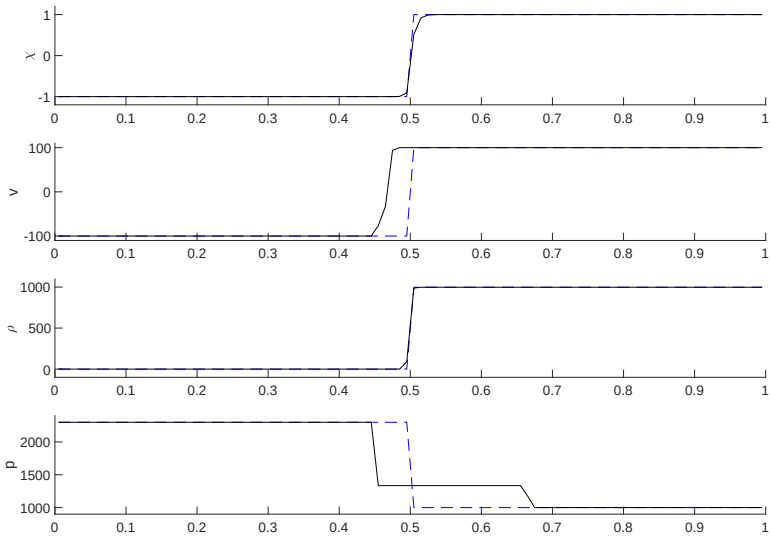

Figure 6.21: HLL. Example 1. Blue: the initial data, Black: the numerical solution.

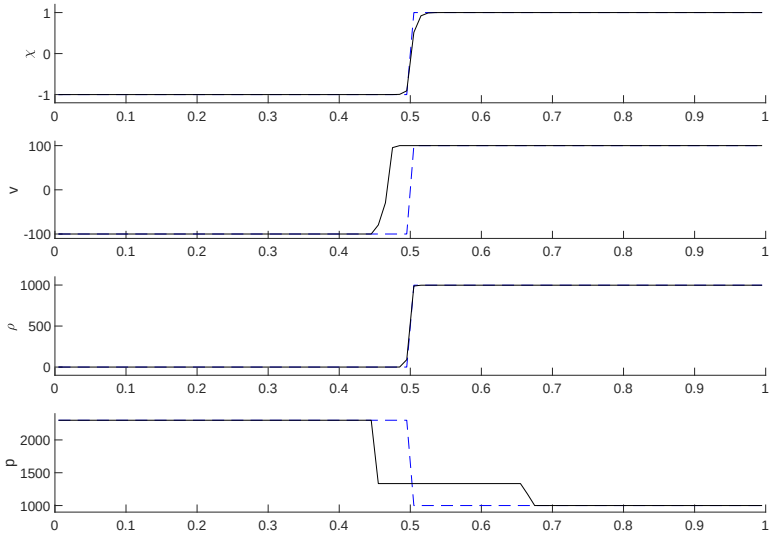

Figure 6.22: Rusanov. Example 1. Blue: the initial data, Black: the numerical solution.

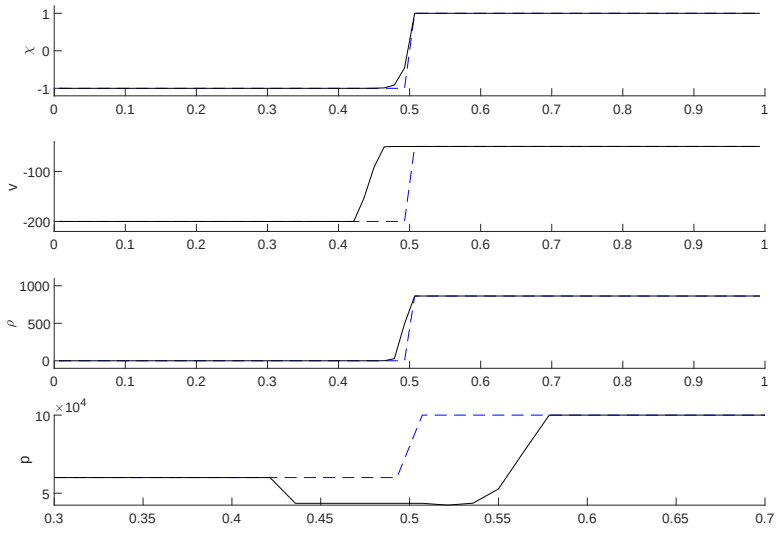

Figure 6.23: HLL. Example 2. Blue: the initial data, Black: the numerical solution.

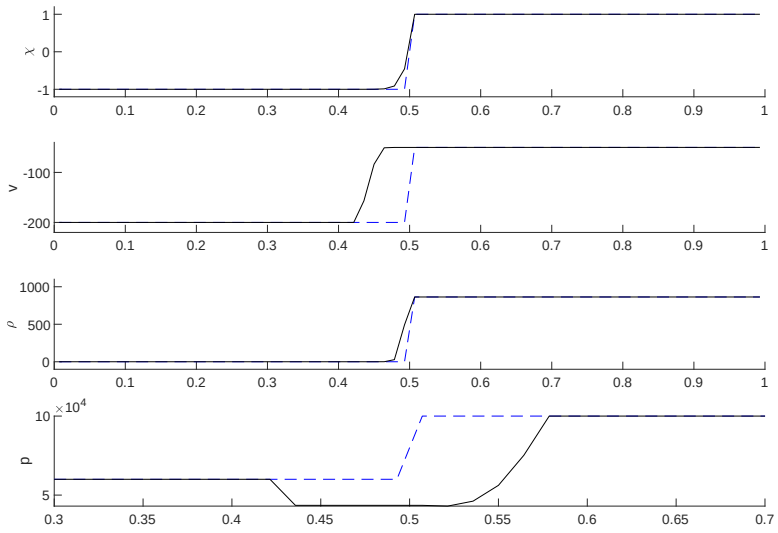

Figure 6.24: Rusanov. Example 2. Blue: the initial data, Black: the numerical solution.

6.5.1 Estimating the pressure using the exact solution

As we have seen before, estimating the pressure by using numerical methods in order to solve a Riemann problem at the wall provided us a solution for the difficulties that we described in this section, but only for few time steps. In this subsection we suggest another way to estimate the pressure by finding the exact solution on the wall.

6.5.2 The related problem and a pressure estimator

The homogeneous part of a diffuse interface model for the case $N = 1$ consists of 2 conservation laws for the mass density and the momentum and the transport equation for the phase variable. The latter is no conservation law. Accordingly, it is not clear how to discretize this equation.
A similar situation is known from the discretization of the non-conservative terms in the two-phase Baer-Nunziato model. In [2] Saurel and Abgrall suggested to use a specific upwind discretization. The idea is based on the knowledge of the properties of the exact Riemann solution. In particular, it is well-known that pressure and velocities are constant across the phase interface in this model. So the discretization has to be carried out in such a away that homogeneous pressure and velocity fields are preserved. The specific design of the discretization depends on the Riemann solver applied.
Unfortunately we are not able to copy this strategy to our system. Nevertheless we will use insight in the exact Riemann solution of the system to develop a solution strategy.

The main idea

This new approach is based on using the exact solution on the wall, instead of estimating a value of the pressure, where the exact solution is known. This Riemann problem is solved numerically using the HLL Riemann solver on a very coarse grid. Of course we do not estimate the pressure but use the pressure from the exact solution in every computational cell. Afterwards we calculate the phase variable χ using the equation of state by Newton's method.
One can notice that in the original problem we have $p(\rho_V^*) = p(\rho_L^*) = p$. Then the problem can be solved explicitly as in Toro [75].
In particular, let the density ρ_V, the sound speed a_V and the relative velocity v of the vapor phase be given. Then for the intermediate pressure $p(\rho_V^*)$ of the related problem we have

$$p(\rho_V^*) = \begin{cases} a_V^2 \rho_V \left(\frac{v}{2a_V} + \sqrt{\frac{v^2}{4a_V^2+1}} \right)^2 & v > 0 \\ \exp(\frac{v}{a_V} + \ln(\rho_V a_V^2)) & v < 0. \end{cases} \tag{6.7}$$

We expect that the intermediate pressure $p(\rho_V^*)$ of the related problem is a good approximation for the intermediate pressure p^* of the original problem.
It will be used as an estimation for the intermediate pressure of the original problem in our numerical simulations.
Now we have the density from the solver and an estimated values of the pressure.

We want again to compute the phase variable χ using the equation of state. For this goal we apply Newton's method to it.

6.6 Numerical examples

In this section we will test the pressure estimator using the exact solution approach introduced previously considering the same two different examples which are discussed in the last section to find the pressure in the intermediate region. Once we have the pressure we will use this value in the numerical solver in order to solve the system considered.
The Riemann problem is solved numerically using the HLL solver on a very coarse grid with $\Delta x = \frac{1}{150}$. The initial data and the parameters for Examples 1 and Example 2 are given Section 6.5. The parameters correspond to water at a Temperature of $T = 473.15K$. One should notice that this is a very high temperature where liquid water is much more compressible than at standard temperature as in Example 1.
Now we will use the pressure estimator using the exact solution approach to approximate the pressure and compare the results to the exact solution as we can see in table 6.13. One can observe that the exact solution and approximated pressure

	approximated pressure	exact pressure
Example 1	1335.3208 Pa	1335.3199 Pa
Example 2	43526 Pa	43531 Pa

Table 6.13: Approximated pressure and exact pressure

are in very good agreement. We can see that the largest discrepancy appears in Example 2 which is not surprising due to the more intense compressibility of the liquid phase that comes along with the very high temperature.
Finally the pressure estimator has to be integrated into the numerical solver. This Riemann solver is based on the idea that the solution of a general initial value problem is a superposition of local Riemann problems that appear between neighboring computational cells.
For all Riemann problems we estimate the pressure. As a consequence for every computational cell we obtain two pressure estimations, a left and a right side value. The estimator gives very good approximations for the pressure as we have seen in Table 6.13.
On the other hand it neglects the wave propagating through the liquid phase. Accordingly the left sided approximations will be used in the vapor and in the mixture region while the right sided estimations are used in the liquid. Alternatively one can use some averaged value.
The overall algorithm for a single time step can be summarized as follows:

- Use any Riemann solver to evolve the conserved quantities
- Solve the related problem at every inner cell boundary
- Update the pressure
- Calculate the corresponding phase function quantity

Using the above algorithm we solve Examples 1 and 2. The phase boundary is smeared. This behavior is not surprising due to the very large density gradient at the phase boundary. The wave speeds are fitted very well. Nevertheless one can observe that the pressure is slightly overestimated.
Using a volume based mean value instead for the pressure estimation the pressure in the intermediate region will be in prefect agreement to the exact pressure. But then the shock speed will be underestimated.
Refining the grid the numerical solution converges.
The numerical solution of Example 2 behaves similarly. There is some deviance in the left rarefaction. This discrepancy disappears when the grid is refined.
Our estimating the pressure approach enabled us to overcome difficulties that appeared in the study of the numerical solution of the homogeneous part of the diffuse interface model in the case vapor-liquid flow. It gives a satisfactory results and a is promising concept which can easily be extended to multicomponent flows.

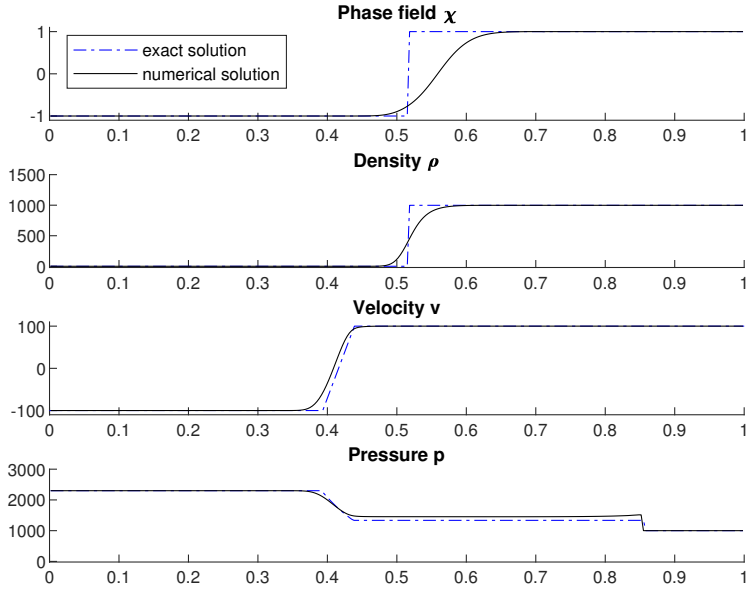

Figure 6.25: Exact and numerical solution of Example 1

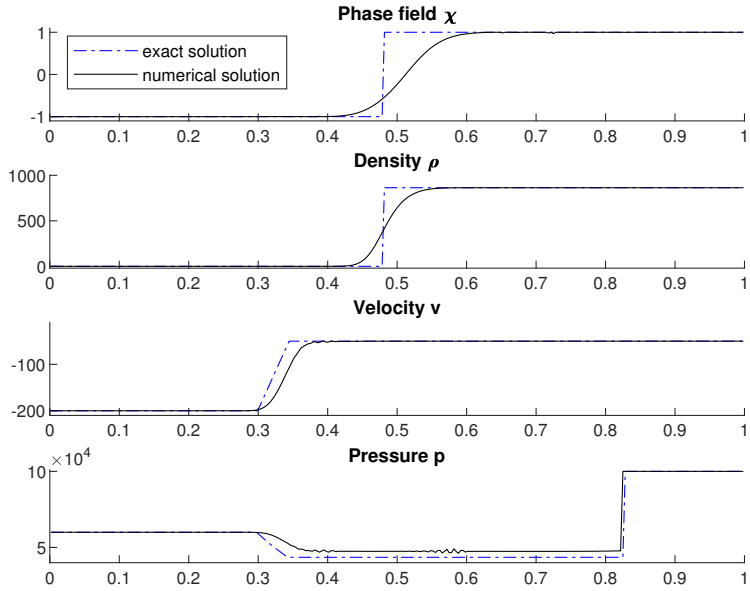

Figure 6.26: Exact and numerical solution of Example 1

Chapter 7

The model with chemical reaction

Many physical problems of fluid dynamics are governed by hyperbolic conservation laws with a source or production term. The source term is related to physical effects or to geometric effects. A non-linear system of conservation laws with source term has the form

$$\mathbf{U}_t + \mathbf{F}(\mathbf{U})_x = \mathbf{S}(\mathbf{U}), \tag{7.1}$$

where $\mathbf{U}$ is the vector of unknowns, $\mathbf{F}$ is the vector of fluxes and $\mathbf{S}$ is a vector of sources.
In Chapter 4 we studied the homogeneous system

$$\mathbf{U}_t + \mathbf{F}(\mathbf{U})_x = 0, \tag{7.2}$$

in which $\mathbf{S}(\mathbf{U}) = 0$. There no source was considered.
Assuming no spatial flux variations, where $\mathbf{F}(\mathbf{U})_x = 0$, gives another simplification of (7.1). This leads to a system of ordinary differential equations

$$\frac{d}{dt}\mathbf{U} = \mathbf{S}(\mathbf{U}), \tag{7.3}$$

In this chapter we want to study the approximate solution of the homogeneous part of the diffuse interface multiphase mixture model with source term using the splitting method.
For further details about conservation laws with source terms we refer the reader to the work of Hantke and Müller [33], the PhD theses by Helzel [36] as well as Fedkiw [28].

7.1 Splitting method for a system of equations

In this section we present the approach so called splitting method. This is used to solve systems of conservation laws with a source term. This method is a first order method. In this approach we split the system into two subproblems. The first one is the homogeneous system (7.2) and the other one is the source subproblem (7.3). The homogeneous subproblem can be solved numerically as we have seen in Chapters 5 and 6 or by any other appropriate method. In order to solve the source term problem one can use any ODE solver. For more details see Papalexandris et al. [58], Tang [72], LeVeque [45] as well as LeVeque and Yee [48].

We consider the initial value problem

$$\mathbf{U}_t + \mathbf{F}(\mathbf{U})_x = \mathbf{S}(\mathbf{U}), \tag{7.4}$$

$$\mathbf{U}(x, t^n) = \mathbf{U}^n, \tag{7.5}$$

where $\mathbf{U}^n$ is the solution at t^n and we want to evolve the solution to the new value $\mathbf{U}^{n+1}$ at t^{n+1} in a time step $\Delta t = t^{n+1} - t^n$.
We discretise the spatial domain $[0, L]$ into M numbers of cells or grid points i. We split the system (7.1) into (7.2) and (7.3). The splitting scheme is

$$\left.\begin{array}{l} \mathbf{U}_t + \mathbf{F}(\mathbf{U})_x = 0, \\ \mathbf{U}(x, t^n) = \mathbf{U}^n \end{array}\right\} \Rightarrow \overline{\mathbf{U}}^{n+1},$$

where the initial data for this subproblem is the initial data of the complete problem (7.1) and $\overline{\mathbf{U}}^{n+1}$ is the solution of the homogeneous subproblem. This solution will be used as an initial data for the second subproblem (7.3)

$$\left.\begin{array}{l} \frac{d}{dt}\mathbf{U} = \mathbf{S}(\mathbf{U}), \\ \overline{\mathbf{U}}^{n+1} \end{array}\right\} \Rightarrow \mathbf{U}^{n+1}.$$

The solution of the main problem (7.1) using splitting method is given as

$$\mathbf{U}^{n+1} = S^{(\Delta t)} C^{(\Delta t)}(\mathbf{U}^n), \tag{7.6}$$

where $C^{(\Delta t)}$ is the solution operator for the problem (7.2) and $S^{(\Delta t)}$ is the solution operator for the problem (7.3) over time t.

7.2 The homogeneous model with chemical reactions

The diffuse interface multiphase mixture model with chemical reaction was presented in Chapter 3. In this section, we want to solve this model after neglecting the second order terms. This is nothing else than supplying the homogeneous part of the model with source terms. We will solve this part of the system using splitting method presented in previous section.
As we have seen in Chapter 3, we consider multi-component liquids (L) and/or vapors (V) mixture of N constituents A_1, A_2, ... , A_N where the constituents A_α where $\alpha = 1, ..., N$ of a fluid mixture allow the chemical reactions. This means that we have N_R reactions of the type

$$a_1^i A_1 + a_2^i A_2 + ... + a_N^i A_N \rightleftharpoons b_1^i A_1 + b_2^i A_2 + ... + b_N^i A_N,$$

where the constants a_α^i and b_α^i are positive integers and $\nu_\alpha^i = b_\alpha^i - a_\alpha^i$ denotes the stoichiometric coefficients of constituent α in the possible reaction $i = 1, ..., N$.
Again we emphasize that the model considers reactions with forward f and backward b path and the corresponding reaction rates R_f^i and R_b^i give the number of forward and backward reactions per volume and per time. Hence

$$r_\alpha = \sum_{i=1}^{N} m_\alpha \nu_\alpha^i (R_f^i - R_b^i). \tag{7.7}$$

But the 2nd law of thermodynamics prescribes the ratio of the reaction rates as

$$R_b^i = R_f^i \exp(\frac{A^i}{kT}), \tag{7.8}$$

where T is the temperature, k is the Boltzmann constant and the chemical affinity A^i is defined by

$$A^i = \sum_{\alpha=1}^{N} m_\alpha \nu_\alpha^i \mu_\alpha.$$

We substitute (7.8) into (7.7) and get

$$r_\alpha = \sum_{i=1}^{N} m_\alpha \nu_\alpha^i R_f^i (1 - \exp(\frac{A^i}{kT})).$$

As either the forward or the backward rate can be modeled, we set $R_f^i = M_r^i$ where the constant $M_r^i > 0$ is the reaction mobility.
As we have seen before, the partial mass densities and the partial velocities define the total mass density ρ and the mixture velocity v according to

$$\rho = \sum_{i=1}^{N} \rho_i \quad \text{and} \quad \rho v = \sum_{i=1}^{N} \rho_i v_i.$$

The diffuse interface model is given by the following system of PDEs after neglecting the second order terms and adding the source term

$$\begin{aligned} \partial_t \rho + \operatorname{div}(\rho v) &= 0, \\ \partial_t \rho_\alpha + \operatorname{div}(\rho_\alpha v) &= \sum_{i=1}^{N_R} \nu_\alpha^i m_\alpha M_r^i (1 - \exp(\frac{A^i}{kT})), \\ \partial_t (\rho v) + \operatorname{div}(\rho v^2 + p) &= 0, \\ \partial_t (\rho \chi) + \operatorname{div}(\rho v \chi) &= -M_p (\frac{\partial \rho \psi}{\partial \chi}), \end{aligned} \tag{7.9}$$

where p is the pressure, m_α is the atomic mass of constituents α, $\rho\psi$ is the given equation of state, μ_α is the chemical potential and M_p and M_r^i are the mobilities. For more details see Chapter 3 and the references therein.
We supply the model with the equation of state (3.8) which was derived in Chapter 3. It has the form

$$p(\chi, \rho_1, ..., \rho_N) = -W(\chi) + \sum_{i=1}^{N} [h(\chi)(a_{Li}^2 \rho + d_{Li}) + (1 - h(\chi))(a_{Vi}^2 \rho + d_{Vi})].$$

7.3 Solving the system using the splitting method

Now we want to solve the system (7.9) numerically using the splitting method which means we will split our problem into two subproblems. The first one is the homogeneous part of the system. This has been discussed in Chapters 5 and 6. Then we

will solve the chemical reaction subproblem by solving the following ODEs system

$$\frac{d\rho}{dt} = 0,$$
$$\frac{d\rho_\alpha}{dt} = \sum_{i=1}^{N_R} \gamma_\alpha^i m_\alpha M_r^i (1 - \exp(\frac{A^i}{kT})),$$
$$\frac{d\rho v}{dt} = 0,$$
$$\frac{d\rho\chi}{dt} = -M_p(\frac{\partial \rho\psi}{\partial \chi}).$$

Afterwards, we obtain the solution by applying (7.6) as explained before in this chapter.

7.4 Examples

In this section we want to present two examples and discuss the solutions using the splitting approach. For comparison reasons we will choose examples from Hantke and Müller [33]. In each example we will discuss the solution of the ODEs (7.3) using Rung-Kutta method. Then we will present the complete solution of the full system with source term (7.1). In order to do this we will involve the solution of the ODE system in the homogeneous system according to the formula

$$\mathbf{U}^{n+1} = S^{(\Delta t)} C^{(\Delta t)}(\mathbf{U}^n),$$

where $C^{(\Delta t)}$ is the solution operator for the problem (7.2) and $S^{(\Delta t)}$ is the solution operator for the problem (7.3) over time t. We will choose the parameters as follows:

	γ	c_v	π	ρ_0	m_α
vapor	1.43	1040	0	0.9	0.01802
liquid	2.35	1816	10^9	999	0.01802
oxygen	1.4	920	0	1.429	0.032
hydrogen	1.4	14304	0	0.09	0.00202

Table 7.1: parameters

In both examples we have only one reaction so that $N_R = 1$ and there will be no need to sum over i.

Example 1a
In this example we consider a mixture of a pure liquid water (l) and a pure vapor water (v). It is a phase transition not chemical reaction between the vapor and the liquid. But we consider this example to test the source term r_α, and show its ability to deal with such situations. A further reason, this example is considered in paper [33] where the model presented therein can deal with both cases phase transition and chemical reaction. The chemical reactions is just the phase transition.

$$(H_2O)_{vapor} \rightleftharpoons (H_2O)_{liquid} \tag{7.10}$$

In this case the mixture consists of two components ($N = 2$). The model has the form

$$\begin{aligned}
\partial_t \rho + \partial_x(\rho v) &= 0,\\
\partial_t \rho_l + \partial_x(\rho_l v) &= \nu_l m_l M_r(1 - \exp(\frac{A}{kT})),\\
\partial_t(\rho v) + \partial_x(\rho v^2 + p) &= 0,\\
\partial_t(\rho\chi) + \partial_x(\rho v\chi) &= -M_p(\frac{\partial \rho\psi}{\partial \chi}),
\end{aligned}$$

where ρ is the total density $\rho = \rho_l + \rho_{\mathrm{v}}$. We replace the transport equation of the total density by the transport equation of the partial density of the second component. The model becomes

$$\begin{aligned}
\partial_t \rho_{\mathrm{v}} + \partial_x(\rho_{\mathrm{v}} v) &= \nu_{\mathrm{v}} m_{\mathrm{v}} M_r(1 - \exp(\frac{A}{kT})),\\
\partial_t \rho_l + \partial_x(\rho_l v) &= \nu_l m_l M_r(1 - \exp(\frac{A}{kT})),\\
\partial_t(\rho v) + \partial_x(\rho v^2 + p) &= 0,\\
\partial_t(\rho\chi) + \partial_x(\rho v\chi) &= -M_p(\frac{\partial \rho\psi}{\partial \chi}).
\end{aligned}$$

From (7.10) we observe that $a_l = 0$, $a_{\mathrm{v}} = 1$, $b_l = 1$ and $b_{\mathrm{v}} = 0$ which gives the coefficients $\nu_{_{\mathrm{v}}} = 1$ and $\nu_{_l} = -1$.
As we have seen in Chapter 2 for constant temperature the chemeical potential μ (2.8) is given as

$$\mu_\alpha = (\gamma_\alpha - 1)c_\alpha T \ln \frac{\rho_\alpha}{\rho_{ref_\alpha}} + (\gamma_\alpha - 1)c_\alpha T - \frac{\pi_\alpha}{\rho_{ref_\alpha}},$$

which can be calculated using the parameters in Table 7.1. Here α denotes to liquid or vapor component.
In this case the chemical affinity A is given as

$$\begin{aligned}
A = \sum_{\alpha=1}^{N} m_\alpha \nu_\alpha \mu_\alpha &= m_l \nu_l \mu_l + m_{\mathrm{v}} \nu_{\mathrm{v}} \mu_{\mathrm{v}}\\
&= m_l \mu_l - m_{\mathrm{v}} \mu_{\mathrm{v}} = m(\mu_l - \mu_{\mathrm{v}}),
\end{aligned}$$

where $m_l = m_{\mathrm{v}} = m$, which gives by linearization

$$1 - \exp(\frac{A}{kT}) \approx 1 - (1 + \frac{A}{kT}) = \frac{-A}{kT} = \frac{m(\mu_{\mathrm{v}} - \mu_l)}{kT}.$$

The system now has the form

$$\begin{aligned}
\partial_t \rho + \partial_x(\rho v) &= 0,\\
\partial_t \rho_{\mathrm{v}} + \partial_x(\rho_{\mathrm{v}} v) &= \nu_{\mathrm{v}} m M_r(\frac{m(\mu_{\mathrm{v}} - \mu_l)}{kT}),\\
\partial_t \rho_l + \partial_x(\rho_l v) &= \nu_l m M_r(\frac{m(\mu_v - \mu_l)}{kT}),\\
\partial_t(\rho v) + \partial_x(\rho v^2 + p) &= 0,\\
\partial_t(\rho\chi) + \partial_x(\rho v\chi) &= -M_p(\frac{\partial \rho\psi}{\partial \chi}).
\end{aligned}$$

Next we apply the splitting method approach in order to solve the system. In this example we choose the initial data with $p_{\mathrm{v}} = 2 \cdot 10^5$ and $p_l = 10^5$ and $T = 298K$. We first solve the system of the ODEs numerically which in his case have the form

$$\begin{aligned}
\frac{d\rho}{dt} &= 0, \\
\frac{d\rho_l}{dt} &= \nu_l m M_r (1 - \exp(\frac{A}{kT})), \\
\frac{d\rho_{\mathrm{v}}}{dt} &= \nu_{\mathrm{v}} m M_r (1 - \exp(\frac{A}{kT})), \\
\frac{d\rho v}{dt} &= 0, \\
\frac{d\rho\chi}{dt} &= -M_p(\frac{\partial \rho\psi}{\partial \chi}).
\end{aligned}$$

We obtain the results in Figure 7.1 and we observe that the pressure in the liquid water increases and decreases in vapor water. The same behavior is seen for the densities where the density of the water liquid increases whereas the density of the vapor decreases.

Example 1b
Now we want to solve the submodel with source terms. As a test case we consider the initial data on both sides as $p_{vapor} = 2 \cdot 10^5$ and $p_{liquid} = 10^5$ and $T = 298K$. We obtain the results as in Figure 7.3.
One can notice that χ is constant because nothing is changed and the same for v. But we can notice that the density of the liquid ρ_1 is going up and the density of the vapor ρ_2 is going down. This matches the results in Figure 7.1 where the liquid density ρ_L increases and the vapor density ρ_V decreases. The pressure p_L shows the same behavior.
We consider the initial condition as $p_{vapor} = 2 \cdot 10^5$ and $p_{liquid} = 10^5$ to the left and $p_{vapor} = 10^5$ and $p_{liquid} = 2 \cdot 10^5$ to the right, we obtain the results as in Figure 7.4.

Example 2a
In this example we consider a mixture of three components Oxygen (O_2), Hydrogen (H_2) and vapor water (v). The chemical reaction is the so-called oxyhydrogen reaction

$$2H_2 + O_2 \rightleftharpoons 2(H_2O)_{vapor}$$

In this case the system has the form

$$\begin{aligned}
\partial_t \rho_{O_2} + \partial_x(\rho_{O_2} v) &= \nu_{O_2} m_{O_2} M_r (1 - \exp(\frac{A}{kT})), \\
\partial_t \rho_{H_2} + \partial_x(\rho_{H_2} v) &= \nu_{H_2} m_{H_2} M_r (1 - \exp(\frac{A}{kT})), \\
\partial_t \rho_{H_2O} + \partial_x(\rho_{H_2O} v) &= \nu_{H_2O} m_{H_2O} M_r (1 - \exp(\frac{A}{kT})), \\
\partial_t(\rho v) + \partial_x(\rho v^2 + p) &= 0, \\
\partial_t(\rho\chi) + \partial_x(\rho v \chi) &= -M_p(\frac{\partial \rho\psi}{\partial \chi}).
\end{aligned}$$

In this case

$$A = \sum_{\alpha=1}^{N} m_\alpha \nu_\alpha \mu_\alpha = m_{O_2}\nu_{O_2}\mu_{O_2} + m_{H_2}\nu_{H_2}\mu_{H_2} + m_{H_2O}\nu_{H_2O}\mu_{H_2O}$$
$$= -m_{O_2}\mu_{O_2} - 2m_{H_2}\mu_{H_2} + 2m_{H_2O}\mu_{H_2O}.$$

Which gives by linearizatuion

$$1 - \exp(\frac{A}{kT}) \approx \frac{1}{kT}(m_{O_2}\mu_{O_2} + 2m_{H_2}\mu_{H_2} - 2m_{H_2O}\mu_{H_2O}).$$

The chemical reaction term has the form

$$r_\alpha = \nu_\alpha m_\alpha M_r((\frac{-A}{kT})).$$

The system in this case has the form

$$\begin{aligned}
\partial_t \rho + \partial_x(\rho v) &= 0,\\
\partial_t \rho_{_{O_2}} + \partial_x(\rho_{_{O_2}} v) &= r_{_{O_2}}\\
\partial_t \rho_{_{H_2}} + \partial_x(\rho_{_{H_2}} v) &= r_{_{H_2}}\\
\partial_t \rho_{_{H_2O}} + \partial_x(\rho_{_{H_2O}} v) &= r_{_{H_2O}}\\
\partial_t(\rho v) + \partial_x(\rho v^2 + p) &= 0,\\
\partial_t(\rho\chi) + \partial_x(\rho v \chi) &= -M_p(\frac{\partial \rho\psi}{\partial \chi}),
\end{aligned}$$

the stoichiometric coefficients are $\nu_{_{H_2O}} = 2$, $\nu_{_{H_2}} = -2$ and $\nu_{_{O_2}} = -1$.
Now we solve the following ODE system

$$\begin{aligned}
\frac{d\rho}{dt} &= 0,\\
\frac{d\rho_{_{O_2}}}{dt} &= r_{_{O_2}},\\
\frac{d\rho_{_{H_2}}}{dt} &= r_{_{H_2}},\\
\frac{d\rho_{_{H_2O}}}{dt} &= r_{_{H_2O}},\\
\frac{d\rho v}{dt} &= 0,\\
\frac{d\rho\chi}{dt} &= -M_p(\frac{\partial \rho\psi}{\partial \chi}).
\end{aligned}$$

We choose the initial data as $p_{H_2O} = 10^4$, $p_{O_2} = 10^5$, $p_{H_2} = 2 \cdot 10^5$ and $T = 298K$. The results are shown in Figure 7.2. We can see the same behavior of the densities and the pressure of the components, only now for 3 components. The densities of the oxygen and hydrogen decrease, the pressure as well, whereas the density of the water vapor increases and the pressure of the vapor water behaves in the same manner. This meets our expectations due to the recombination reaction.

Example 2b

As a test case we consider the initial data on both sides as $p_{H_2O} = 10^4$, $p_{O_2} = 10^5$, $p_{H_2} = 2.10^5$ and $T = 298K$. We obtain the results as in Figure 7.5.
Now we consider the initial condition as $p_{H_2O} = 10^4$, $p_{O_2} = 10^5$ and $p_{H_2} = 2.10^5$ to the left and $p_{H_2O} = (10^4)^2$, $p_{O_2} = (10^5)^2$ and $p_{H_2} = (2.10^5)^2$ from the right, we obtain the results as in Figure 7.6.

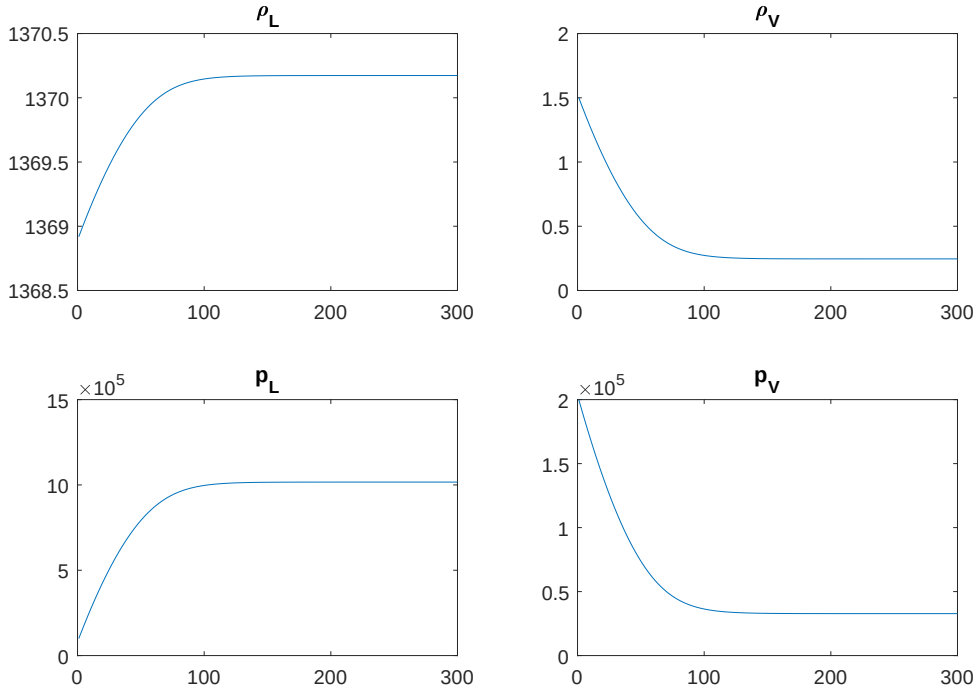

Figure 7.1: Example 1.

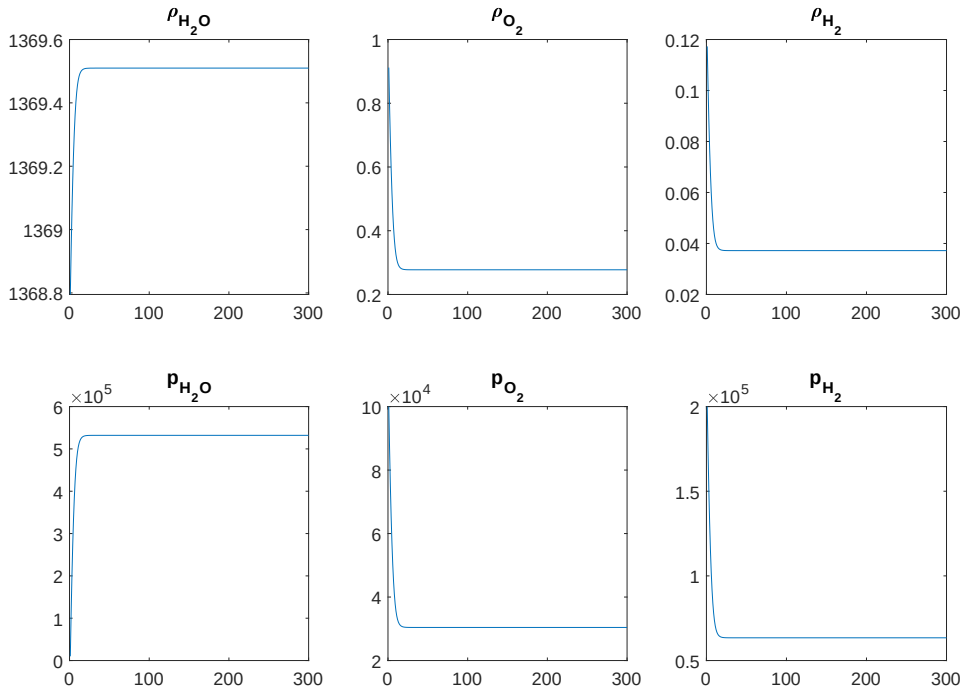

Figure 7.2: Example 2.

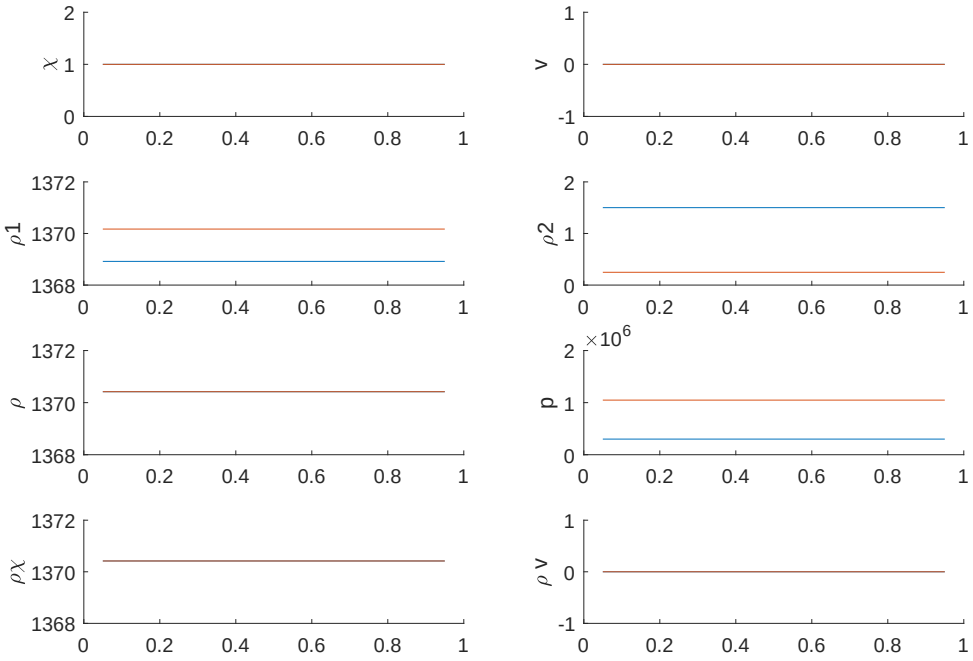

Figure 7.3: The full system, Example 1, test case. Blue: the initial data, Red: the numerical solution.

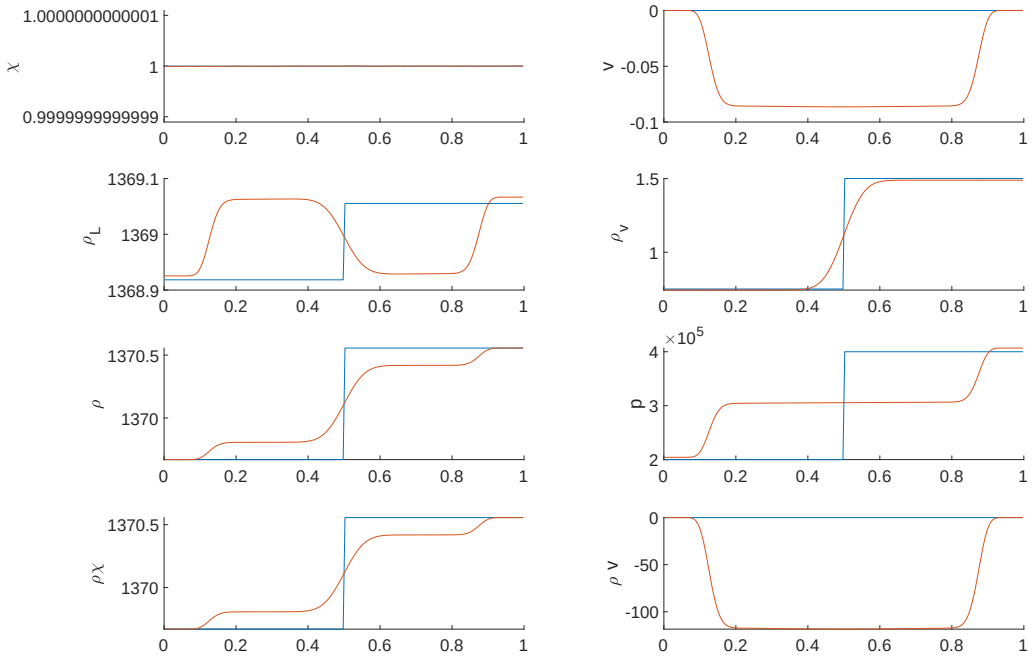

Figure 7.4: The full system, Example 1. Blue: the initial data, Red: the numerical solution.

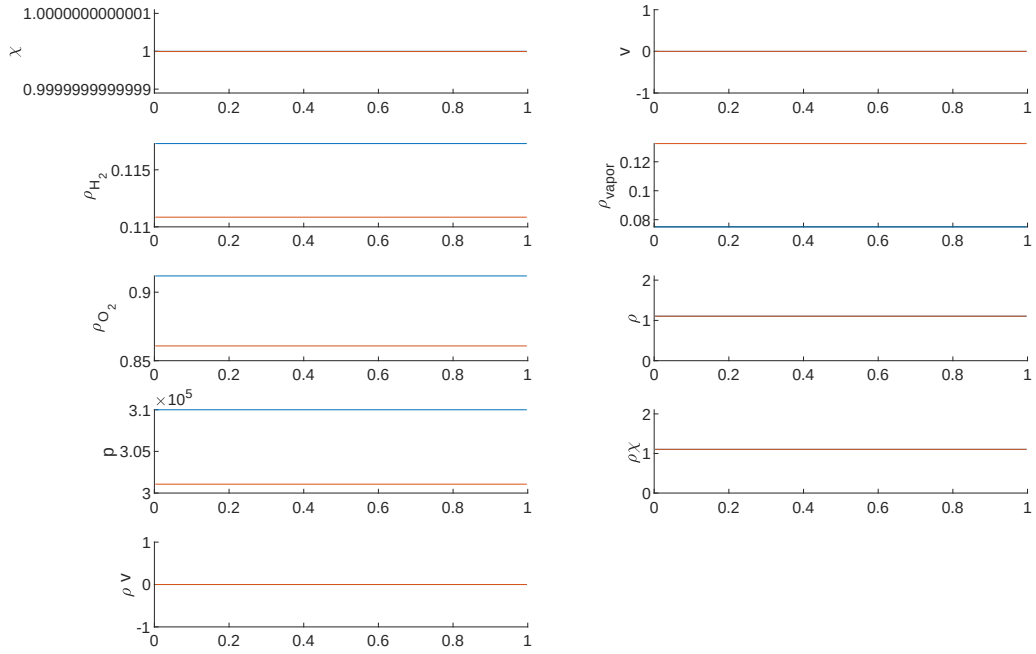

Figure 7.5: The full system, Example 2, test case, 200 cells, 90 time steps, time=3.10^{-04}. Blue: the initial data, Red: the numerical solution.

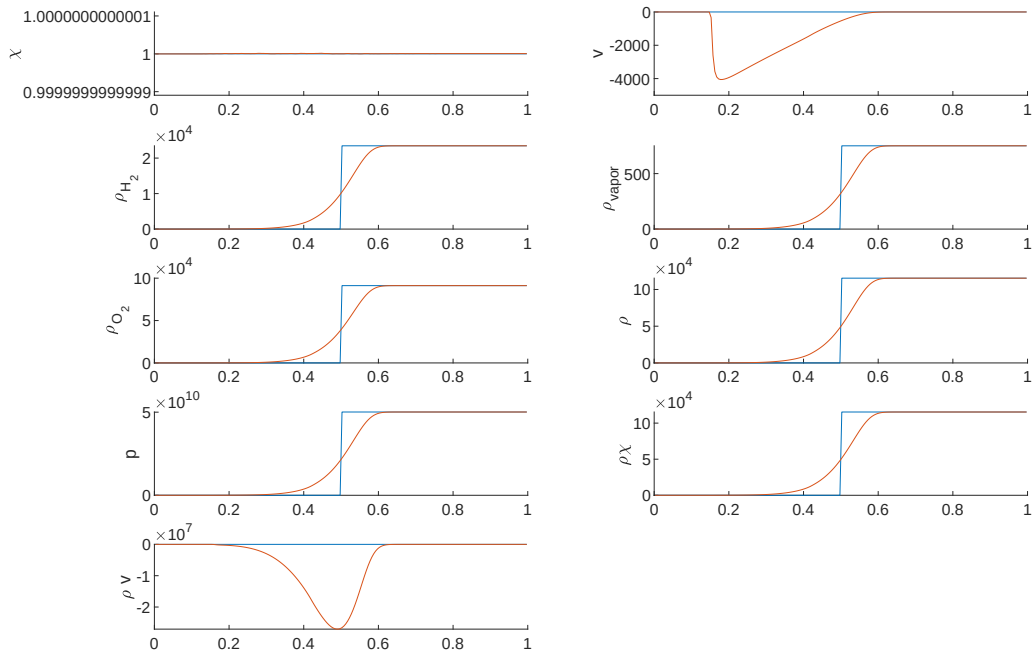

Figure 7.6: The full system, Example 2, test case, 200 cells, 90 time steps, time=9.10^{-05}. Blue: the initial data, Red: the numerical solution.

Chapter 8

Conclusion

In this thesis, we recalled a diffuse interface multiphase mixture model proposed by Dreyer, Giesselmann, and Kraus in [24]. In order to close the model, an equation of state was considered. Our main focus in this work was on the isothermal case where the temperature is fixed. We introduced the model in detail. Then we considered the homogeneous part of it as a submodel. It is a system of hyperbolic conservation laws. The main goal of this thesis was to solve the Riemann initial value problem for the sub-model analytically and numerically.
We started the analytical study by discussing the analytical structure of the submodel and introduced its mathematical properties. The eigenstructure of the model was presented which enabled us to understand the wave patterns of the solutions.
We presented the exact solution to the Riemann problem for the two phase multicomponent model. Further we proved the existence and uniqueness of this solution. We constructed the exact solution of the case $N = 1$. Here we have one component in each phase. We applied the solution to different test cases and we gave a comparison with different references.
One of the main advantages of this work was to generalize the exact solution to the multicomponent flow, i.e. the case $N > 1$. We obtained the complete solution and many examples are discussed.
In the numerical part of the study, we considered two cases the vapor-vapor flow and the vapor-liquid flow.
Discussing the flow of vapor-vapor is considered a good test case in order to test the performance of our solvers and to illustrate the structure of the solution. We wanted to show that the model can be solved numerically. We presented the numerical solution of this case using the isothermal and isentropic equation of state. We used different Riemann solvers namely the HLL, Rusanov, and HLLC solvers for the first order accuracy. In order to achieve the second order we used the MUSCL method. As we have the exact solution, we discussed different test cases and compared the results with it.
The more interesting case was the vapor-liquid flow. In this case, unexpected difficulties appeared. We obtained negative pressures and unphysical results in the mixture cells. We explained why we got those results and we developed strategies in order to overcome them.
The first strategy was using tracking the interface approach. In this approach, in each time step, we check if the interface lies at the cell boundary or not. If we have a mixture cell we split it into two cells. This approach enabled us to find a

numerical solution for the case of vapor-liquid. But it handled the interface as a sharp interface and used a part of the equation of state which is not our aim. So another approach was required.
In this thesis, we developed a new approach in order to find a numerical solution for the homogeneous part of the diffuse interface model in the case of vapor-liquid flow. We called this new approach estimating the mixture pressure. It is based on the physical properties of the vapor and the liquid. Due to the fact that most of the effects appear in the vapor phase, we considered the liquid phase as a wall. We solved the Riemann problem on the wall in two ways, using the exact solution and numerically using Riemann solvers. We used this estimated value of the pressure to find the numerical solution of the system.
The new method avoids expensive techniques like interface tracking and it is very cheap because it does not require an iterative procedure.
We tested this approach in different examples and the results presented are satisfactory.
Finally in this thesis, we included diffusion and source terms in the sub-model. We presented the numerical solution using the splitting method and we applied it to two examples.
Future work and open problems. In the numerical study, we considered the liquid phase as a solid wall in order to estimate the pressure. This means that we neglected the changes in the liquid phase.
A further interesting topic is extending estimating the pressure approach to solve other models where large density gradients lead to difficulties in discretization.
On the other hand, solving the submodel supplied with chemical reaction terms is an interesting subject. This can be applied to more complicated examples.

Bibliography

[1] R. Abgrall. How to prevent pressure oscillations in multicomponent flow calculations: A quasi conservative approach. *Journal of Computational Physics*, 1(125):150–160, 1996.

[2] R. Abgrall and R. Saurel. A multiphase Godunov method for compressible multifluid and multiphase flows. *Journal of Computational Physics*, 2(150):425–467, 1999.

[3] R. Abgrall and R. Saurel. Discrete equations for physics and numerical compressible multiphase mixtures. *Journal of Computational Physics*, 2(186):361–369, 2003.

[4] R. Acarl. Simulation of interface dynamics: a diffuse interface model. *Visual Comput.*, (25):101–115, 2009.

[5] A. Alzain. *Numerical methods for multiphase mixture canservation laws with phse transition.* Doctoral thesis, Otto-von-Guericke Universität Magdeburg, 2010.

[6] D. M. Anderson, G. B. McFadden, and A. A. Wheeler. Diffuse interface methods in fluid mechanics. *Annu. Rev. Fluid Mech.*, (30):139–165, 1998.

[7] J. D. Anderson. *Modern Compressible Flow.* McGraw Hill Publishing Company, 1990.

[8] N. Andrianov. *Analytical and numerical investigation of two-phase flows.* Doctoral thesis, Otto-von-Guericke Universität Magdeburg, 2003.

[9] N. Andrianov and G. Warnecke. The Riemann problem for the Baer-Nunziato two phase flow model. *Journal of Computational Physics*, (195):434–464, 2004.

[10] N. Andrianov, G. Warnecke, and R. Saurel. A simple method for compressible multiphase mixtures and interfaces. *Int. J. Numer. Meth. Fluids*, (41):109–131, 2003.

[11] Peter Atkins and Julio De Paula. *Physical Chemistry.* Oxford University Press, 2006.

[12] M. Bachmann. *Dynamics of cavitation bubbles in compressible two-phase fluid flow.* PhD thesis, RWTH Aschen University, 2012.

[13] M. Baer and J. Nunziato. A two-phase mixture theory for the deflagration to detonation transition in reactive granular materials. *International Journal of Multiphase Flow*, (12):861–889, 1986.

[14] T. Blesgen. A generalization of the Navier-Stokes equations to two-phase flows. *Journal of Physics. D, Applied Physics*, 32(10):1119–1123, 1999.

[15] D. Bothe and W. Dreyer. Continum thermodynamics of chemically reacting fluid mixtures. *Acta Mech*, 226:1757–1805, 2015.

[16] C. M. Brad and J. C. Dorelli. A simple GPU- accelerated two dimentional MUSCL-Hancock solver for ideal magnetohydrodynamics. *Journal of Computational Physics*, 259:444–460, 2018.

[17] C. Chalons, P. Engel, and C. Rohde. A conservative and convergent scheme for undercompressive shock waves. *SIAM Journal on Numerical Analysis*, (52):554–579, 2014.

[18] C. Chalons, C. Rohde, and M. Wiebe. A finite volume method for undercompressive shock waves in two space dimentions. *ESAIM: Mathematical Modelling Numerical Analysis*, (51):1987–2015, 2017.

[19] A. Chertock, S. Karni, and A. Kurganov. Interface tracking method for compressible multifluids. *ESAIM: Mathematical Modelling and Numerical Analysis*, 42:991–1019, 2008.

[20] A. Chertock, A. Kurganov, and Y. Liu. Central-upwind schemes for the system of shallow water equations with horizontal temperature gradients. *Numerische Mathematik*, 127(4):595–639.

[21] J. P. Cocchi, R. Saurel, and J. Loraud. Treatment of interface problems with Godunov-type schems. *Shock waves*, 5:347–357, 1996.

[22] C. M. Dafermos. *Hyperbolic Conservation Laws in Continumm Physics*. Grundlehren der mathematischen Wissenschaften, Berlin Heidelberg, 2016.

[23] J. Paulo Dias and M. Figueira. On the approximation of the solutions of the Riemann problem for a discontinuous conservation law. *Bull Braz. Math Soc.*, 36(1):115–125, 2005.

[24] W. Dreyer, J.Giesselmann, and C. Kraus. A compressible mixture model with phase transition. *Physica D:Nonlinear Phenomena*, 273:1–13, 2014.

[25] E. Rocca E. Feireisl, H. Petzeltova and G. Schimperna. Analysis of a phase-field model for two phase compressible fluids. *Math. Models Methods Appl. Sci.*, 20(7):1129–1160, 2010.

[26] L. C. Evans. *Partial Differential Equations*, volume 19. American Math. Soc., Providence, RI, 1998.

[27] S. Fechter, C. D. Munz, C. Rohde, and C. Zeiler. A sharp interface method for comperessible liquid-vapor flow with phase transition and surface tension. *Journal of Computational Physics*, (336):347–374, 2017.

[28] R. P. Fedkiw. *A survey of chemically reacting compressible flow*. PhD thesis, UCLA, 1996.

[29] T. Flatten, A. Morin, and S. T. Munkejord. On solutions to equilibrium problems for systems of stiffened gases. *SIAM Journal on Applied Mathematics*, 71(1):41,67.

[30] T. Gallouet, J. M. Herard, and N. Seguin. Some recent finite volume schemes to compute Euler equations using real gas EOS. *International Journal for Numerical Methods in Fluids*, 39(12):1073–1138, 2002.

[31] E. Godlewski and P.A. Raviart. *Numerical Approximation of Hyperbolic Systems of Conservation Laws*. Springer New York, 1996.

[32] M. Hantke, W. Dreyer, and G. Warnecke. Exact solutions to the Riemann problems for compressible isothermal Euler equations for two-phase flows with and without phase transition. *Quarterly of Applied Mathematics*, LXXI(3):509–540, 2013.

[33] M. Hantke and S. Müller. Analysis and simulation of a new multi-component two-phase flow model with phase transition and chemical reactions. *Quarterly of Applied Mathematics*, LXXVI(2):253–287, 2018.

[34] M. Hantke, G. Warnecke, C. Matern, and H. Yaghi. A new method to discretize a muliticomponent phase field model. *Journal of Computational and Applied Mathematics*, (422), 2022.

[35] M. Hantke, G. Warnecke, C. Matern, and H. Yaghi. The Riemann problem for a two phase mixture hyperbolic system with phase function and multi-phase equation of state . *Quarterly of Applied Mathematics*, Submitted, 2022.

[36] C. Helzel. *Numerical approximation of conservation laws with stiff source term for the modeling of detonation waves*. Doctoral thesis, Otto-von-Guericke Universität Magdeburg, 2000.

[37] J. Herard. A three phase flow model. *Math. Comput. Model*, (45):732–755, 2007.

[38] L. Hoermander. *Lectures on Nonlinear Hyperbolic Differential Equations*. Springer-Verlag, 1997.

[39] H. H. Hu, N. A. Patankarb, and M. Y. Zhua. Direct numerical simulations of fluid solid systems using the arbitrary Lagrangian-Eulerian technique. *Journal of Computational Physics*, (169):427–462, 2001.

[40] B. Keyfitz and H. C. Kranzer. *A Viscosity Approximation to a System of Hyperbolic Conservation Laws with No Classical Riemann Solution*, volume 1402. Lecture Notes in Mathematics, 1988.

[41] M. Kotschote. Strong solutions of the Navier-Stockes equations for a compressible fluid of Alles-Cahn type. *Arch. Ration. Mech. Anal.*, 206(2):489–514, 2012.

[42] D. Kröner. *Numerical Schemes for Conservation Laws*. Advances in Numerical Mathematics, Wiley, 1997.

[43] L. D. Landau and E. M. Lifshitz. *Course of Theoretical Physics*, volume 5. Statistical physics, London, Paris, New Yourk, Los Angeles: Pergamon Press X, 1958.

[44] P. LeFloch. *Hyperbolic Systems of Conservation Laws: The Theory of Classical and Nonclassical Shock Waves*. Lectures in Mathematics, Birkhäuser Verlag, 2002.

[45] R. LeVeque. Wave propagation algorithms for multidimensional hyperbolic systems. *Journal of Computational Physics*, 131:327–353, 1997.

[46] R. J. LeVeque. A large time step generalization of Godunov's method for systems of conservation laws. *SIAM: J. Numer. Anal.*, 22:1051–1073, 1985.

[47] R. J. LeVeque. *Numerical Methods for Conservation Laws*, volume 132. Springer-Verlag, 1992.

[48] R. J. LeVeque and H. C. Yee. A study of numerical methods for hyperbolic conservation laws with stiff source terms. *Journal of Computational Physics*, 86:187–210, 1990.

[49] F. D. Lora-Clavijo, J. P. Cruz-Perez, F. Siddhartha Guzman, and J. A. Gonzalez. Exact solution of the 1D Riemann problem in Newtonian and relativistic hydrodynamics. *Revista Mexicana de Fisica*, E(59):28–50, 2013.

[50] J. Marie, I. Faille, and T. Gallouet. On an approximate Godunov scheme. *International Journal of Computational Fluid Dynamics*, 12(2):133–149, 1999.

[51] C. Matern. *The Riemann problem for a weakly hyperbolic two-phase flow model of a dispersed phase in a carrier fluid*. Doctoral thesis, Otto-von-Guericke Universität Magdeburg, 2022.

[52] R. Menikoff and B. J. Plohr. The Riemann problem for fluid flow of real materials. *Reviews of Modern Physics*, 61(1):75–130, 1989.

[53] A. Mignone and G. Bode. An HLLC Riemann solver for relativistic flows. *Monthly Notices of the Royal Astronomical Society*, 364(1):126–136, 2005.

[54] L.A. Monthe, F. Benkhaldoun, and I. Elmahi. Positivity preserving finite volume Roe schemes for transport-diffusion equations. *Computer Methods in Applied Mechanics and Engineering*, 178(3):215–232, 1999.

[55] K. Murawski, Jr. K. Murawski, and P. Sticzyneski. Implementation of MUSCL-Hancock method into C++ code for the Euler equation. *Bullentin of the Polish Academy of Science*, 60(1):45–53, 2012.

[56] I. Müller and W. Müller. *Fundamentals of Thermodynamics and Applications*. Springer-Verlag, 2009.

[57] S. Müller, , M. Hantke, and P. Richter. Closure conditions for non-equilibrium multi-component models. *Continuum Mechanics and Thermodynamics*, (28):1157–1189, 2016.

[58] M. V. Papalexandris, A. Leonard, and P. E. Dimotaksi. Unsplit schemes for hyperbolic conservation laws with source terms. *Journal of Computational Physics*, (134):31–61, 1997.

[59] P. A. Raviart and D. Serre. *First International Conference on Hyperbolic Problems*. Spriger-Verlag, 1986.

[60] P. L. Roe. Approximate Riemann solvers, parameter vectors, and difference schemes. *Journal of Computational Physics*, 43(2):357–372, 1981.

[61] E. Romenski, A. D. Resenyansky, and E. F. Toro. Conservative hyperbolic formulation for compressible two-phase flow with different phase pressures and temperature. *Quarterly of Applied Mathematics*, (65):259–279, 2007.

[62] R. Saural, F. Petitpas, and R. Abgrall. Modelling phase transition in metastable liquids. Application to cavitating and flashing flows. *Journal of Fluid Mechanics*, (607):313–350, 2008.

[63] R. Saurel. *Interfaces, Detonation Waves, Cavitation and Multiphase Godunov Method*. Kluwer Academic/ Plenum Publishers, 2001.

[64] R. Saurel and R. Abgrall. A simple method for compressible multifluid flows. *SIAM J. Sci. Comput.*, (21):1115–1145, 1999.

[65] R. Saurel and O. Le Metayer. A multiphase model for interfaces, schocks, detonation waves and cavitation. *J. Fluid Mech*, (431):239–271, 2001.

[66] R. Scardovelli and S. Zaleski. Direct numerical simulation of free surface and interface flow. *Annu. Rev. Fluid Mech*, (31):567–603, 1999.

[67] V. Schleper. A HLL-type Riemann solver for two-phase flow with surface forces and phase transition. *Applied Numerical Mathematics*, (108):256–270, 2016.

[68] K. M. Shyue. An efficient shock-capturing algorithm for compressible multicomponent problems. *Journal of Computational Physics*, (142):208–242, 1998.

[69] J. Smoller. *Shock Waves and Reaction-Diffusion Equations*, volume 256. Springer Science and Business Media, 2012.

[70] Gary Sod. A survey of several finite difference methods for systems of nonlinear hyperbolic conservation laws. *Journal of Computational Physics*, (27):1–31, 1978.

[71] S. I. Sohn. A new TVD-MUSCL schem for hyperbolic conservation laws. *Computers and Mathematics with Applications*, 50:231–248, 2005.

[72] T. Tang. Conservation analysis for operator splitting method applied to conservation laws with stiff source terms. *SIAM Journal on Numerical Analysis*, 5(35):1939–1968, 1998.

[73] F. Thein. *Results for two phase flows with phase transition*. Doctoral thesis, Otto-von-Guericke Universität Magdeburg, 2018.

[74] F. Thein, E. Romenski, and M. Dumbser. Exact and numerical solutions of the Riemann problem for a conservative model of comperessible two-phase flows. *Journal of Scientific Computing*, 93(3), 2022.

[75] E. F. Toro. *Riemann Solvers and Numerical Methods for Fluid Dynamics.* Springer-Verlag, 2009.

[76] E .F. Toro. The HLLC Riemann solver. *Springer-Verlag GmbH Germany, Part of Springer Nature*, 2019.

[77] G. Tryggvason, B. Bunner, and A. Esmaeeli. A front tracking method for the computations of multiphase flow. *Journal of Computational Physics*, (100):25–37, 1992.

[78] A. Tveito and R. Winther. *Introduction to Partial Differential Equations.* Springer-Verlag, 1998.

[79] J. Wang and G. Warnecke. On entropy consistency of large time step schemes I. the Godunov and Glimm schemes. *SIAM: J. Numer. Anal.*, 30(5):1229–1251, 1993.

[80] J. Wang and G. Warnecke. On entropy consistency of large time step schemes II. approximate Riemann solvers. *SIAM: J. Numer. Ana.*, 30(5):1252–1267, 1993.

[81] G. Warnecke. *Analytische Methoden in der Theorie der Erhalyungsgleichung.* B. G. Teubner, Stuttgart-Leipzig, 1999.